SPONSORED CONTENT

nature reprint collection

www.nature.com/reprintcollections/microrna_2013

July 2013

MicroRNAs from bench to clinic

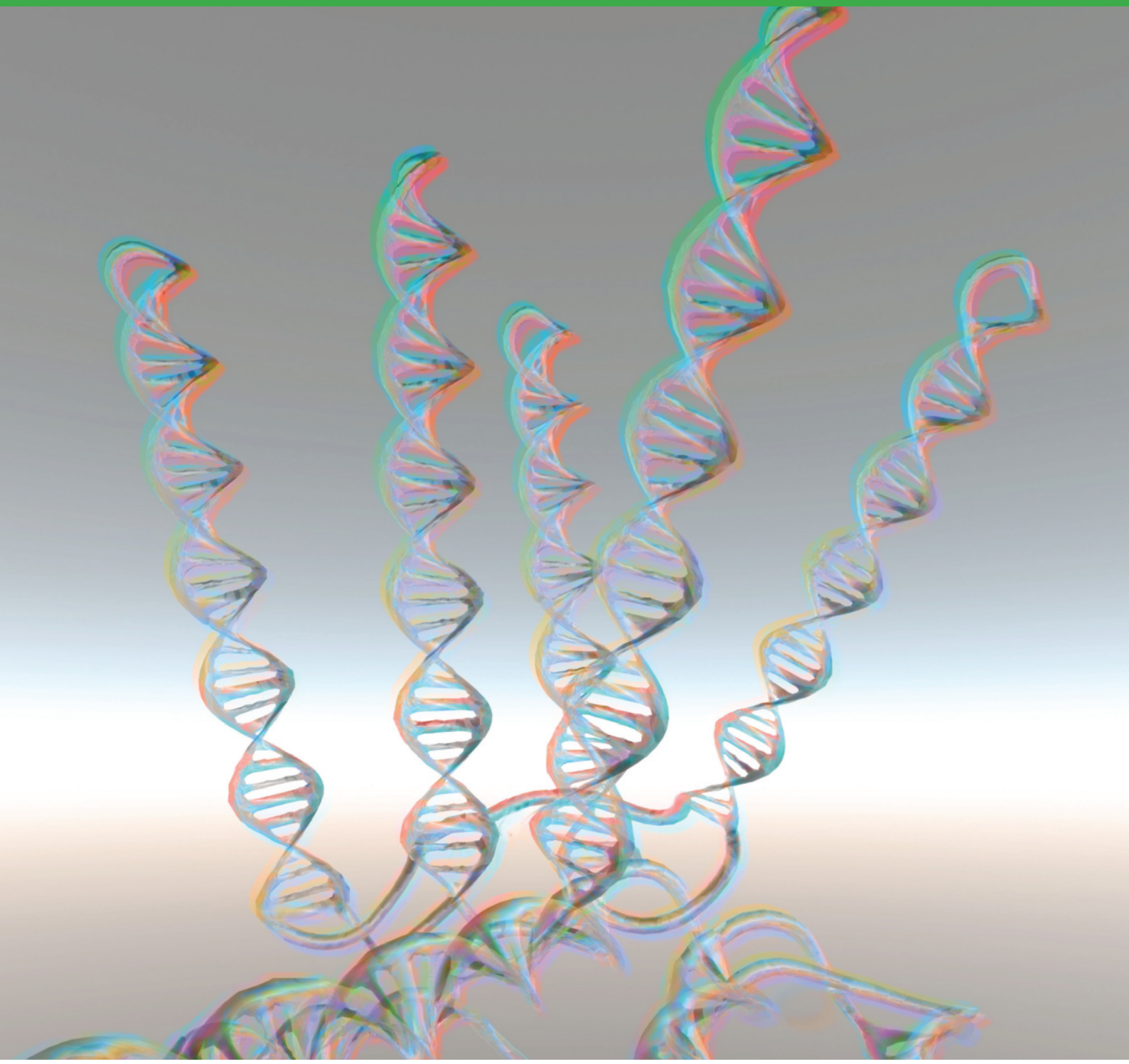

Content selected by: EXIQON Seek Find Verify

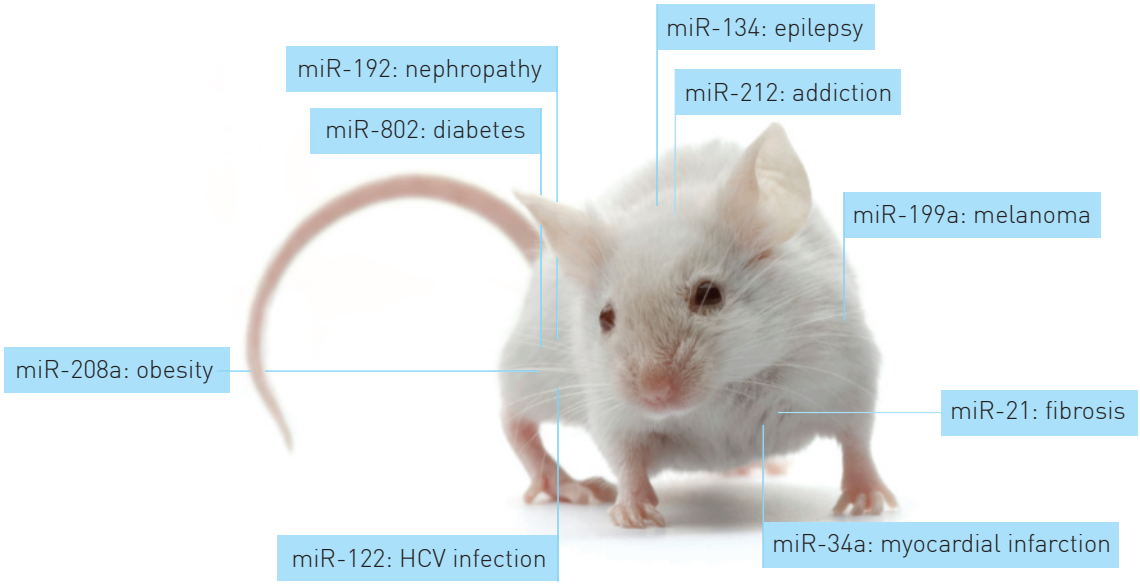

Explore microRNA as therapeutic targets

Efficient silencing *in vivo* using LNA™-enhanced inhibitors

In vivo LNA™ microRNA inhibitors have enabled numerous groundbreaking discoveries about microRNA function and their potential as therapeutic targets in disease. Designed by experts to ensure:

- Unmatched potency even at low concentrations
- Superior serum stability and nuclease resistance
- Low toxicity and limited off target effects

Get expert advice

exiqon.com/in-vivo-mirna-inhibitors

EXIQON
Seek Find Verify

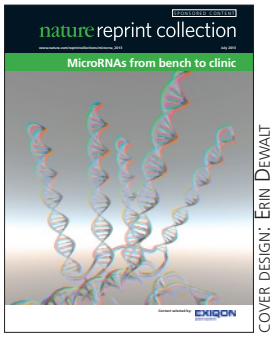

COVER DESIGN: ERIN DEWALT
© CAROL AND MIKE WERNER / ALAMY

nature

nature medicine

Nature Reprint Collection

MicroRNAs from bench to clinic

publisher: MELANIE BRAZIL
editorial production: MATT HANSEN, RENEE LUCAS
manufacturing production: MABEL ENG, KELLY HOPKINS
marketing: NAZLY DE LA ROSA
sponsorship: EVELINA RUBIO HAKANSSON, WILL PIPER, YVETTE SMITH, REYA SILAO
sponsor: EXIQON

Nature Medicine - www.nature.com/nm
75 Varick Street, 9th Floor
New York NY 10013-1917
(212) 726-9325
e-mail: medicine@us.nature.com

CITING THE COLLECTION
All papers have been previously published in *British Journal of Cancer, Nature, Nature Medicine* and *Nature Reviews Drug Discovery*. Please use original citation, which can be found on the table of contents.

VISIT THE COLLECTION
www.nature.com/reprintcollections/microrna_2013

SUBSCRIPTIONS AND CUSTOMER SERVICES
For UK/ROW (excluding Japan):
Nature Publishing Group, Subscriptions, Brunel Road, Basingstoke, Hants, RG21 6XS, UK. Tel: +44 (0) 1256 329242.
Subscriptions and customer services for Americas—including Canada, Latin America and the Caribbean: Nature Publishing Group, Subscription Department, PO Box 5161, Brentwood, TN 37024-5161, USA. Tel: +1 (800) 524 2688 (US) or +1 615 850 5315 (outside the US).

npg
nature publishing group

Sponsor foreword

Progress in the microRNA field over the last 12 years has been nothing but remarkable. MicroRNAs were only discovered in humans in 2001, but since then they have revolutionized cell biology and completely changed the way we view the regulation of gene expression. They are now known to be involved, at some level, in all cellular and developmental pathways and all major types of disease, including all cancers, as well as metabolic, cardiovascular, neuronal and immune-related disorders. Exiqon's LNA™-based microRNA research tools have been instrumental in many of the groundbreaking discoveries in the field. In this collection, we are thrilled to present some of the recent advances in moving microRNAs from basic research into the clinic both as biomarkers and therapeutic targets.

Since the discovery of circulating or extracellular microRNAs, their potential as minimally invasive diagnostic and prognostic markers for disease has been actively investigated. Here we feature two articles where qPCR profiling of microRNAs in biofluids have been shown to have diagnostic potential. Another promising area with clinical prospects is microRNA *in situ* hybridization (ISH) in FFPE samples. We have included an article detailing the prognostic potential of microRNA ISH in this collection.

Due to their extensive involvement in human disease, microRNAs are naturally interesting targets for therapeutic intervention. One of the most advanced areas in this respect is the potential of microRNAs as therapeutic targets in cardiovascular disease and we have included a review of this area. In addition, two very recent and groundbreaking studies that have shown the exciting potential for microRNA inhibition in diabetes and epilepsy are also included.

The transition of microRNAs from basic research to applied clinical use is well underway. We hope you find this collection interesting and inspiring and look forward to following the progress of this exciting area in the future.

Lars Kongsbak, CEO, Exiqon A/S

This supplement is published by Nature Publishing Group on behalf of Exiqon.
All content has been chosen by Exiqon.

FULL PAPER

BJC

British Journal of Cancer (2013) 108, 1712–1719 | doi: 10.1038/bjc.2013.121

Keywords: colorectal cancer; diagnostic; biomarker; microRNA profile; serum

Identification of serum microRNA profiles in colon cancer

E Hofsli*[,1,2,7], W Sjursen[3,4,7], W S Prestvik[5], J Johansen[2], M Rye[2], G Tranø[6], H H Wasmuth[6], I Hatlevoll[1] and L Thommesen[5]

[1]Department of Oncology, St Olavs Hospital, Trondheim University Hospital, Olav Kyrresgt 17, Trondheim 7006, Norway; [2]Faculty of Medicine, Department of Cancer and Molecular Medicine, Norwegian University of Science and Technology, Olav Kyrresgt 17, Trondheim 7006, Norway; [3]Department of Laboratory Medicine Children's and Women's Health, Norwegian University of Science and Technology, Olav Kyrresgt 17, Trondheim 7006, Norway; [4]Department of Pathology and Medical Genetics, St Olavs Hospital, Trondheim University Hospital, Olav Kyrresgt 17, Trondheim 7006, Norway; [5] Faculty of Technology, Sør-Trøndelag University College, E.C. Dahlsgt 2, Trondheim 7004, Norway and [6]Department of Gastrointestinal Surgery, St Olavs Hospital, Trondheim University Hospital, Olav Kyrresgt 17, Trondheim 7006, Norway

Background: microRNAs (miRNAs) exist in blood in an apparently stable form. We have explored whether serum miRNAs can be used as non-invasive early biomarkers of colon cancer.

Methods: Serum samples from 30 patients with colon cancer stage IV and 10 healthy controls were examined for the expression of 375 cancer-relevant miRNAs. Based on the miRNA profile in this study, 34 selected miRNAs were measured in serum from 40 patients with stage I–II colon cancer and from 10 additional controls.

Results: Twenty miRNAs were differentially expressed in serum from stage IV patients compared with controls ($P<0.01$). Unsupervised clustering revealed four subgroups; one corresponding mostly to the control group and the three others to the patient groups. Of the 34 miRNAs measured in the follow-up study of stage I–II patients, 21 showed concordant expression between stage IV and stage I–II patient. Based on the profiles of these 21 miRNAs, a supervised linear regression analysis (Partial Least Squares Regression) was performed. Using this model we correctly assigned stage I–II colon cancer patients based on miRNA profiles of stage IV patients.

Conclusion: Serum miRNA expression profiling may be utilised in early detection of colon cancer.

Colorectal cancer (CRC) is the second leading cause of cancer-related death in developed countries (Jemal *et al*, 2010; Hrasovec and Glavac, 2012). Early detection improves survival, as 5-year survival rate declines from nearly 90% in early-stage disease (stage I–II) to 12–13% in metastatic disease (stage IV; http://www.kreftregisteret.no). To detect early cancer or adenomas, various population-based screening programmes have been implemented (Geiger and Ricciardi, 2009; Hol *et al*, 2010). Colonoscopy is the gold standard method for early detection of CRC, but widespread use is limited due to its invasive nature and high costs. The most widely used non-invasive screening method, the fecal occult blood test, is compromised by limited diagnostic accuracy. Thus, new non-invasive methods are needed.

MicroRNAs (miRNAs) are small, 19–25 nucleotide noncoding RNAs, which negatively regulate gene transcription at transcriptional or post-transcriptional level (Iorio and Croce, 2012a) and have an important role in the control of biological processes, such as cellular development, differentiation, proliferation and apoptosis. Prior studies have demonstrated the impact of miRNAs in tumour biology and oncogenesis (Stefani and Slack, 2008; Inui

*Correspondence: Dr E Hofsli, E-mail: eva.hofsli@stolav.no
[7]The first two authors are joint first authors.

Received 3 January 2013; revised 27 February 2013; accepted 28 February 2013; published online 4 April 2013

et al, 2010; Babashah and Soleimani, 2011). MicroRNAs are frequently dysregulated in cancer and have shown great potential as tissue-based markers for cancer classification and prognostication (Paranjape *et al*, 2009; Gandellini *et al*, 2011; Kong *et al*, 2012; Iorio and Croce, 2012b).

In CRC tissue, various miRNAs have been found differentially expressed compared with matched normal tissue (Liu and Chen, 2010; Schee *et al*, 2010; Dong *et al*, 2011; Hrasovec and Glavac, 2012). Some miRNAs, as mir-21 (Schetter *et al*, 2008; Dong *et al*, 2011), miR-31 (Bandres *et al*, 2006; Dong *et al*, 2011) and miR-429 (Li *et al*, 2013), have been characterised as possible prognostic markers of CRC (Dong *et al*, 2011; Menendez *et al*, 2013), whereas others such as miR-126 (Hansen *et al*, 2012) and miR-150 (Ma *et al*, 2012) have been proposed as predictive markers of response to chemotherapy. Specific miRNA signatures have also been reported to predict response to neoadjuvant chemoradiotherapy in rectal cancer (Della Vittoria Scarpati *et al*, 2012; Kheirelseid *et al*, 2012).

MiRNAs are found in serum, plasma and other body fluids (Chen *et al*, 2008; Cortez *et al*, 2011), and exist in an apparently stable extracellular form (Zheng *et al*, 2011). The mechanism underlying their stability in the RNase-rich environment of blood is not well understood, but the current model posits that circulating miRNAs are stabilised by the formation of the Ago2-miRNA complex and/or protected of degradation by encapsulation in exosomes (Valadi *et al*, 2007; Meckes *et al*, 2010; Zomer *et al*, 2010; Russo *et al*, 2012). Exosomes containing miRNA produced by malignant cells may have an important role in metastasis by promoting angiogenesis, cell proliferation and/or tumour cell invasion (Iorio and Croce, 2009; Liu *et al*, 2011; Zheng *et al*, 2011). The current comprehension involves that miRNA profiles in serum from cancer patients may mirror the profiles of the tumours. Several recent studies have characterised miRNA profiles in serum and urine aiming to identify appropriate diagnostic markers of cancer (Huang *et al*, 2010; Ohshima *et al*, 2010; Wittmann and Jack, 2010).

A limited number of studies have been undertaken searching for miRNA expression in blood from CRC patients (Chen *et al*, 2008; Ng *et al*, 2009; Huang *et al*, 2010; Pu *et al*, 2010; Nugent *et al*, 2012). The aim of this study was to identify miRNAs for early diagnosis of colon cancer. Serum samples from patients with newly diagnosed colon cancer and from blood donors were assessed for miRNA expression. We characterise a serum miRNA profile in colon cancer that may serve as a new non-invasive approach in early detection of colon cancer.

MATERIALS AND METHODS

Patients and controls. Newly diagnosed colon cancer patients from two hospitals in Norway (St Olavs Hospital, Trondheim and Hamar Hospital, Hamar) were included, as described in Trano *et al* (2009). Blood, tumour tissue and adjacent normal mucosa were collected from the patients after informed consent had been obtained. The selected groups consisted of 30 patients with metastatic (stage IV) colon cancer, and 40 patients with early-stage colon cancer (7 patients with stage I and 33 with stage II). Serum from 20 blood donors aged $\geqslant 50$ years (10 females and 10 males) were used as controls (Blood bank, St Olavs Hospital, Trondheim).

MiRNA profiling by miRCURY LNA Universal RT miRNA PCR. Isolation of RNA and all real-time quantitative PCR (Q-PCR) experiments were performed by Exiqon Company, Vedbaek, Denmark (www.exiqon.com). RNA was purified from 250 μl serum with the miRNeasy mini kit from Qiagen (Venlo, Holland) according to the manufacturers' protocol. Q-PCR was performed by using the miRCURY LNA Universal RT microRNA PCR system containing 375 miRNA assays in Study 1, and 34 miRNAs in Study 2. In Study 1, there were no replicas, whereas in Study 2 three replicates per sample were polyadenylated and reverse transcribed (RT) into cDNA for all miRNA. One real-time Q-PCR amplification was performed for each RT reaction. Detectable miRNAs were those with a Cp (crossing point) <37, or 5 Cp below the negative control.

Study design. Increasing numbers of studies postulate that colon and rectal cancer differ with respect to molecular and genetic characteristics (Li and Lai, 2009; Koga *et al*, 2010; Slattery *et al*, 2011). To ensure a homogenous patient population, only colonic cancer was included. Initially, we measured 375 cancer-relevant miRNAs in serum from 30 patients with stage IV disease and from 10 control samples (5 females and 5 males; Study 1). Twenty miRNAs were differentially expressed in serum from stage IV patients compared with controls ($P<0.01$). Subsequently, serum from 40 patients with stage I–II colon cancer was analysed for the expression of 34 miRNAs (Study 2). In all, 20 of these miRNAs were selected based on differential expression in Study 1 ($P<0.01$), 10 miRNAs were chosen from review of the miRNA literature and 4 miRNAs were additional reference miRNAs provided by Exiqon.

Statistical analysis. All miRNA profiles from Study 1 and Study 2 were normalised using the geometric mean for each sample over all miRNAs. Profiles of the 20 most differentially expressed miRNAs ($P<0.01$) in Study 1 were subjected to hierarchical clustering to create a heatmap. Missing values were imputed using the K-nearest-neighbour method.

The 21 miRNAs that showed concordant expression in advanced (Study 1) and localised (Study 2) disease were used to construct a Partial Least Squares Regression (PLSR) model. The 21 miRNA profiles from Study 1 were used as model variables, and cancer status ($1/-1$ for cancer/control) for the 30 colon cancer patients and 10 controls in Study 1 was used as a target variable. Root-mean-square error after cross-validation indicated that two principal components were optimal for this model. The two-component PLSR model was then used to investigate whether the difference between cancer and control samples in Study 2 could be recognised using the miRNA profiles of the same 21 miRNAs used to create the model from Study 1. The profiles from Study 2 thus represent a completely independent test set for model evaluation. Results were displayed graphically to determine the optimal threshold separating cancers from controls. The analysis was performed using the statistical scripting language R (http://www.r-project.org/).

RESULTS

MiRNA profile in serum from patients with stage IV colon cancer. To investigate a possible difference in miRNA expression profile between colon cancer stage IV patients and healthy subjects, 375 cancer-relevant miRNAs were assessed in sera from 30 patients and 10 healthy blood donors (Study 1). Patients and tumour characteristics are shown in Table 1. We observed a distinct different expression pattern in cancer *vs* healthy subjects. Twenty miRNAs were significantly differentially expressed with $P<0.01$. A total of 9 miRNAs were upregulated and 11 downregulated. We performed a hierarchical clustering of the 20 miRNAs with highest differential expression between serum from patients and controls (Figure 1). This clustering analysis revealed four subgroups; one corresponding principally to the control group and the three others to the patient groups.

MicroRNA profile in serum from patients with stage I and II colon cancer. To examine whether a corresponding serum miRNA profile as demonstrated in colon cancer stage IV could

Table 1. Patients' characteristics

Characteristic	Patients with metastatic disease ($n = 30$), n (%)	Patients with localised disease ($n = 40$), n (%)
Age (years)		
<60	9 (30)	8 (20)
60–75	8 (26.7)	12 (30)
⩾75	13 (43.3)	20 (50)
Median (range)	68.6 (41–86)	72.4 (30–93)
Sex		
Male	14 (46.7)	18 (45)
Female	16 (53.3)	22 (55)
K-RAS mutation		
Yes	8 (26.7)	11 (27.5)
No	22 (73.3)	29 (72.5)
B-RAF mutation		
Yes	13 (43.3)	14 (35)
No	17 (56.7)	26 (65)
Microsatellite instability		
Stable (MSS)	23 (76.7)	15 (37.5)
Unstable (MSI-H)	7 (23.3)	25 (62.5)
Tumour location		
Coecum	9 (30)	9 (22.5)
Ascending colon	4 (13.3)	8 (20)
Right flexure	0 (0)	4 (10)
Transverse colon	7 (23.3)	4 (10)
Left flexure	2 (6.7)	1 (2.5)
Descending colon	0 (0)	0 (0)
Sigmoid colon	8 (26.7)	14 (35)
TNM status		
T1	0 (0)	3 (7.5)
T2	1 (3.3)	4 (10)
T3	19 (63.3)	28 (70)
T4	9 (30)	5 (12.5)
Missing	1 (3.3)	0 (0)
N0	8 (26.7)	40 (100)
N1	7 (23.3)	0 (0)
N2	15 (50)	0 (0)
M0	0 (0)	40 (100)
M1	30 (100)	0 (0)
CEA		
<5	8 (26.7)	
5–100	11 (36.7)	
⩾100	5 (16.7)	
Missing	6 (20)	

Abbreviations: CEA = carcinoembryonal antigen; MSI-Hi = microsatellite instability-high; MSS = microsatellite stable; TNM = TNM staging; .

be found in early stage cancer, 34 miRNAs were further analysed in sera from 40 patients with stage I or II colon cancer and 10 healthy controls (Study 2). Figure 2 shows that 21 of the 26 detected miRNAs displayed the same expression profile as in advanced colon cancer, suggesting that most of these miRNAs are relevant as diagnostic markers. Of these 21 miRNAs, miR-423-5p, miR-210, miR-720, miR-320a and miR-378 showed the highest expression compared with controls, whereas miR-106a, miR-143, miR-103, miR-199a-3p, miR-382 and miR-151-5p showed the lowest expression. The relevance to CRC of these 26 miRNAs according to literature is summarised in Table 2.

The five miRNAs that showed different expression in early- *vs* late-stage cancer were miR-34a, miR-146a, miR-21, miR-484 and mir-425 (Figure 2). MiR-484 and miR-21 were highly expressed in stage IV as compared with controls, but lower expressed than controls in blood samples from early-stage I–II patients. The opposite was found for miR-34a and miR-146a. The expression level of miR-425 was reduced at stage I–II compared with controls, but no significant changes detected in samples from stage IV patients.

The PLSR model correctly assigns stage I–II colon cancer patients based on miRNA profiles of stage IV patients. We generally observed a good correspondence between expression profiles of stage IV (Study 1) and stage I–II cancer patients (Study 2), as 21 out of 26 miRNAs showed the same pattern of expression. This suggests that the miRNAs selected for analysis in Study 2 may be relevant as diagnostic markers. To investigate whether our miRNA expression profiles of stage IV colon cancer could be used to recognise cancer in early-stage I–II patients, we used PLSR, a supervised linear regression method, which is used for prediction and classification in multivariate analyses (Martens, 1989). Patient to patient variation in miRNA expression profiles makes it difficult to create reliable recognition models using individual miRNAs. Utilising information from several miRNA expression profiles simultaneously (multivariate analysis) is a powerful strategy to improve the confidence of such models. We thus used PLSR to model and validate our results. The model was trained using miRNA profiles from the 40 subjects (30 stage IV colon cancer patients and 10 controls) analysed in Study 1, and evaluated using cross-validation. The resulting model was then used to assign the 50 subjects (40 stage I–II cancer patients and 10 controls) from Study 2 to either the cancer or control group. In this setting, the subjects from Study 2 is regarded as a completely independent test set, and is not involved at any stage in the modelling phase. Partial Least Squares Regression can only assign independent data using the same set of miRNAs in the modelling and test set. We thus selected from Study 1 only the miRNAs assessed further in Study 2 to build our PLSR model. As five miRNAs showed clear inconsistencies in expression profiles between Study 1 and Study 2, these were not suited for modelling. The remaining set of 21 miRNAs was thus used in the final modelling and validation. The results are illustrated in Figure 3, showing that 9 out of 10 controls (specificity of 90%) and 35 out of 40 cancer patients (sensitivity of 87.5%) from Study 2 could be correctly assigned using the selected threshold.

DISCUSSION

In this study, we demonstrate distinct differences in the expression profile of miRNA in sera from colon cancer patients *vs* healthy subjects, and identify a 21 miRNA serum colon cancer profile that may be utilised to identify colon cancer patients at an early stage of the disease. The generation of a PLSR model correctly assigned stage I–II patients based on the miRNA profiles of stage IV patients, which mathematically support the trend observed in our data.

The miRNA profile in sera from CRC patients did not show a uniform profile; but showed up to be clustered into three subgroups. These three subgroups may reflect the heterogeneity in gene expression and signalling pathways leading to CRC development. MicroRNA profiling may thus be a valuable supplement to the gene expression profiling of CRC subgroups.

Our demonstration of a difference in serum miRNA expression in colon cancer patients compared with healthy individuals are in

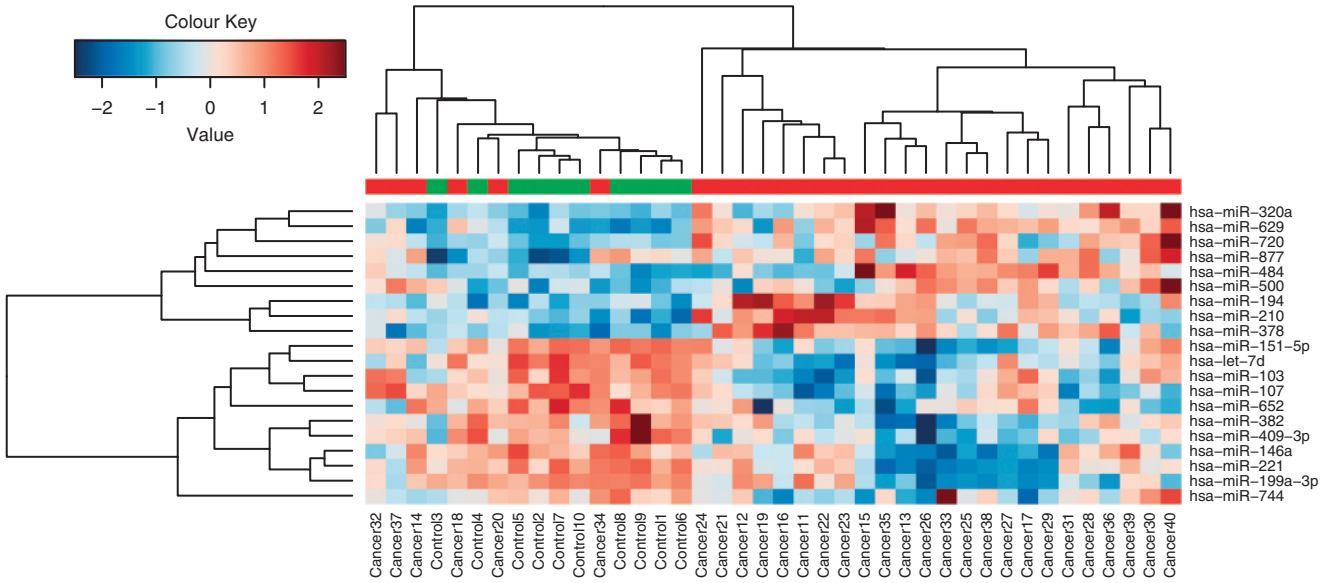

Figure 1. Heat-map diagram of a two-way hierarchical clustering analysis consisting of the 20 most differentially expressed miRNAs in serum from 30 metastatic (stage IV) colon cancer patients as compared with 10 healthy subjects (*P*-value <0.01). Red colour represents an expression level above mean, blue colour represents expression lower than the mean. Upper colour labelling show patient samples in red and controls in green.

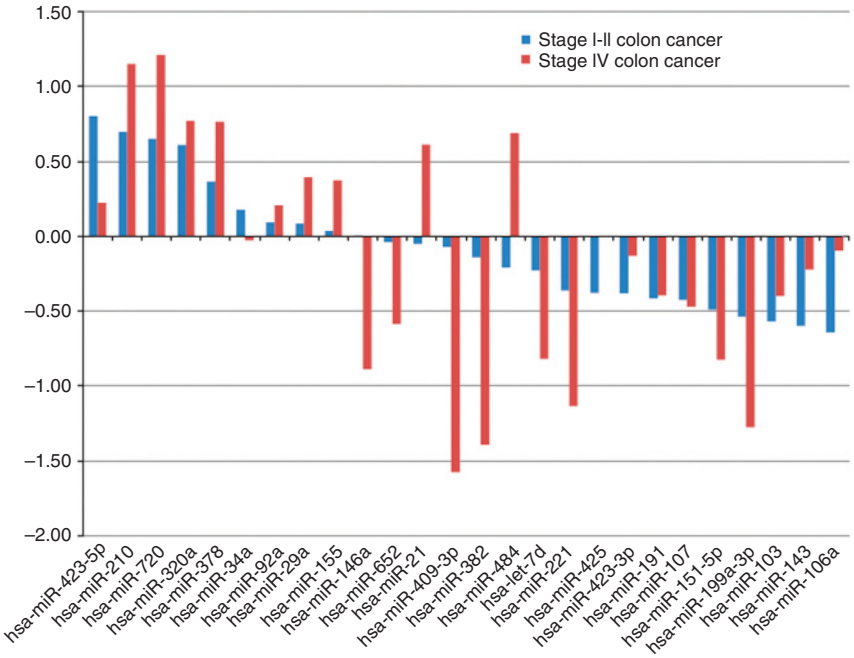

Figure 2. Differentially expressed miRNAs in stage IV (red bars) *vs* stage I–II (blue bars) colon cancer. The expression of 34 miRNAs was compared, and 26 miRNAs were detected. In all, 21 of 26 detected miRNAs showed the same expression profile in early-stage I–II *vs* metastatic stage IV colon cancer.

accordance with the relatively few studies that have assessed miRNA expression in serum of CRC patients (Chen *et al*, 2008; Ng *et al*, 2009; Huang *et al*, 2010; Pu *et al*, 2010; Nugent *et al*, 2012; Menendez *et al*, 2013). However, with regard to single miRNAs that have been reported differentially expressed, these studies present some conflicting results (Ng *et al*, 2009; Huang *et al*, 2010; Cheng *et al*, 2011; Nugent *et al*, 2012). Our finding of an upregulation of miR-92a in sera from colon cancer patients is in accordance with studies by Ng *et al* (2009) and Huang *et al* (2010), but in contrast to studies by Cheng *et al* (2011) and Nugent *et al* (2012). The reasons for opposite results may be several. Whereas most studies have included both colon and rectal cancers in their analyses, our study involves only patients with colon cancer. Thus, the issue of possible differences in miRNA expression in colon *vs* rectal cancer has been omitted in our study. Differential expression of miRNAs by tumour location could not be excluded (Slattery *et al*, 2011; Gaedcke *et al*, 2012), as well as ethnical differences in miRNA expression, which is reflected in studies from Norway (Cekaite *et al*, 2012) and China (Ng *et al*, 2009; Huang *et al*, 2010). Moreover, the detection of miRNAs still involves challenges that are reflected both in the study design and the analytical methods. We therefore suggest that a serum miRNA

Table 2. Examples of relevance to CRC of miRNAs found in sera from patients with metastatic (stage IV) and early stage (stage I-II) CRC

microRNA	Selection criteria	microRNA expression in CRC compared with controls (literature)	Concordance present study and literature	References
Upregulated in present study (stage I–II and IV colon cancer)				
miR-423-5p	Reference	Not reported in CRC	New	
miR-210	$P<0.01$	Upregulated (cells)	Yes	Ota *et al* (2012)
miR-720	$P<0.01$	Upregulated (tissue)	Yes	Ragusa *et al* (2012) Della Vittoria Scarpati *et al* (2012)
miR-320a	$P<0.01$	Downregulated (tissue and cells)	No	Schepeler *et al* (2008) Sun *et al* (2012)
miR-378	$P<0.01$	Downregulated (tissue)	No	Wang *et al* (2010); Faltejskova *et al* (2012)
miR-92a	Literature	Upregulated (plasma)	Yes and no	Ng *et al* (2009)
		Downregulated (plasma)		Huang *et al* (2010) Cheng *et al* (2011)
miR-29a	Literature	Upregulated (plasma)	Yes	Huang *et al* (2010); Weissmann-Brenner *et al* (2012)
miR-155	Literature	Upregulated (tissue)	Yes	Wang *et al* (2012) Valeri *et al* (2010)
Downregulated in present study (stage I–II and IV colon cancer)				
miR-106a	Literature	Upregulated (stool)	No	Link *et al* (2010) Diaz *et al* (2008)
miR-143	Literature	Downregulated in CRC	Yes	Michael *et al* (2003)
miR-103	$P<0.01$	Upregulated (cell lines and tissue)	No	Gottardo *et al* (2007); Li *et al* (2011b); Chen *et al* (2012)
miR-199a-3p	$P<0.01$	Not reported in CRC	New	
miR-151-5p	$P<0.01$	Not reported in CRC	New	
miR-107	$P<0.01$	Upregulated (cell lines and tissue)	No	Chen *et al* (2012)
miR-191	Reference	Upregulated	No	Xi *et al* (2006)
miR-423-3p	Reference	Not reported in CRC	New	
miR221	$P<0.01$	Upregulated (blood)	No	Pu *et al* (2010)
miR-let7d	$P<0.01$	Not reported in CRC	New	
miR-382	$P<0.01$	Downregulated	New	
miR-409-3p	$P<0.01$	Not reported in CRC	New	
miR-652	$P<0.01$	Upregulated (rectal cancer)	No	Lulla *et al* (2011) Gao *et al* (2011)
Different expression in the present study between stage I–II and IV colon cancer				
miR-34a	Literature	Upregulated	Yes (present study: upreg stage I–II; weak downreg stage IV)	Wang *et al* (2012)
		Downregulated (serum)		Nugent *et al* (2012)
miR-146a	$P<0.01$	No difference (serum)	No (present study: downreg stage IV)	Huang *et al* (2010)
miR-21	Literature	Upregulated (tissue and blood)	Yes (present study: upreg stage IV; weak downreg stage I–II)	Schetter *et al* (2008); Pu *et al* (2010); Dong *et al* (2011); Kanaan *et al* (2012)
miR-484	$P<0.01$	Not reported in CRC	New	
miR-425	Reference	No difference (tissue)	No (present study: downreg stage I–II)	Chang *et al* (2010)

Abbreviations: CRC = colorectal cancer; miRNA = microRNA.

profile may be more reliable than the detection of few individual miRNAs.

Several of the 21 miRNAs that constitute our colon cancer serum miRNA profile have been described to be involved in the development of cancer. Our demonstration of an enhanced expression of miR-21 is in accordance with previous reports showing elevated levels of miR-21 both in CRC tissue (Schetter *et al*, 2008; Dong *et al*, 2011) and blood (Pu *et al*, 2010; Kanaan *et al*, 2012). In a recent systematic review, overexpression of miR-21 and a reduced expression of let-7d were the two miRNAs that most frequently were associated with poor outcome across diverse malignancies (Nair *et al*, 2012). Interestingly, a recent large study from Denmark characterised the mir-21 expression as a prognostic factor in stage II colon cancer (Kjaer-Frifeldt *et al*, 2012). Members of the Let-7 family are reduced in a wide range of cancers and target-known oncogenes, like c-myc, RAS and HMGA2, and are therefore considered as to function as tumour suppressor-like miRNAs (Menendez *et al*, 2013). Our demonstration of a reduced level of miR-let-7d in sera from colon cancer patients was therefore not surprisingly, but to our knowledge, no previous assessment of

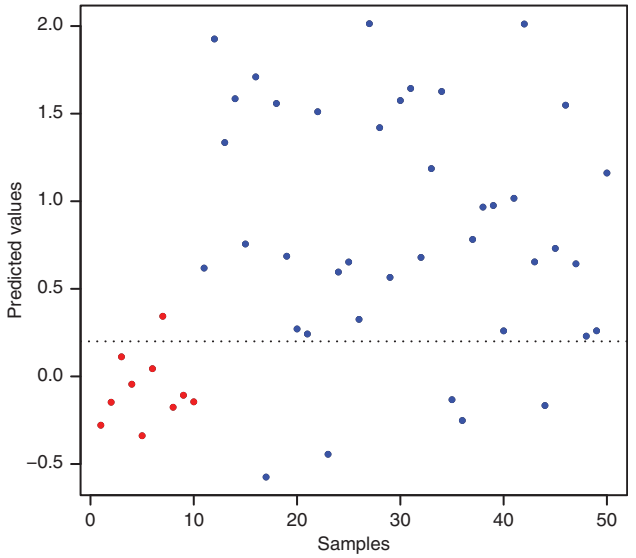

Figure 3. Prediction analysis of early-stage colon cancer patients. Controls are shown in red and cancer samples in blue. 9 out of 10 healthy controls were correctly predicted as true negatives and 35 out of 40 patients with cancer as true positives.

let-7d expression in sera from colon cancer patients has been reported. MiR-378 has been shown to function as an oncogene-like miRNA (Lee *et al*, 2007), to be functionally important for c-Myc-driven transformation (Feng *et al*, 2011) and to correlate with progression of human breast cancer (Eichner *et al*, 2010). However, in other studies, miR-378 has been found to be downregulated in CRC tissue (Wang *et al*, 2010; Faltejskova *et al*, 2012). In accordance with our results, a higher expression of miR-720 has been demonstrated in CRC tissue than in normal colon epithelial tissue controls (Ragusa *et al*, 2012).

Perhaps, somewhat unexpected was our findings of reduced serum levels of miR-103 and miR-107 in colon cancer patients compared with controls. MiR-103 and miR-107 have been found highly expressed in several solid tumours (Gottardo *et al*, 2007; Li *et al*, 2011b; Kim *et al*, 2012), and have been associated with poor prognosis in CRC. (Chen *et al*, 2012). On the other hand, a downregulation of miR-103 has been found in haematological malignancies (Li *et al*, 2011a; Machova Polakova *et al*, 2011). Notably, the miR-103/107 family is located to chromosomal loci prone to deletions or amplifications, and miR-103/107 is consequently reported to be deregulated in various diseases (Finnerty *et al*, 2010). We cannot exclude that the decreased miRNA expression found in our study reflects such genomic alterations. In our opinion, the diagnostic value of these miRNAs in blood should thus be evaluated with caution and at least compared with genomic analysis of the tumour sample.

Although our results have to be confirmed in larger clinical studies, the identification of a miRNA profile in serum of early-stage colon cancer patient that is quite similar to the late-stage cancer patients is promising and suggests that the miRNA profile may be used to identify early-stage cancer. Taken into consideration the complex regulation of miRNAs, we advocate that the miRNA profile – rather than assessment of a single miRNA expression – must be the foundation in establishing potentially new biomarkers.

In conclusion, we have identified a 21 miRNA profile in blood samples from colon cancer patients consisting of miRNAs that have been previously reported as possible markers of CRC, others not. Our study identifying miRNA expression profiles indicates that serum miRNA may be utilised to detect colon cancer in early curative stages.

REFERENCES

Babashah S, Soleimani M (2011) The oncogenic and tumour suppressive roles of microRNAs in cancer and apoptosis. *Eur J Cancer* **47**(8): 1127–1137.

Bandres E, Cubedo E, Agirre X, Malumbres R, Zarate R, Ramirez N, Abajo A, Navarro A, Moreno I, Monzo M, Garcia-Foncillas J (2006) Identification by Real-time PCR of 13 mature microRNAs differentially expressed in colorectal cancer and non-tumoral tissues. *Mol Cancer* **5**: 29.

Cancer Genome Atlas Network (2012) Comprehensive molecular characterization of human colon and rectal cancer. *Nature* **487**(7407): 330–337.

Cekaite L, Rantala JK, Bruun J, Guriby M, Agesen TH, Danielsen SA, Lind GE, Nesbakken A, Kallioniemi O, Lothe RA, Skotheim RI (2012) MiR-9, -31, and -182 deregulation promote proliferation and tumor cell survival in colon cancer. *Neoplasia.* (New York, NY) **14**(9): 868–881.

Chang KH, Mestdagh P, Vandesompele J, Kerin MJ, Miller N (2010) MicroRNA expression profiling to identify and validate reference genes for relative quantification in colorectal cancer. *BMC Cancer* **10**: 173.

Chen HY, Lin YM, Chung HC, Lang YD, Lin CJ, Huang J, Wang WC, Lin FM, Chen Z, Huang HD, Shyy JY, Liang JT, Chen RH (2012) miR-103/107 promote metastasis of colorectal cancer by targeting the metastasis suppressors DAPK and KLF4. *Cancer Res* **72**(14): 3631–3641.

Chen X, Ba Y, Ma L, Cai X, Yin Y, Wang K, Guo J, Zhang Y, Chen J, Guo X, Li Q, Li X, Wang W, Wang J, Jiang X, Xiang Y, Xu C, Zheng P, Zhang J, Li R, Zhang H, Shang X, Gong T, Ning G, Zen K, Zhang CY (2008) Characterization of microRNAs in serum: a novel class of biomarkers for diagnosis of cancer and other diseases. *Cell Res* **18**(10): 997–1006.

Cheng H, Zhang L, Cogdell DE, Zheng H, Schetter AJ, Nykter M, Harris CC, Chen K, Hamilton SR, Zhang W (2011) Circulating plasma MiR-141 is a novel biomarker for metastatic colon cancer and predicts poor prognosis. *PLoS One* **6**(3): e17745.

Cortez MA, Bueso-Ramos C, Ferdin J, Lopez-Berestein G, Sood AK, Calin GA (2011) MicroRNAs in body fluids–the mix of hormones and biomarkers. *Nat Rev Clin Oncol* **8**(8): 467–477.

Della Vittoria Scarpati G, Falcetta F, Carlomagno C, Ubezio P, Marchini S, De Stefano A, Singh VK, D'Incalci M, De Placido S, Pepe S (2012) A specific miRNA signature correlates with complete pathological response to neoadjuvant chemoradiotherapy in locally advanced rectal cancer. *Int J Rad Oncol Biol Phys* **83**(4): 1113–1119.

Diaz R, Silva J, Garcia JM, Lorenzo Y, Garcia V, Pena C, Rodriguez R, Munoz C, Garcia F, Bonilla F, Dominguez G (2008) Deregulated expression of miR-106a predicts survival in human colon cancer patients. *Genes Chromosomes Cancer* **47**(9): 794–802.

Dong Y, Wu WK, Wu CW, Sung JJ, Yu J, Ng SS (2011) MicroRNA dysregulation in colorectal cancer: a clinical perspective. *Br J Cancer* **104**(6): 893–898.

Eichner LJ, Perry MC, Dufour CR, Bertos N, Park M, St-Pierre J, Giguere V (2010) miR-378(*) mediates metabolic shift in breast cancer cells via the PGC-1beta/ERRgamma transcriptional pathway. *Cell Metab* **12**(4): 352–361.

Faltejskova P, Svoboda M, Srutova K, Mlcochova J, Besse A, Nekvindova J, Radova L, Fabian P, Slaba K, Kiss I, Vyzula R, Slaby O (2012) Identification and functional screening of microRNAs highly deregulated in colorectal cancer. *J Cell Mol Med* **16**(11): 2655–2666.

Feng M, Li Z, Aau M, Wong CH, Yang X, Yu Q (2011) Myc/miR-378/TOB2/cyclin D1 functional module regulates oncogenic transformation. *Oncogene* **30**(19): 2242–2251.

Finnerty JR, Wang WX, Hebert SS, Wilfred BR, Mao G, Nelson PT (2010) The miR-15/107 group of microRNA genes: evolutionary biology, cellular functions, and roles in human diseases. *J Mol Biol* **402**(3): 491–509.

Gaedcke J, Grade M, Camps J, Sokilde R, Kaczkowski B, Schetter AJ, Difilippantonio MJ, Harris CC, Ghadimi BM, Moller S, Beissbarth T, Ried T, Litman T (2012) The rectal cancer microRNAome–microRNA expression in rectal cancer and matched normal mucosa. *Clin Cancer Res* **18**(18): 4919–4930.

Gandellini P, Profumo V, Folini M, Zaffaroni N (2011) MicroRNAs as new therapeutic targets and tools in cancer. *Exp Opin Ther Targets* **15**(3): 265–279.

Gao W, Shen H, Liu L, Xu J, Shu Y (2011) MiR-21 overexpression in human primary squamous cell lung carcinoma is associated with poor patient prognosis. *J Cancer Res Clin Oncol* **137**(4): 557–566.

Geiger TM, Ricciardi R (2009) Screening options and recommendations for colorectal cancer. *Clin Colon Rectal Surg* **22**(4): 209–217.

Gottardo F, Liu CG, Ferracin M, Calin GA, Fassan M, Bassi P, Sevignani C, Byrne D, Negrini M, Pagano F, Gomella LG, Croce CM, Baffa R (2007) Micro-RNA profiling in kidney and bladder cancers. *Urol Oncol* **25**(5): 387–392.

Hansen TF, Sorensen FB, Lindebjerg J, Jakobsen A (2012) The predictive value of microRNA-126 in relation to first line treatment with capecitabine and oxaliplatin in patients with metastatic colorectal cancer. *BMC Cancer* **12**: 83.

Hol L, de Jonge V, van Leerdam ME, van Ballegooijen M, Looman CW, van Vuuren AJ, Reijerink JC, Habbema JD, Essink-Bot ML, Kuipers EJ (2010) Screening for colorectal cancer: comparison of perceived test burden of guaiac-based faecal occult blood test, faecal immunochemical test and flexible sigmoidoscopy. *Eur J Cancer* **46**(11): 2059–2066.

Hrasovec S, Glavac D (2012) MicroRNAs as novel biomarkers in colorectal cancer. *Front Genet* **3**: 180.

Huang Z, Huang D, Ni S, Peng Z, Sheng W, Du X (2010) Plasma microRNAs are promising novel biomarkers for early detection of colorectal cancer. *Int J Cancer* **127**(1): 118–126.

Inui M, Martello G, Piccolo S (2010) MicroRNA control of signal transduction. *Nat Rev Mol Cell Biol* **114:** 252–263.

Iorio MV, Croce CM (2009) MicroRNAs in cancer: small molecules with a huge impact. *J Clin Oncol* **27**(34): 5848–5856.

Iorio MV, Croce CM (2012a) MicroRNA dysregulation in cancer: diagnostics, monitoring and therapeutics. A comprehensive review. *EMBO Mol Med* **4**(3): 143–159.

Iorio MV, Croce CM (2012b) microRNA involvement in human cancer. *Carcinogenesis* **33**(6): 1126–1133.

Jemal A, Siegel R, Xu J, Ward E (2010) Cancer statistics, 2010. *CA: a Cancer J Clin* 60(5): 277–300.

Kanaan Z, Rai SN, Eichenberger MR, Roberts H, Keskey B, Pan J, Galandiuk S (2012) Plasma miR-21: a potential diagnostic marker of colorectal cancer. *Ann Surg* **256**(3): 544–551.

Kheirelseid EA, Miller N, Chang KH, Curran C, Hennessey E, Sheehan M, Newell J, Lemetre C, Balls G, Kerin MJ (2012) miRNA expressions in rectal cancer as predictors of response to neoadjuvant chemoradiation therapy. *Int J Colorectal Dis* **18**: 18.

Kim BH, Hong SW, Kim A, Choi SH, Yoon SO (2012) Prognostic implications for high expression of oncogenic microRNAs in advanced gastric carcinoma. *J Surg Oncol* **20**(10): 23271.

Kjaer-Frifeldt S, Hansen TF, Nielsen BS, Joergensen S, Lindebjerg J, Soerensen FB, Depont Christensen R, Jakobsen A (2012) The prognostic importance of miR-21 in stage II colon cancer: a population-based study. *Br J Cancer* **107**(7): 1169–1174.

Koga Y, Yasunaga M, Takahashi A, Kuroda J, Moriya Y, Akasu T, Fujita S, Yamamoto S, Baba H, Matsumura Y (2010) MicroRNA expression profiling of exfoliated colonocytes isolated from feces for colorectal cancer screening. *Cancer Prev Res* **3**(11): 1435–1442.

Kong YW, Ferland-McCollough D, Jackson TJ, Bushell M (2012) microRNAs in cancer management. *Lancet Oncol* **13**(6): e249–e258.

Lee DY, Deng Z, Wang CH, Yang BB (2007) MicroRNA-378 promotes cell survival, tumor growth, and angiogenesis by targeting SuFu and Fus-1 expression. *Proc Natl Acad Sci USA* **104**(51): 20350–20355.

Li FY, Lai MD (2009) Colorectal cancer, one entity or three. *J Zhejiang Univ Sci B* **10**(3): 219–229.

Li J, Du L, Yang Y, Wang C, Liu H, Wang L, Zhang X, Li W, Zheng G, Dong Z (2013) MiR-429 Is an Independent Prognostic Factor in Colorectal Cancer and Exerts Its Anti-apoptotic Function by Targeting SOX2. *Cancer Lett* **329**(1): 84–90.

Li S, Moffett HF, Lu J, Werner L, Zhang H, Ritz J, Neuberg D, Wucherpfennig KW, Brown JR, Novina CD (2011a) MicroRNA expression profiling identifies activated B cell status in chronic lymphocytic leukemia cells. *PLoS One* **6**(3): e16956.

Li X, Zhang Y, Zhang H, Liu X, Gong T, Li M, Sun L, Ji G, Shi Y, Han Z, Han S, Nie Y, Chen X, Zhao Q, Ding J, Wu K, Daiming F (2011b) miRNA-223 promotes gastric cancer invasion and metastasis by targeting tumor suppressor EPB41L3. *Mol Cancer Res* **9**(7): 824–833.

Link A, Balaguer F, Shen Y, Nagasaka T, Lozano JJ, Boland CR, Goel A (2010) Fecal MicroRNAs as novel biomarkers for colon cancer screening. *Cancer Epidemiol Biomarkers Prev* **19**(7): 1766–1774.

Liu F, Lou YL, Wu J, Ruan QF, Xie A, Guo F, Cui SP, Deng ZF, Wang Y (2011) Upregulation of MicroRNA-210 regulates renal angiogenesis mediated by activation of VEGF signaling pathway under ischemia/perfusion injury *in vivo* and *in vitro*. *Kidney Blood Press Res* **35**(3): 182–191.

Liu M, Chen H (2010) The role of microRNAs in colorectal cancer. *J Genet Genomics* **37**(6): 347–358.

Lulla RR, Costa FF, Bischof JM, Chou PM, de F Bonaldo M, Vanin EF, Soares MB (2011) Identification of differentially expressed microRNAs in osteosarcoma. *Sarcoma* **2011**: 732690.

Ma Y, Zhang P, Wang F, Zhang H, Yang J, Peng J, Liu W, Qin H (2012) miR-150 as a potential biomarker associated with prognosis and therapeutic outcome in colorectal cancer. *Gut* **61**(10): 1447–1453.

Machova Polakova K, Lopotova T, Klamova H, Burda P, Trneny M, Stopka T, Moravcova J (2011) Expression patterns of microRNAs associated with CML phases and their disease related targets. *Mol Cancer* **10**: 41.

Martens HNT (1989) *Multivariate Calibration* ChichesterWiley.

Meckes Jr. DG, Shair KH, Marquitz AR, Kung CP, Edwards RH, Raab-Traub N (2010) Human tumor virus utilizes exosomes for intercellular communication. *Proc Natl Acad Sci USA* **107**(47): 20370–20375.

Menendez P, Villarejo P, Padilla D, Menendez JM, Montes JA (2013) Diagnostic and prognostic significance of serum MicroRNAs in colorectal cancer. *J Surg Oncol* **107**(2): 217–220.

Michael MZ, O' Connor SM, van Holst Pellekaan NG, Young GP, James RJ (2003) Reduced accumulation of specific microRNAs in colorectal neoplasia. *Mol Cancer Res* **1**(12): 882–891.

Nair VS, Maeda LS, Ioannidis JP (2012) Clinical outcome prediction by microRNAs in human cancer: a systematic review. *J Natl Cancer Inst* **104**(7): 528–540.

Ng EK, Chong WW, Jin H, Lam EK, Shin VY, Yu J, Poon TC, Ng SS, Sung JJ (2009) Differential expression of microRNAs in plasma of patients with colorectal cancer: a potential marker for colorectal cancer screening. *Gut* **58**(10): 1375–1381.

Nugent M, Miller N, Kerin MJ (2012) Circulating miR-34a levels are reduced in colorectal cancer. *J Surg Oncol* **106**(8): 947–952.

Ohshima K, Inoue K, Fujiwara A, Hatakeyama K, Kanto K, Watanabe Y, Muramatsu K, Fukuda Y, Ogura S, Yamaguchi K, Mochizuki T (2010) Let-7 microRNA family is selectively secreted into the extracellular environment via exosomes in a metastatic gastric cancer cell line. *PLoS One* **5**(10): e13247.

Ota T, Doi K, Fujimoto T, Tanaka Y, Ogawa M, Matsuzaki H, Kuroki M, Miyamoto S, Shirasawa S, Tsunoda T (2012) KRAS up-regulates the expression of miR-181a, miR-200c and miR-210 in a three-dimensional-specific manner in DLD-1 colorectal cancer cells. *Anticancer Res* **32**(6): 2271–2275.

Paranjape T, Slack FJ, Weidhaas JB (2009) MicroRNAs: tools for cancer diagnostics. *Gut* **58**(11): 1546–1554.

Pu XX, Huang GL, Guo HQ, Guo CC, Li H, Ye S, Ling S, Jiang L, Tian Y, Lin TY (2010) Circulating miR-221 directly amplified from plasma is a potential diagnostic and prognostic marker of colorectal cancer and is correlated with p53 expression. *J Gastroenterol Hepatol* **25**(10): 1674–1680.

Ragusa M, Statello L, Maugeri M, Majorana A, Barbagallo D, Salito L, Sammito M, Santonocito M, Angelica R, Cavallaro A, Scalia M, Caltabiano R, Privitera G, Biondi A, Di Vita M, Cappellani A, Vasquez E, Lanzafame S, Tendi E, Celeste S, Di Pietro C, Basile F, Purrello M (2012) Specific alterations of the microRNA transcriptome and global network structure in colorectal cancer after treatment with MAPK/ERK inhibitors. *J Mol Med* **4**: 4.

Russo F, Di Bella S, Nigita G, Macca V, Lagana A, Giugno R, Pulvirenti A, Ferro A (2012) miRandola: Extracellular Circulating MicroRNAs Database. *PLoS One* **7**(10): e47786.

Schee K, Fodstad O, Flatmark K (2010) MicroRNAs as biomarkers in colorectal cancer. *Am J Pathol* **177**(4): 1592–1599.

Schepeler T, Reinert JT, Ostenfeld MS, Christensen LL, Silahtaroglu AN, Dyrskjot L, Wiuf C, Sorensen FJ, Kruhoffer M, Laurberg S, Kauppinen S, Orntoft TF, Andersen CL (2008) Diagnostic and prognostic microRNAs in stage II colon cancer. *Cancer Res* **68**(15): 6416–6424.

Schetter AJ, Leung SY, Sohn JJ, Zanetti KA, Bowman ED, Yanaihara N, Yuen ST, Chan TL, Kwong DL, Au GK, Liu CG, Calin GA, Croce CM, Harris CC (2008) MicroRNA expression profiles associated with prognosis and therapeutic outcome in colon adenocarcinoma. *JAMA* **299**(4): 425–436.

Slattery ML, Wolff E, Hoffman MD, Pellatt DF, Milash B, Wolff RK (2011) MicroRNAs and colon and rectal cancer: differential expression by tumor location and subtype. *Genes Chromosomes Cancer* **50**(3): 196–206.

Stefani G, Slack FJ (2008) Small non-coding RNAs in animal development. *Nat Rev Mol Cell Biol* **9**(3): 219–230.

Sun JY, Huang Y, Li JP, Zhang X, Wang L, Meng YL, Yan B, Bian YQ, Zhao J, Wang WZ, Yang AG, Zhang R (2012) MicroRNA-320a suppresses human

colon cancer cell proliferation by directly targeting beta-catenin. *Biochem Biophys Res Commun* **420**(4): 787–792.

Trano G, Wasmuth HH, Sjursen W, Hofsli E, Vatten LJ (2009) Awareness of heredity in colorectal cancer patients is insufficient among clinicians: a Norwegian population-based study. *Colorectal Dis* **11**(5): 456–461.

Valadi H, Ekstrom K, Bossios A, Sjostrand M, Lee JJ, Lotvall JO (2007) Exosome-mediated transfer of mRNAs and microRNAs is a novel mechanism of genetic exchange between cells. *Nat Cell Biol 9* **6**: 654–659.

Valeri N, Gasparini P, Fabbri M, Braconi C, Veronese A, Lovat F, Adair B, Vannini I, Fanini F, Bottoni A, Costinean S, Sandhu SK, Nuovo GJ, Alder H, Gafa R, Calore F, Ferracin M, Lanza G, Volinia S, Negrini M, McIlhatton MA, Amadori D, Fishel R, Croce CM (2010) Modulation of mismatch repair and genomic stability by miR-155. *Proc Natl Acad Sci USA* **107**(15): 6982–6987.

Wang M, Zhang P, Li Y, Liu G, Zhou B, Zhan L, Zhou Z, Sun X (2012) The quantitative analysis by stem-loop real-time PCR revealed the microRNA-34a, microRNA-155 and microRNA-200c overexpression in human colorectal cancer. *Med Oncol* **29**(5): 3113–3118.

Wang YX, Zhang XY, Zhang BF, Yang CQ, Chen XM, Gao HJ (2010) Initial study of microRNA expression profiles of colonic cancer without lymph node metastasis. *J Dig Dis* **11**(1): 50–54.

Weissmann-Brenner A, Kushnir M, Lithwick Yanai G, Aharonov R, Gibori H, Purim O, Kundel Y, Morgenstern S, Halperin M, Niv Y, Brenner B (2012) Tumor microRNA-29a expression and the risk of recurrence in stage II colon cancer. *Int J Oncol* **40**(6): 2097–2103.

Wittmann J, Jack HM (2010) Serum microRNAs as powerful cancer biomarkers. *Biochimica et Biophysica Acta* **1806**(2): 200–207.

Xi Y, Formentini A, Chien M, Weir DB, Russo JJ, Ju J, Kornmann M (2006) Prognostic Values of microRNAs in Colorectal Cancer. *Biomark Insights* **2**: 113–121.

Zheng D, Haddadin S, Wang Y, Gu LQ, Perry MC, Freter CE, Wang MX (2011) Plasma microRNAs as novel biomarkers for early detection of lung cancer. *Int J Clin Exp Pathol* **4**(6): 575–586.

Zomer A, Vendrig T, Hopmans ES, van Eijndhoven M, Middeldorp JM, Pegtel DM (2010) Exosomes: Fit to deliver small RNA. *Commun Integr Biol* **3**(5): 447–450.

British Journal of Cancer (2012) 107, 1354–1360

www.bjcancer.com

MicroRNA profiling of diagnostic needle aspirates from patients with pancreatic cancer

S Ali[1], H Saleh[2,3], S Sethi[2], FH Sarkar[1,2] and PA Philip[*,1]

[1]Department of Oncology, Wayne State University School of Medicine, Detroit, MI 48201, USA; [2]Department of Pathology, Wayne State University School of Medicine, Detroit, MI 48201, USA; [3]Karmanos Cancer Institute, Detroit Medical Center, Wayne State University School of Medicine, Detroit, MI 48201, USA

BACKGROUND: A major challenge to the development of biomarkers for pancreatic cancer (PC) is the small amount of tissue obtained at the time of diagnosis. Single-gene analyses may not reliably predict biology of PC because of its complex molecular makeup. MicroRNA (miRNA) profiling may provide a more informative molecular interrogation of tumours. The primary objective of this study was to determine the feasibility of performing miRNA arrays and quantitative real-time PCR (qRT–PCR) from archival formalin-fixed paraffin-embedded (FFPE) cell blocks obtained from fine-needle aspirates (FNAs) that is the commonest diagnostic procedure for suspected PC.

METHODS: MicroRNA expression profiling was performed on FFPE from FNA of suspicious pancreatic masses. Subjects included those who had a pathological diagnosis of pancreatic adenocarcinoma and others with a non-malignant pancreatic histology. Exiqon assay was used to quantify miRNA levels and qRT–PCR was used to validate abnormal expression of selected miRNAs.

RESULTS: A total of 29 and 15 subjects had pancreatic adenocarcinoma and no evidence of cancer, respectively. The RNA yields per patient varied from 25 to 100 ng. Profiling demonstrated deregulation of over 228 miRNAs in pancreatic adenocarcinoma of which the top 7 were further validated by qRT–PCR. The expression of let-7c, let-7 f, and miR-200c were significantly reduced in most patients whereas the expression of miR-486-5p and miR-451 were significantly elevated in all pancreas cancer patients. MicroRNAs let-7d and miR-423-5p was either downregulated or upregulated with a significant inter-individual variation in their expression.

CONCLUSION: This study demonstrated the feasibility of using archival FFPE cell blocks from FNAs to establish RNA-based molecular signatures unique to pancreatic adenocarcinoma with potential applications in clinical trials for risk stratification, patient selection, and target validation.

British Journal of Cancer (2012) **107,** 1354–1360. doi:10.1038/bjc.2012.383 www.bjcancer.com
Published online 28 August 2012

Keywords: miRNAs; fine-needle aspirates; pancreatic cancer; biomarker; qRT–PCR

Pancreatic cancer (PC) is the fourth leading cause of cancer related deaths in the United States (Jemal *et al*, 2010). Mortality from this disease has not changed over the past few decades partly because of lack of screening methods for early detection. Most patients present with advanced disease without any effective systemic therapies. Future advances in targeted therapies must be based on better selection of patients and on the ability to establish molecular signatures from representative tissues. However, progress in tissue-based research is challenged by the paucity of material obtained during diagnostic procedures. The majority of patients with PC are diagnosed by an image-guided fine-needle aspiration (FNA) of the primary or metastatic tumour site (Chen *et al*, 2007; Touchefeu *et al*, 2009). Szafranska *et al* (2008b) reported that miRNA analysis from fresh FNA biopsy samples differentiated malignant from benign PC tissues. Another similar study on FNA samples identified markers in PDAC patients diagnosed with non-resectable tumours (Bournet *et al*, 2012). Despite evidence for miRNAs in tumour tissue obtained at surgery from patients with PC there is little knowledge on miRNA profiling from formalin-fixed paraffin-embedded (FFPE) cell blocks of FNAs material.

*Correspondence: Dr PA Philip; E-mail: philipp@karmanos.org
Revised 18 June 2012; accepted 3 August 2012; published online 28 August 2012

It is well recognised that the development of cancer involves alterations in the expression of multiple genes regulated by transcriptional, post-transcriptional, translational, and post-translational modifications. Therefore, a single gene or protein expression may not reliably predict the biological behaviour of the disease. Nevertheless, traditional approaches to developing biomarkers continue to be based on single-gene assays. MicroRNA expression assays expand the scope to study tumour biology by interrogating multiple target perturbations that are related to key target molecule(s). This may be a better strategy to study PC because of the multiplicity of gene mutations and pathway deregulations that underlie its aggressiveness and resistance to therapy (Sarkar *et al*, 2010; Wang *et al*, 2010). MicroRNAs by virtue of their molecular interactions influence gene and gene products that are amenable to drug effects. Understanding the miRNAs that are involved in gene regulation and others that are 'effectors' in the downstream signalling will provide an opportunity to interrogate these miRNAs to develop biomarkers for the gene in question, and will also provide a means to target the biological effects of the gene(s) of interest and certain undruggable molecules. Establishing signatures that are based on a constellation of upregulated (oncogenic) and downregulated (tumour suppressor) miRNAs that are unique to each patient will risk stratify newly diagnosed patients and provide invaluable tools for personalised therapy.

Experimental evidence supports an increasing role for miRNAs in the molecular biology of PC. Underexpression of miR-200 and let-7 families is associated with shorter survival (Ali *et al*, 2010a; Bao *et al*, 2011a). We and others have shown that miR-200 is a marker of chemo-resistance and that its re-expression or reactivation leads to increased expression of E-cadherin and reduced expression of ZEB1/2 and vimentin that would reverse drug resistance (Hurteau *et al*, 2009; Bao *et al*, 2011b). By its regulation of epithelial to mesenchymal transition (EMT) miR-200 also promotes invasion and metastases (Li *et al*, 2009; Yu *et al*, 2010). Other studies have shown that downregulation of let-7 expression in PC that was inversely associated with worsening tumour and patient survival (Li *et al*, 2009; Torrisani *et al*, 2009; Ali *et al*, 2010b). Interestingly, the frequently mutated oncogene *RAS* in PC is known to be translationally downregulated by the let-7 family (Takamizawa *et al*, 2004; Ali *et al*, 2010b).

The goal of this study was to establish the feasibility of miRNA expression profiling of localised PC using material obtained from diagnostic FNA. In this study, we evaluated the expression profiles of miRNAs in FFPE cell blocks from 29 patients with pancreatic adenocarcinoma and from 15 non-malignant pancreatic tissues. We further validated the expression of selected miRNAs by quantitative real-time-PCR (qRT–PCR) in individual samples to provide quantitative analysis of miRNA expression in real time.

MATERIALS AND METHODS

Tissue collection

Diagnostic FNAs from patients who underwent computerised tomography or endoscopic ultrasound-guided biopsy of a suspicious mass using 20–23 gauge needle were studied (Supplementary Table 1). Two to five needle passes from primary tumour were undertaken per patient with a mean of 3. Diagnostic smears were evaluated using Deff-Quick staining (Mercedes Medical, Sarasota, FL, USA). The remaining needle aspirates were placed in fixative fluid from which pellets were obtained after centrifugation. Cellular pellets were fixed using formalin and embedded in paraffin using standard protocol. Hematoxylin and eosin staining was used for histological confirmation of cancer, to determine the cellularity of representative sections, and to confirm the presence of tumour cells together with lymphocytes and macrophage without any evidence of desmoplastic cells. Minimums of 50 cells were considered necessary to obtain a satisfactory quantity of RNA to perform qRT–PCR, which represented $\sim$80% of the patients. Moreover, this number of cells would also allow for a reliable distinction between benign and malignant histology. The lack of sufficient amount of RNA from the other 20% of the patients could have been due to the lack of sufficient cells but less likelier due to RNA degradation because pre-miRNA template is typically $<$150 nucleotide. We collected FFPE morphologically normal appearing pancreas tissue from 15 patients that were anatomically farther away from the pancreatic tumour to serve as the controls. The institutional human investigation Review Board approved the study. All analyses were performed without knowing the origin of samples.

RNA isolation

Total RNA was isolated from FFPE tissue using the RNeasy Kit (Qiagen, Valencia, CA, USA) according to the manufacturer's protocol with some modifications. Four freshly cut tissue sections of 10 μm thick and $\sim$1 cm in diameter were placed in micro tubes along with 1 ml xylene. After vigorous shaking for 10 s, samples were centrifuged for 2 min at room temperature. The supernatant was removed, 1 ml of ethanol was added, and centrifuged again for 2 min. The resultant pellet was resuspended in 240 μl of buffer PKD along with 10 μl of proteinase K and incubated at 55 °C for 15 min, and then at 80 °C for 15 min. Approximately 500 μl of buffer RBC was added and transferred to a DNA column, centrifuged, and the flow-through was collected. Ethanol of 1200 μl was added to the aliquot that was subsequently applied directly to the RNeasy column. RNA was washed with buffer solution to remove impurities and eluted in a final volume of 15 μl. RNA was quantified and its purity evaluated by the absorption ratio at 260/280 nm using NanoDrop 2000 (Thermo Scientific, Pittsburgh, PA, USA). The ratio of 260/280 varied from 1.8–2.1. Samples with values less or more were considered to be not usable.

MicroRNA profiling

Purified RNA pooled separately from normal and patient samples were analysed by LC Sciences for miRNA microarray profiling (LC Sciences Houston, TX, USA) as an initial step. The miRNA profiling was performed by miRBase version 16 (LC Sciences). Data were normalised using selected housekeeping genes. Network analysis was performed with the web-based bioinformatics tool Ingenuity pathway analysis software (Ingenuity Systems, Redwood City, CA, USA) functional network analysis.

Real-time reverse transcriptase-PCR (qRT–PCR)

Real time qRT–PCR was conducted on all samples to validate the miRNA profiling results using SYBR Green miRNA-based assay. The Universal cDNA Synthesis Kit (Exiqon, Woburn, MA, USA) was used per manufacturer's protocol. Approximately 10 ng of RNA from tissue was reverse transcribed using 5 μl of master mix containing 5 $\times$ reaction buffer and enzyme mix. The mixture was incubated at 42 °C for 60 min, followed by 95 °C for 5 min. Reverse transcriptase (RT)–PCR reactions were then carried out in a total volume of 10 μl reaction mixture containing 4 μl of RT product mixed with 1.0 μl PCR primer mix, and 5 μl of SYBR Green master mix. All reactions, including controls were performed in triplicate using StepOnePlus Real-Time PCR (Applied Biosystems, Foster City, CA, USA). Relative expression of miRNAs was analysed using the C_t method and was normalised by RNU48 expression.

RESULTS

Expression profiling of miRNAs

RNA from archival FNA cell blocks of PC and control samples ($\sim$5 μl each) were pooled separately. Expression profiling revealed 228 miRNAs that were differentially expressed in subjects with or without PC: 103 were upregulated and 125 were downregulated. The top 10 up and downregulated miRNAs are shown in Table 1. The up or downregulated miRNAs included miR-486-5p, miR-451, miR-423-5p, let-7c, d, f, and miR-200c.

Pathway analysis of expressed miRNAs

Ingenuity modelling of the miRNA profiling was undertaken to better understand the pathways involved and target genes as shown in Figures 1 and 2. Networks involving selected miRNAs were then algorithmically generated based on their connectivity. This analysis showed that many of the miRNAs were regulated through each other either directly or indirectly, and were also regulated by several target genes. We observed upregulation of miR-451, miR-122, miR-150, and downregulation of the let-7 family, miR-200c, and miR-146a, which is a target of E2F1, E2F3, and LIN28A. This was in agreement with our previous observations showing downregulation of the let-7 family and miR-146a in plasma samples from patients with PC (Ali *et al*, 2010b). We also observed that the profiles obtained were within what was seen in 15 bio functional network groups relating to cancer, genetic

disorder, and gastrointestinal disease (Figure 2B). Of the seven miRNAs chosen for further analysis, three were oncomirs (miR-486-5p, miR-423-5p, and miR-451) and four were tumour-suppressor miRNAs (miR-200c, let-7c, let-7d, and let-7f).

Table 1 The top 10 up and downregulated miRNAs by miRNA profiling

	Normal (N)		Tumour (T)			
Reporter name	**Mean**	**s.d.**	**Mean**	**s.d.**	**Log2 (T/N)**	***P*-value**
Top 10 downregulated miRNAs						
hsa-miR-4286	1248	132	36	10	−5.11	2.64E−03
hsa-let-7f	716	90	31	3	−4.54	5.29E−05
hsa-miR-720	13484	514	863	8	−3.97	6.89E−05
hsa-let-7d	815	140	63	7	−3.70	2.29E−04
hsa-miR-1280	7230	1155	575	49	−3.65	1.74E−04
hsa-miR200c	987	146	87	14	−3.51	3.27E−04
hsa-miR-26a	886	18	85	29	−3.38	6.14E−03
hsa-let-7c	982	26	233	46	−2.07	7.09E−03
hsa-miR-146a	24	41	8	4	−1.58	5.42E−01
hsa-let-7b	1212	172	426	39	−1.51	1.91E−03
Top 10 upregulated miRNAs						
hsa-miR-486-5p	11	1	1306	65	6.87	2.65E−04
hsa-miR-451	107	17	5452	344	5.67	6.07E−04
hsa-miR-92a	96	18	1024	27	3.41	1.98E−03
hsa-miR-423-5p	30	2	271	16	3.17	2.40E−05
hsa-miR-124	6	1	57	10	3.15	5.22E−04
hsa-miR-3687	150	15	1251	67	3.06	6.35E−05
hsa-miR-1246	288	30	1847	77	2.68	1.22E−03
hsa-miR-1275	395	60	2264	516	2.52	1.84E−03
hsa-miR-17	15	2	37	8	1.32	7.85E−03
hsa-miR-320a	142	23	329	31	1.21	4.07E−03

qRT–PCR of selected miRNAs

We further analysed the miRNA expression level of seven miRNAs based on the miRNA profiling described above and validated their expression in individual samples using qRT–PCR. Analyses were blinded to source of the samples and performed in parallel to avoid batch effects. The expression level in controls was set at 1.0. The reproducibility of the qRT–PCR assay showed that miRNAs can be efficiently extracted from FNA cell blocks and could be compared across multiple samples. The miRNA expression analysis of four functional tumour-suppressor miRNAs, miR-200c (Figure 3), let-7c, let-7d, and let-7f (Figure 4), showed significant reduction in tumours compared with controls. Moreover, analyses clearly indicated that the expression levels of miR-200c, let-7c, and let-7f were significantly downregulated in almost all the PC patients compared with controls. Conversely, the expression of let-7d was differentially expressed between the samples compared with normal controls (Figure 4). Compared with miRNA levels from controls, the expression levels of oncogenic miR-486-5p and miR-451 were significantly upregulated, and in more than half of the PC specimens the level was increased to >20-fold (Figure 5). On the other hand, the expression levels of miR-423-5p were varied between the samples compared with normal controls (Figure 5), which suggest that some miRNAs can function differently between patients.

Comparative expression of seven miRNAs tested in FNA samples

The expression levels of all seven miRNAs are presented as a box plot in Figure 6. The analysis of the individual samples for miRNA expression level by qRT–PCR revealed that three of the four tumour-suppressor miRNAs were significantly downregulated

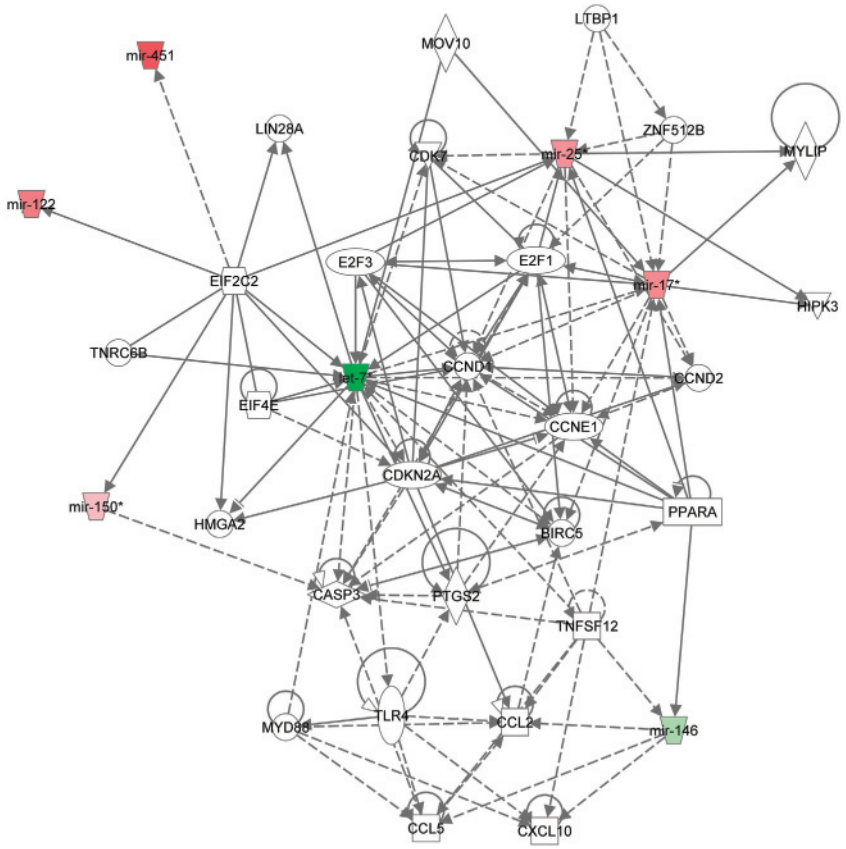

Figure 1 Ingenuity network analysis showing up (red) and downregulation (green) of miRNAs analysed by miRNA profiling in PC and their targeted genes.

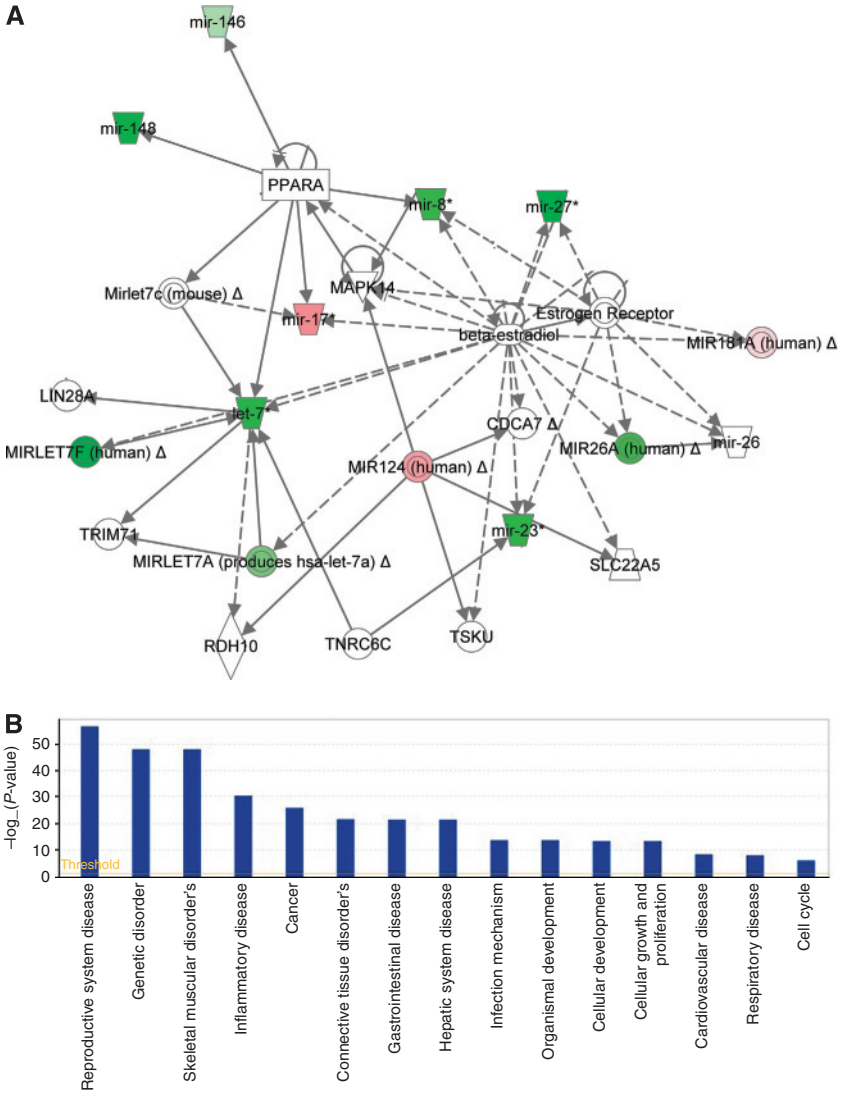

Figure 2 Ingenuity network analysis showing up (red) and downregulation (green) of miRNAs involved in PC and their target genes (**A**). The solid lines connecting genes represent a direct relation and dotted lines indirect relation. We also observed 15 bio functional network groups that included cancer, genetic disorder, and gastrointestinal disease (**B**).

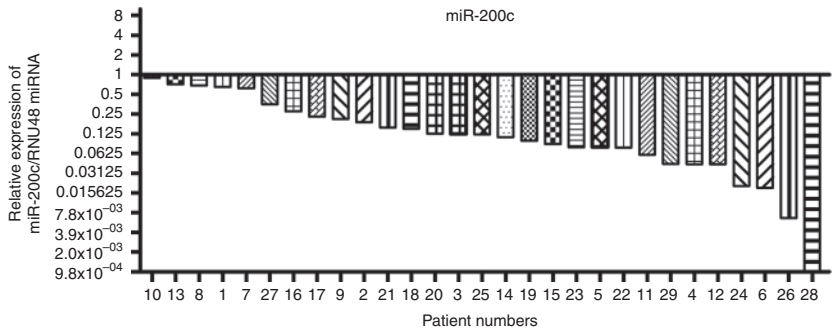

Figure 3 Comparative expression analysis of miR-200c in 29 FNA cell blocks from PC patients analysed individually compared with FNA cell blocks obtained from 15 normal controls by using qRT–PCR. The graph is presented in log2 values and 1.0 represents average of normal subjects ($n = 15$). There was a significant downregulation of miR-200c in all 29 PC patients compared with normal subjects.

compared with controls. Similarly two of the three oncogenic miRNAs were significantly upregulated relative to controls. However, tumour-suppressor miRNA let-7d and oncogenic miRNA miR-423-5p showed differential expression in patients with PC.

DISCUSSION

The understanding of biological functions of miRNAs in patients with PC will significantly help the development of new targeted anticancer drugs and testing of novel therapies. Most investigators

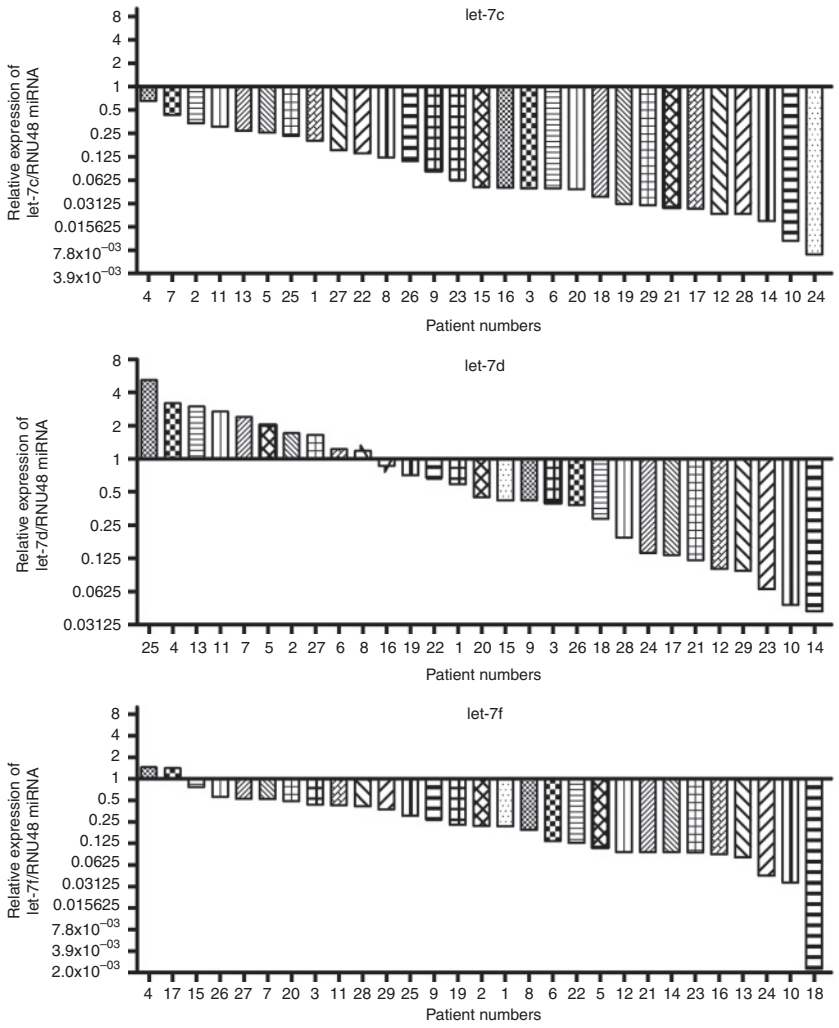

Figure 4 Comparative expression analysis of let-7c, let-7d, and let-7f in 29 FNA cell blocks from PC patients analysed individually compared with FNA cell blocks obtained from 15 normal controls by using qRT–PCR. The graph is presented in log2 values and 1.0 represents average of normal subjects ($n = 15$). The results showed a significant decrease in the expression of let-7c, and let-7f in almost all PC patients compared with normal subjects. In contrast, the expression level of let-7d showed a differential expression between samples in PC patients.

agree that miRNA expression profiling is an accurate method for the analysis of archived surgical specimens from tumours including PC (Li *et al*, 2007; Doleshal *et al*, 2008; Szafranska *et al*, 2008a; Goswami *et al*, 2010). We previously identified miRNA expression from plasma samples that were characteristic of PCs (Ali *et al*, 2010b). The primary objective of this study was to determine the feasibility of performing miRNA arrays and qRT–PCR from FFPE cell blocks obtained from diagnostic FNAs.

To the best of our knowledge this is the first study to determine miRNA expression from FNAs of FFPE cell blocks in patients with PC. We found 228 miRNAs that were differentially expressed in the PC patients compared with normal controls. Consistent with published literature using surgical specimens, we found higher expression of miR-451 and miR-486-5p, and lower expression of let-7c, let-7d, let-7f, and miR-200c in the FNA samples of PC patients. Further analyses revealed marked downregulation of the let-7 family that is well known for its tumour suppressive characteristics and consistent with previous independent studies showing that let-7 is underexpressed in PC (Li *et al*, 2009; Torrisani *et al*, 2009; Watanabe *et al*, 2009; Oh *et al*, 2010; Ngi-Garimella *et al*, 2011). We confirmed the expression of let-7c, let-7d, and let-7f in PC individually and compared with controls by qRT–PCR. We found that the expression of let-7c and let-7f was significantly reduced in all PC specimens, whereas the expression of let-7d was differentially expressed between these samples.

Emerging evidence indicates that EMT has a crucial role in cancer progression and drug resistance and is associated with loss of miR-200c expression (Burk *et al*, 2008; Li *et al*, 2009; Wellner *et al*, 2009; Yu *et al*, 2010). A recent study from our group showed that re-expression of miR-200 suppressed pulmonary metastases of breast cancer cells *in vivo*, whereas anti-miR-200 treatment *in vivo* resulted in increased metastases (Ahmad *et al*, 2011). Here, we report that the expression of miR-200c is significantly reduced in all PC patients tested compared with controls. In addition to downregulated miRNAs in PC, our results also demonstrated a significant upregulation of miR-486-5p, miR-451, and miR-423-5p. These findings are in concordance with the findings of another recent study in gastric cancer where a significant increase in serum miR-423-5p was demonstrated by Solexa sequencing. Furthermore, miR-423-5p expression level showed a substantial increase in patients with metastatic disease compared with those with stages I or II (Liu *et al*, 2011).

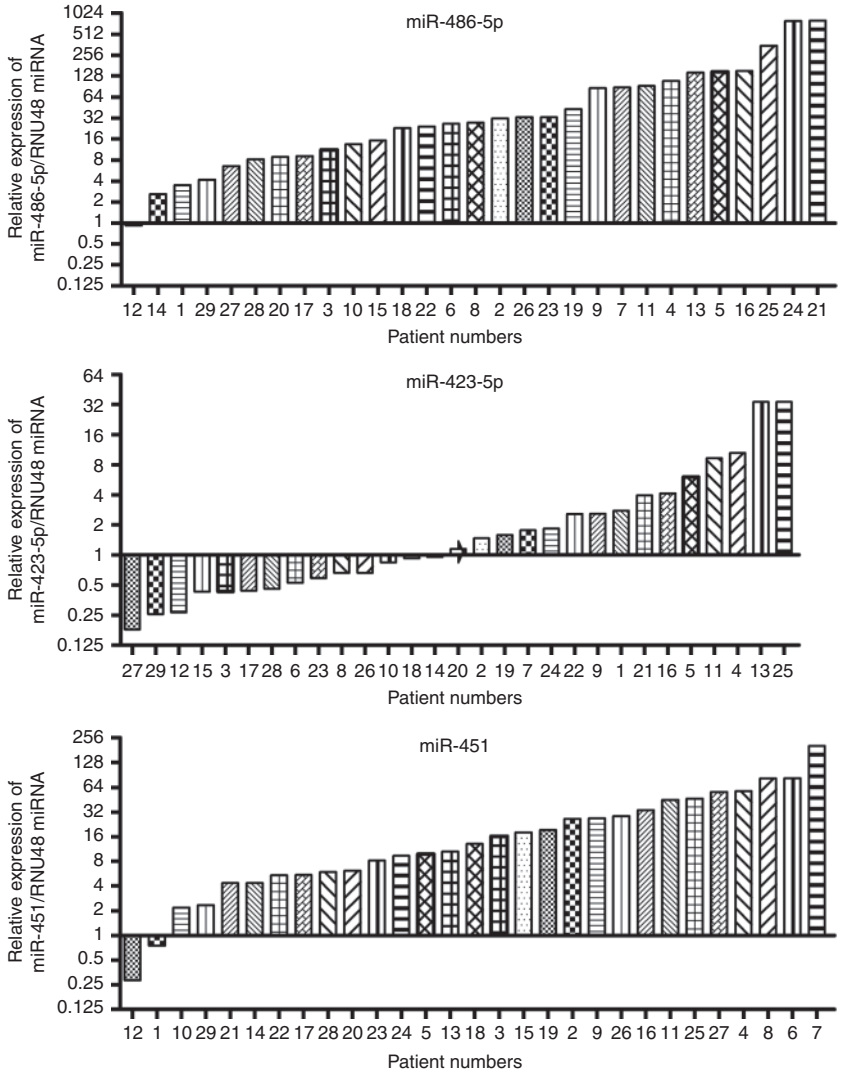

Figure 5 Comparative expression analysis of miR-486-5p, miR-423-5p, and miR-451 in 29 FNA cell blocks from PC patients analysed individually compared with FNA cell blocks obtained from 15 normal controls by using qRT–PCR. The graph is presented in log2 values and 1.0 represents average of normal subjects ($n = 15$). The results showed a significant increase in the expression of miR-486-5p, and miR-451 in almost all PC patients compared with normal subjects. In contrast, the expression level of miR-423-5p showed a differential expression between samples in PC patients.

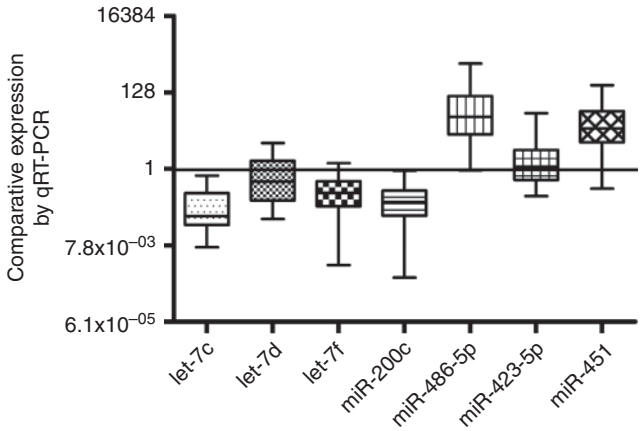

Figure 6 Box plot representing the expression of 7 miRNAs as assessed by qRT–PCR in 29 FNA cell blocks from PC patients analysed individually compared with FNA cell blocks obtained from 15 normal controls by using qRT–PCR. The graph is presented in log2 values and 1.0 represents average of normal subjects ($n = 15$).

It is obvious that with a molecularly very complex disease such as pancreatic adenocarcinoma a single gene product or pathway is unlikely neither to be a robust target for therapy nor to predict biology of disease. A systems biology approach provides a unique strategy to study networks of molecular events that drive various signalling pathways resulting from the deregulations of miRNAs (Azmi *et al*, 2011). The miRNAs and their targets are arranged in complex regulatory networks (Figures 1 and 2), but as the functional roles of miRNAs in PC are better defined, it will improve the sub-classification of PC with respect to prognosis and patterns of response to specific therapies.

In conclusion, this study demonstrates the feasibility of undertaking analyses of miRNAs in very small diagnostic specimens from FNAs of PC that may provide an invaluable research tool to individualise therapy and develop rationally based targeted therapies. Moreover, a unique group of miRNAs were identified that can serve as a tool for investigating the biology of PC with respect to prognosis and response to therapy at the individual level. Prospective clinical trials will be needed to better understand the functions of these miRNAs. The role of miRNAs may also be extended to *in vivo* monitoring of targeted therapies.

ACKNOWLEDGEMENTS

We sincerely thank the Guido and Puschelberg Foundation for providing some financial support to complete our study. We also acknowledge the financial support provided through R01 grant funding from the National Cancer Institutes, National Institute of Health, awarded to FHS (5R01CA131151, 3R01CA131151-02S1, 5R01CA132794, and 1R01CA154321).

Supplementary Information accompanies the paper on British Journal of Cancer website (http://www.nature.com/bjc)

REFERENCES

Ahmad A, Aboukameel A, Kong D, Wang Z, Sethi S, Chen W, Sarkar FH, Raz A (2011) Phosphoglucose isomerase/autocrine motility factor mediates epithelial-mesenchymal transition regulated by miR-200 in breast cancer cells. *Cancer Res* **71**(9): 3400–3409

Ali S, Ahmad A, Banerjee S, Padhye S, Dominiak K, Schaffert JM, Wang Z, Philip PA, Sarkar FH (2010a) Gemcitabine sensitivity can be induced in pancreatic cancer cells through modulation of miR-200 and miR-21 expression by curcumin or its analogue CDF. *Cancer Res* **70**(9): 3606–3617

Ali S, Almhanna K, Chen W, Philip PA, Sarkar FH (2010b) Differentially expressed miRNAs in the plasma may provide a molecular signature for aggressive pancreatic cancer. *Am J Transl Res* **3**(1): 28–47

Azmi AS, Ali S, Banerjee S, Bao B, Maitah MN, Padhye S, Philip PA, Mohammad RM, Sarkar FH (2011) Network modeling of CDF treated pancreatic cancer cells reveals a novel c-myc-p73 dependent apoptotic mechanism. *Am J Transl Res* **3**(4): 374–382

Bao B, Ali S, Kong D, Sarkar SH, Wang Z, Banerjee S, Aboukameel A, Padhye S, Philip PA, Sarkar FH (2011a) Anti-tumor activity of a novel compound-CDF is mediated by regulating miR-21, miR-200, and PTEN in pancreatic cancer. *PLoS One* **6**(3): e17850

Bao B, Wang Z, Ali S, Kong D, Banerjee S, Ahmad A, Li Y, Azmi AS, Miele L, Sarkar FH (2011b) Over-expression of FoxM1 leads to epithelial-mesenchymal transition and cancer stem cell phenotype in pancreatic cancer cells. *J Cell Biochem* **112**(9): 2296–2306

Bournet B, Pointreau A, Souque A, Oumouhou N, Muscari F, Lepage B, Senesse P, Barthet M, Lesavre N, Hammel P, Levy P, Ruszniewski P, Cordelier P, Buscail L (2012) Gene expression signature of advanced pancreatic ductal adenocarcinoma using low density array on endoscopic ultrasound-guided fine needle aspiration samples. *Pancreatology* **12**(1): 27–34

Burk U, Schubert J, Wellner U, Schmalhofer O, Vincan E, Spaderna S, Brabletz T (2008) A reciprocal repression between ZEB1 and members of the miR-200 family promotes EMT and invasion in cancer cells. *EMBO Rep* **9**(6): 582–589

Chen Y, Zheng B, Robbins DH, Lewin DN, Mikhitarian K, Graham A, Rumpp L, Glenn T, Gillanders WE, Cole DJ, Lu X, Hoffman BJ, Mitas M (2007) Accurate discrimination of pancreatic ductal adenocarcinoma and chronic pancreatitis using multimarker expression data and samples obtained by minimally invasive fine needle aspiration. *Int J Cancer* **120**(7): 1511–1517

Doleshal M, Magotra AA, Choudhury B, Cannon BD, Labourier E, Szafranska AE (2008) Evaluation and validation of total RNA extraction methods for microRNA expression analyses in formalin-fixed, paraffin-embedded tissues. *J Mol Diagn* **10**(3): 203–211

Goswami RS, Waldron L, Machado J, Cervigne NK, Xu W, Reis PP, Bailey DJ, Jurisica I, Crump MR, Kamel-Reid S (2010) Optimization and analysis of a quantitative real-time PCR-based technique to determine microRNA expression in formalin-fixed paraffin-embedded samples. *BMC Biotechnol* **10**: 47

Hurteau GJ, Carlson JA, Roos E, Brock GJ (2009) Stable expression of miR-200c alone is sufficient to regulate TCF8 (ZEB1) and restore E-cadherin expression. *Cell Cycle* **8**(13): 2064–2069

Jemal A, Siegel R, Xu J, Ward E (2010) Cancer statistics, 2010. *CA Cancer J Clin* **60**(5): 277–300

Li J, Smyth P, Flavin R, Cahill S, Denning K, Aherne S, Guenther SM, O'leary JJ, Sheils O (2007) Comparison of miRNA expression patterns using total RNA extracted from matched samples of formalin-fixed paraffin-embedded (FFPE) cells and snap frozen cells. *BMC Biotechnol* **7**: 36

Li Y, Vandenboom TG, Kong D, Wang Z, Ali S, Philip PA, Sarkar FH (2009) Up-regulation of miR-200 and let-7 by natural agents leads to the reversal of epithelial-to-mesenchymal transition in gemcitabine-resistant pancreatic cancer cells. *Cancer Res* **69**(16): 6704–6712

Liu R, Zhang C, Hu Z, Li G, Wang C, Yang C, Huang D, Chen X, Zhang H, Zhuang R, Deng T, Liu H, Yin J, Wang S, Zen K, Ba Y, Zhang CY (2011) A five-microRNA signature identified from genome-wide serum microRNA expression profiling serves as a fingerprint for gastric cancer diagnosis. *Eur J Cancer* **47**(5): 784–791

Ngi-Garimella S, Strouch MJ, Grippo PJ, Bentrem DJ, Munshi HG (2011) Collagen regulation of let-7 in pancreatic cancer involves TGF-beta1-mediated membrane type 1-matrix metalloproteinase expression. *Oncogene* **30**(8): 1002–1008

Oh JS, Kim JJ, Byun JY, Kim IA (2010) Lin28-let7 modulates radiosensitivity of human cancer cells with activation of K-Ras. *Int J Radiat Oncol Biol Phys* **76**(1): 5–8

Sarkar FH, Li Y, Wang Z, Kong D, Ali S (2010) Implication of microRNAs in drug resistance for designing novel cancer therapy. *Drug Resist Updat* **13**(3): 57–66

Szafranska AE, Davison TS, Shingara J, Doleshal M, Riggenbach JA, Morrison CD, Jewell S, Labourier E (2008a) Accurate molecular characterization of formalin-fixed, paraffin-embedded tissues by microRNA expression profiling. *J Mol Diagn.* **10**(5): 415–423

Szafranska AE, Doleshal M, Edmunds HS, Gordon S, Luttges J, Munding JB, Barth RJ Jr, Gutmann EJ, Suriawinata AA, Marc Pipas J, Tannapfel A, Korc M, Hahn SA, Labourier E, Tsongalis GJ (2008b) Analysis of microRNAs in pancreatic fine-needle aspirates can classify benign and malignant tissues. *Clin Chem.* **54**(10): 1716–1724

Takamizawa J, Konishi H, Yanagisawa K, Tomida S, Osada H, Endoh H, Harano T, Yatabe Y, Nagino M, Nimura Y, Mitsudomi T, Takahashi T (2004) Reduced expression of the let-7 microRNAs in human lung cancers in association with shortened postoperative survival. *Cancer Res* **64**(11): 3753–3756

Torrisani J, Bournet B, Du Rieu MC, Bouisson M, Souque A, Escourrou J, Buscail L, Cordelier P (2009) let-7 MicroRNA transfer in pancreatic cancer-derived cells inhibits *in vitro* cell proliferation but fails to alter tumor progression. *Hum Gene Ther* **20**(8): 831–844

Touchefeu Y, Le RM, Coron E, Alamdari A, Heymann MF, Mosnier JF, Matysiak T, Galmiche JP (2009) Endoscopic ultrasound-guided fine-needle aspiration for the diagnosis of solid pancreatic masses: the impact on patient-management strategy. *Aliment Pharmacol Ther* **30**(10): 1070–1077

Wang Z, Li Y, Ahmad A, Azmi AS, Kong D, Banerjee S, Sarkar FH (2010) Targeting miRNAs involved in cancer stem cell and EMT regulation: an emerging concept in overcoming drug resistance. *Drug Resist Updat* **13**(4-5): 109–118

Watanabe S, Ueda Y, Akaboshi S, Hino Y, Sekita Y, Nakao M (2009) HMGA2 maintains oncogenic RAS-induced epithelial-mesenchymal transition in human pancreatic cancer cells. *Am J Pathol* **174**(3): 854–868

Wellner U, Schubert J, Burk UC, Schmalhofer O, Zhu F, Sonntag A, Waldvogel B, Vannier C, Darling D, Zur HA, Brunton VG, Morton J, Sansom O, Schuler J, Stemmler MP, Herzberger C, Hopt U, Keck T, Brabletz S, Brabletz T (2009) The EMT-activator ZEB1 promotes tumorigenicity by repressing stemness-inhibiting microRNAs. *Nat Cell Biol* **11**(12): 1487–1495

Yu J, Ohuchida K, Mizumoto K, Sato N, Kayashima T, Fujita H, Nakata K, Tanaka M (2010) MicroRNA, hsa-miR-200c, is an independent prognostic factor in pancreatic cancer and its upregulation inhibits pancreatic cancer invasion but increases cell proliferation. *Mol Cancer* **9**: 169

British Journal of Cancer (2012) 107, 1169–1174

www.bjcancer.com

The prognostic importance of miR-21 in stage II colon cancer: a population-based study

S Kjaer-Frifeldt*[,1,2], TF Hansen[1], BS Nielsen[3], S Joergensen[3], J Lindebjerg[4], FB Soerensen[2,4], R dePont Christensen[2] and A Jakobsen[1,2] on behalf of Danish Colorectal Cancer Group

[1]Department of Oncology, Danish Colorectal Cancer Group South, Vejle Hospital, Kabbeltoft 25, Vejle, Denmark; [2]University of Southern Denmark, Odense, Denmark; [3]Diagnostic Product Development, Exiqon A/S, Skelstedet 16, Vedbæk 2950, Denmark; [4]Department of Clinical Pathology, Vejle Hospital, Vejle, Denmark

BACKGROUND: Despite several years of research and attempts to develop prognostic models a considerable fraction of stage II colon cancer patients will experience relapse within few years from their operation. The aim of the present study was to investigate the prognostic importance of miRNA-21 (miR-21), quantified by *in situ* hybridisation, in a unique, large population-based cohort.
PATIENTS AND METHODS: The study included 764 patients diagnosed with stage II colon cancer in Denmark in the year 2003. One section from a representative paraffin-embedded tumour tissue specimen from each patient was processed for analysis of miR-21 and quantitatively assessed by image analysis.
RESULTS: The miR-21 signal was predominantly observed in fibroblast-like cells located in the stromal compartment of the tumours. We found that patients expressing high levels of miR-21 had significantly inferior recurrence-free cancer-specific survival (RF-CSS): HR = 1.26; 95% CI: 1.15–1.60; $P < 0.001$. In Cox regression analysis, a high level of miR-21 retained its prognostic importance and was found to be significantly related to poor RF-CSS: HR = 1.41; 95% CI: 1.19–1.67; $P < 0.001$.
CONCLUSION: The present study showed that increasing miR-21 expression levels were significantly correlated to decreasing RF-CSS. Further investigations of the clinical importance of miR-21 in the selection of high-risk stage II colon cancer patients are merited.
British Journal of Cancer (2012) **107,** 1169–1174. doi:10.1038/bjc.2012.365 www.bjcancer.com

Keywords: colon cancer; miRNA-21; population study; prognostic marker; stage II

Colon cancer represents a major challenge all over the Western World (Parkin *et al*, 2005). The incidence has been increasing for decades but screening holds the promise of a shift in distribution towards earlier stages (Gross *et al*, 2006). Surgery is a cornerstone in the treatment, but with operation alone a considerable fraction of patients will experience tumour recurrence, calling for adjuvant chemotherapy. Stage II (no lymph node metastases or distant metastases) patients represent about 25% of all cases and they have a 5-year overall survival (OS) of 73–85%, when surgically resected (O'Connell, 2004).

There is a general agreement on postoperative chemotherapy for stage III colon cancer patients, but there is still a debate on this approach for patients with stage II tumours. Meta-analyses, reviews and international guidelines agree that adjuvant chemotherapy should be offered to a subgroup of patients with high risk of recurrence, including T4 and T3 tumours with lymphovascular invasion, high malignancy grade, perforation and/or inadequate lymph node sampling (Benson III *et al*, 2004; Figueredo *et al*, 2008; Kopetz *et al*, 2008; Bastos *et al*, 2010; Gangadhar and Schilsky, 2010; Lombardi *et al*, 2010). Interestingly, the recent CALBG 9581 study of 24 000 stage II patients from the Medicare Registry found no improvement in 5-year survival in patients receiving adjuvant chemotherapy, irrespective of a division of patients into two groups with high- or low-risk characteristics (O'Connor *et al*, 2011). These results question the current clinical practice and underline the urgent need of new and reliable prognostic and predictive markers in stage II colon cancer.

MicroRNAs (miRNAs) comprise an abundant class of endogenous, small non-coding RNAs, 18–25 nucleotides in length, which regulates protein synthesis at the post-transcriptional level. MicroRNAs are highly conserved in sequence between distantly related organisms, indicating their participation in essential biological processes (Carrington and Ambros, 2003). Abnormal expression of cancer-related miRNAs is characterised by increased or decreased expression levels compared with their levels in the corresponding normal tissue. The miRNA-21 (miR-21) is consistently upregulated in many types of cancers including cancer of the colon (Slaby *et al*, 2007; Schetter *et al*, 2008), breast (Yan *et al*, 2008; Qian *et al*, 2009), lung (Markou *et al*, 2008), stomach (Chan *et al*, 2008) and glioblastoma (Gabriely *et al*, 2008). Among the reported mRNA targets of miR-21 are PTEN, PDCD4, Spry-1 and NF1B, suggesting that miR-21 is involved in regulation of apoptosis, proliferation and migration (Meng *et al*, 2007; Asangani *et al*, 2008; Gabriely *et al*, 2008; Yao *et al*, 2011). Additionally, miR-21 levels seem to increase with increasing stage of the tumour in, for example, colon and breast cancer, suggesting an important role of miR-21 in cancer invasion and dissemination (Slaby *et al*, 2007; Yan *et al*, 2008; Qian *et al*, 2009). These data taken together strongly suggest miR-21 as a potential prognostic marker in early-stage cancer such as stage II colon cancer. Studies have found high levels of miR-21 in colorectal cancer patients to be

*Correspondence: Dr S Kjaer-Frifeldt;
E-mail: Sanne.Kjaer.Frifeldt@slb.regionsyddanmark.dk
Received 12 April 2012; revised 19 July 2012; accepted 23 July 2012

an indicator of poor prognosis, but so far none have been population based (Slaby *et al*, 2007; Schetter *et al*, 2008; Nielsen *et al*, 2011).

Most studies quantifying miRNAs for identification of differential expression have been based on microarrays (Lim *et al*, 2005), real-time PCR (RT-PCR) (Bandres *et al*, 2006) and deep sequencing (Ferdin *et al*, 2010). These quantitative miRNA expression analysis platforms are strong quantitative tools with a high level of precision and reproducibility and have been used to identify valuable biomarker candidates. However, important clinical information may be lost when focal miRNA expression is masked by non-cancerous tissue present in the samples, such as normal mucosa, submucosa and muscularis externa, mucous and necrotic tissue (Bandres *et al*, 2006). Additionally, RNA extraction from formalin-fixed paraffin-embedded (FFPE) tissue blocks is both time-consuming and suboptimal. Current pathological practice is based on FFPE tissue blocks, and the vast majority of archival material is preserved as such. Therefore, new methods should be considered. Recently, it has been reported that *in situ* hybridisation (ISH) using locked nucleic acid (LNA) modified DNA probes, raise the potential of evaluating tissue morphology and to quantitatively assess the miR-21 signal (Nielsen *et al*, 2011; Rask *et al*, 2011). The study by Nielsen *et al* also addressed the prognostic information of miR-21 expression and found that high miR-21 level was associated with poor disease-free survival. However, the patient material was limited (Nielsen *et al*, 2011).

The aim of the present study was to further investigate the prognostic importance of miR-21, quantified by ISH, in a unique, large, homogeneous, population-based cohort consisting of all patients with stage II colon cancer diagnosed and treated exclusively by surgical resection in Denmark in the year 2003.

PATIENTS AND METHODS

Patients

The study population was retrieved by a search in the nationwide registry administered by the Danish Colorectal Cancer Group (DCCG). This database contains prospectively collected surgical and pathological data. The search identified all surgically treated patients diagnosed with stage II colon cancer in 2003 ($N=764$). Patients dying within 30 days from their operation were excluded ($N=66$). All but two hospitals participated in the study and hence patients from those hospitals were not included ($N=56$), thus creating a highly representative cohort (93%) of the Danish population of stage II colon cancer patients in 2003. Furthermore, there were the following exclusions: tumour samples missing in archives ($N=23$); patients being categorised wrongly as stage II colon cancer ($N=14$); patients receiving adjuvant chemotherapy ($N=16$); lack of sufficient tissue for analysis ($N=7$); analysis exclusion criteria regarding number of images acquired <8 ($N=41$) and TR values $<20\,000$ ($N=21$), see below. Thus, 520 patients were included in the statistical analysis. The study was approved by the Regional Scientific Ethical Committee of Southern Denmark according to Danish law. Postoperatively, patients were followed by the treating departments according to local guidelines. The patients were not routinely referred to a Department of Oncology. Thus, the majority of data on recurrence and death were obtained through Danish registries linked to the Danish social security number given to every Danish citizen at birth and to all ethnic immigrants.

The national registry holding all pathology reports in Denmark was used to identify patients with pathologically verified recurrence. Patients experiencing other malignancies were also identified using this registry and subsequently censored from survival analysis on the date of their new cancer diagnosis. To identify patients who had been in contact with the Department of Oncology or who had died, the national registry recording status on all Danish citizens as to their contact to the healthcare system and date of death was used. Patients with non-pathologically verified recurrence and patients receiving adjuvant chemotherapy were found by evaluating patient charts in the Departments of Oncology. A search in the 'Cause of Death Registry' identified patients registered with colon cancer as the cause of death. Follow-up was closed at 1 January 2010. From the study population of 520 patients, we identified the following: 206 patients had died and 73 patients had experienced disease recurrence. According to the registries, 90 patients had died from colon cancer, only 53 of these patients were also identified as having disease recurrence and in the analysis of recurrence-free cancer-specific survival (RF-CSS) events on the remaining 20 patients were added giving 110 events. The date registered was the first coming event of either disease recurrence or death from colon cancer. We also identified 16 patients who had received adjuvant chemotherapy and 23 patients who had been diagnosed with another cancer.

Pathology

One FFPE tissue block representing the invasive front of the tumour of each patient was collected from the Departments of Pathology in Denmark. Information on T-category, malignancy grade, nerve- and vascular-invasion, and the number of lymph nodes assessed was obtained from the pathology reports. Patients were scored as 'not assessed' if the pathological feature was not described. Data on localisation, tumour perforation, and tumour fixation was obtained from the DCCG registry and based on the surgeons' reports.

In situ hybridisation

In situ hybridisation was performed essentially as described previously (Nielsen *et al*, 2011). In brief, the single 6-μm section from each tumour was processed in a Tecan Evo (Männedorf, Switzerland) automated ISH instrument. Predigestion with proteinase-K (15 $\mu g\,ml^{-1}$) was performed at 37°C for 8 min. After pre-hybridisation for 15 min in hybridisation buffer (Exiqon, Vedbaek, Denmark), double-digoxigenin labelled 22'mer LNA probe specific for full-length miR-21 (Exiqon) was incubated at 30 nM for 1 h at 59°C. SSC stringent washes were performed at 59°C. Probe was detected with alkaline phosphatase-conjugated Fab fragments diluted 1 : 800 (Roche, Mannheim, Germany), followed by 1 h incubation with NBT-BCIP substrate (Roche). Sections were dehydrated and mounted using Eukitt (VWR, Herlev, Denmark). All reagents, including the proteinase-K, the DIG-labelled probe and the anti-DIG antibody were from the same batch and prepared identically each day. All steps in the Tecan were controlled regarding volumes, temperature and time.

Image analysis

Quantification of relative expression levels was obtained essentially as described earlier (Nielsen, 2012). In brief, the tumour area was identified on overview images and digitally selected as a region of interest. The areas containing normal mucosa and submucosa and ulcerating areas were not included. Within the selected area, 25 random images were collected per slide using a $\times 20$ objective. Exposure of sample images was strictly controlled and locked at 6.993 ms with RGB (red–green–blue) values at 170–180 in non-stained blank areas. Sample images with staining artifacts were discarded, as were also images with $<10\%$ cancer cells in the image field. Thus, all images contained both cancer cells and stromal cells. A Bayesian pixel classifier to discriminate blue (B, ISH signal), red (R, nuclear counter stain), purple (P, blue ISH signal overlaying nuclear stain) and tissue background was designed based on three images from three different tumours that

represented variations in blue and red colour. The following parameters were obtained for each sample image; B, R, P, total blue (TB = B + P), total red (TR = R + P) and TBR = TB/TR.

Series of 50 slides were analysed and included two control slides in each series to obtain a precision estimate of the measurements. The series also included replicates of adjacent sections obtained from three tumours (CV < 49%). The variation of TBR between individuals was 215%, indicating that the precision of the measurements was sufficiently high to justify statistical analyses (25).

A test run, using four sections from each of 12 tumours was performed to adjust the probe concentration and the hybridisation temperature for optimal signal intensity.

Statistical analysis

Overall survival was defined as time from surgery until death from any cause. Recurrence-free cancer-specific survival (RF-CSS) was defined as the time from surgery until documented tumour recurrence or death from colon cancer, death from other causes was censored and also patients diagnosed with other malignancies were censored from the date of their new cancer diagnosis. Survival was estimated according to the Kaplan–Meier method, and the log-rank test was used to test for differences among groups. The Cox regression model was used to adjust for known prognostic factors; Gender, age, T-category, malignancy grade, localisation, perforation, fixation and number of lymph nodes (dichotomized into above and under 12). The proportional hazard assumption was tested for all variables used in the Cox model, using Schoenfeld residuals. All statistical calculations were carried out using the STATA 11.0 (StataCorp LP, College Station, TX, USA), and all statistical tests were two-sided with a significance level of 0.05.

By visual inspection of the relevant qq-plots, the log-transformed miR-21 values (TB and TBR) followed normal distributions.

RESULTS

Patient characteristics

Patient characteristics are presented in Table 1. The majority of the patients were female patients with a medium differentiated T3 tumour. Location of the tumours was evenly distributed between left (left flexure, descendent, sigmoid) and right colon (coecum, ascendant, right flexure, transverse). Owing to the low number and uncertainty of the low malignancy grade classification, tumours of low and medium malignancy were pooled together in the survival analysis. No significant associations were found between miR-21 expression and patient characteristics.

Localisation of miR-21 ISH signal

The miR-21 ISH signal intensity and prevalence varied considerably within the tumours and between patients, and it was predominantly seen in fibroblastic stromal cells (Figure 1C). We found that miR-21 was predominantly expressed in fibroblast-like cells in the stromal compartment of the tumour. In a smaller fraction of the samples (10–20%) some miR-21-positive cancer cells were also seen (Figure 1F), and in these cases only sub-populations of cancer cells were miR-21 positive. The miR-21-positive cancer cells also included budding cancer cells. The intensity varied from patient to patient and locally within the tumour slide. The miR-21 expression pattern was characterised by intense expression in the tumour area in contrast to the normal mucosa, where weakly stained mononuclear cells were observed.

Table 1 Patient characteristics of the study population (all excluded patients have been subtracted)

Parameter	Number of patients
Study population	520
Gender	
Male	231 (44.4%)
Female	289 (55.6%)
Age (years)	
Median	71.9
Range	33–95
T-category	
3	454 (87.3%)
4	66 (12.7%)
Malignancy grade	
Low	34 (6.5%)
Medium	391 (75.2%)
High (including mucinous, signet)	95 (18.3%)
Localisation[a]	
Right	269 (51.7%)
Left	251 (48.3%)
Tumour perforation	45 (8.7%)
Tumour fixation	93 (17.9%)
Lymph nodes	
Median	11.3
Range	0–40
Nerve invasion	
Yes	34 (6.5%)
No	360 (69.2%)
Not assessed	126 (24.2%)
Vascular invasion	
Yes	30 (5.8%)
No	372 (71.5%)
Not assessed	118 (22.7%)

Information on T-category and malignancy grade was obtained from HE-stained sections. Nerve and vascular invasion was obtained from the pathology reports and was scored 'not assessed' when the histopathological feature was not described.
[a]Left = left flexur, descendens, sigmoideum; right = coecum, ascendens, right flexur, transversum.

Quantification of miR-21 ISH signal

To quantify the ISH signal in the tissue sections, systematic random non-overlapping image fields were compiled from each tumour section. A mean of 16 image fields (range: 8–26) were compiled from each tumour. If the number of image fields was less than eight for one tumour section, the patient was excluded from the statistical analyses. All image fields that passed the inclusion criteria (see Patients and Methods) were processed with a pixel classifier that discriminated the blue ISH signal (B), the red nuclear stain (R), the blue signal located over red nuclear stain (P) and all other tissue structures (see Figures 1C and F). Total blue area (TB = B + P), total red area (TR = R + P) and total blue area per total red area (TBR = TB/TR) were obtained of which the TB and TBR values represent estimates of miR-21 expression, and TR the overall nuclear density. Sections cut too thin, samples fixed inadequately and tumours with poor cell density (prevalent in mucinous lesions) generally had low TR, and cases with TR $< 20\,000\ \mu m^2$ were excluded, see patients paragraph. As expected, substantial variation of both TB and TBR was observed; TB range = 23.61–185 274 μm^2; TBR range = 0.0001814–13.085, as

Epidemiology

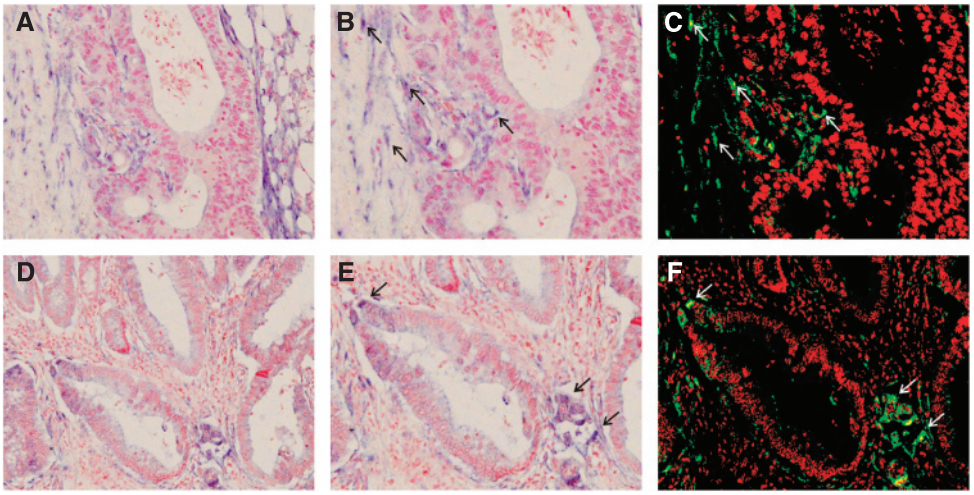

Figure 1 Localisation and image analysis of miR-21 *in situ* hybridisation signal in colon cancer. Paraffin sections from two representative colon cancers (**A**–**C** and **D**–**F**) stained for miR-21 using LNA-based *in situ* hybridisation. The images, **A** and **D**, are selected random images obtained with a ×20 objective. A selected area in **A** and **D** has been enlarged in **B** and **E**, and is presented after colour segmentation in **C** and **F**. The miR-21 *in situ* hybridisation signal (blue, examples indicated by arrows in **B** and **C**) is seen in tumour-associated stromal fibroblast-like cells (**B**, arrows) in virtually all colon tumours, whereas miR-21 signal in cancer cells (**E**, arrows) was less frequently seen. For quantitation of the *in situ* hybridisation signal, the blue and purple stain in **A**/**B** and **D**/**E** are translated into green and yellow pixels in **C** and **F**. The nuclear red counterstain is likewise translated into red and the tissue background into black in **C** and **F**. Bars are 50 μm.

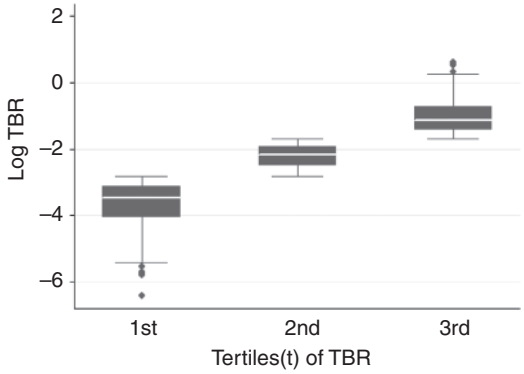

Figure 2 Box-plot of miR-21 expression levels in patients divided into tertiles of log(TBR). Substantial variation of both TB and TBR was observed; TB range = 23.61–185 274 μm^2; TBR range = 0.0001814–13.085.

illustrated in Figure 2 where patients were divided into tertiles according to their mean log(TBR) value.

The prognostic value of miR-21

Results from the log-rank analysis of mean log(TBR) are listed in Table 2. Patients expressing high levels of miR-21 (high mean log(TBR)) had significantly inferior RF-CSS (HR = 1.26; 95% CI: 1.15–1.60; $P<0.001$), and the same applied to mean log(TB) (HR = 1.12; 95% CI: 1.0–1.42; $P=0.05$). Proportional hazard assumptions were tested for all variables. Results from the multiple Cox regression are outlined in Table 3 and included age, gender, T-category, malignancy grade, localisation, tumour perforation, tumour fixation and number of lymph nodes. Mean log(TBR) was found to be an independent predictive marker of poor RF-CSS (HR = 1.41; 95% CI: 1.19–1.67; $P<0.001$), and the same applied to high levels of mean log(TB) ($P=0.018$). In addition to mean log(TBR), the following parameters were found to be predictive of a poor outcome regarding RF-CSS in the Cox regression analysis: male gender ($P=0.033$), T4-category ($P<0.001$), and tumour perforation ($P<0.001$). In the Cox regression analysis of OS, the following parameters were found to be prognostic of a poorer outcome; increasing age ($P<0.001$), male gender ($P<0.001$) and T4-category ($P=0.017$). We did not find any significant relation between miR-21 expression and OS.

Vascular and nerve invasion were not described in a large fraction of the patients (22.7% and 24.2%, respectively). Thus, the Cox regression analysis was only performed with respect to these two pathological features in the limited subsets of patients. However, high levels of mean log(TBR) was consistently found

Table 2 Log-rank test on OS and RF-CSS related to log-transformed mean values of log(TBR)

	OS		RF-CSS	
	Hazard ratio (95% CI)	***P*-value**	**Hazard ratio (95% CI)**	***P*-value**
Mean log(TBR)	1.05 (0.94–1.18)	0.38	1.26 (1.15–1.60)	**<0.001**

Abbreviations: OS = overall survival; RF-CSS = recurrence-free cancer-specific survival. *P* value <0.001 is indicated in bold.

Table 3 Cox regression analysis on OS and RF-CSS related to log-transformed mean log(TBR), including gender, T-category, malignancy grade, localisation, tumour perforation, tumour fixation and number of lymph nodes

	OS		RF-CSS	
	Hazard ratio (95% CI)	***P*-value**	**Hazard ratio (95% CI)**	***P*-value**
Mean log(TBR)	1.08 (0.97–1.22)	0.17	1.41 (1.19–1.67)	**<0.001**
Age	1.06 (1.04–1.07)	**<0.001**	1.02 (1.00–1.04)	0.055
Male gender	1.81 (1.36–2.42)	**<0.001**	1.54 (1.04–2.29)	0.033
T4-category	1.59 (1.09–2.32)	0.017	2.51 (1.58–3.97)	**<0.001**
Left localisation	0.93 (0.70–1.25)	0.64	1.04 (0.69–1.55)	0.87
Perforation	1.57 (0.99–2.49)	0.056	2.69 (1.56–4.63)	**<0.001**
Fixation	1.41 (0.98–2.04)	0.064	1.41 (0.86–2.32)	0.17
Lymph nodes ⩾12	1.03 (0.78–1.37)	0.84	0.93 (0.64–1.38)	0.74
High malignancy grade	1.24 (0.87–1.77)	0.24	1.54 (0.95–2.50)	0.08

Abbreviations: CI = confidence interval; OS = overall survival; RF-CSS = recurrence-free cancer-specific survival. *P* values <0.001 are indicated in bold.

Epidemiology

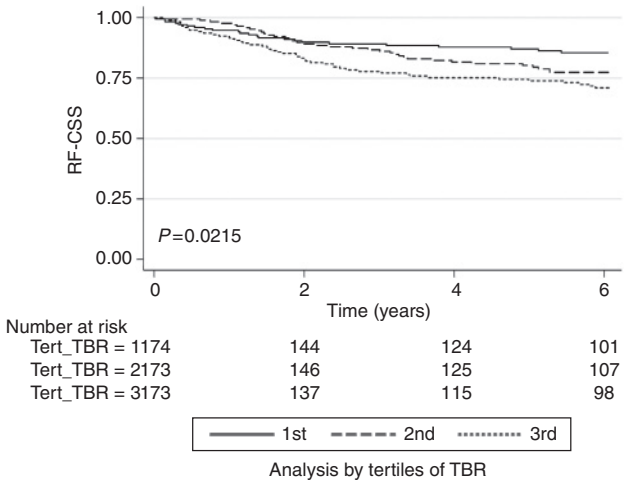

Figure 3 Kaplan–Meier plot illustrating recurrence-free cancer-specific survival (RF-CSS) of the patients divided into tertiles of log(TBR). Patients with mean log(TBR) values in the upper tertile had significantly shorter RF-CSS (HR = 1.92; 95% CI: 1.19–3.09; $P = 0.008$) compared with patients with mean log(TBR) values in the lower tertile.

to be significantly related to poor RF-CSS (HR = 1.52; 95% CI: 1.23–1.88; $P < 0.001$). The same applied to log(TB) ($P = 0.008$).

To illustrate the effect of increasing mean log(TBR), the population cohort was stratified into tertiles according to their mean log(TBR) value. As illustrated in Figure 3, patients with mean log(TBR) values in the upper tertile had significantly shorter RF-CSS (HR = 1.92; 95% CI: 1.19–3.09; $P = 0.008$) compared with patients with mean log(TBR) values in the lower tertile.

DISCUSSION

At present, the decision on adjuvant chemotherapy for stage II colon cancer patients is based on clinical and pathological markers of risk, which are inadequately informative in most of the patients, and better methods are certainly needed (Tournigand and de Gramont, 2011). For several years, new prognostic markers of significant importance have been a central topic in cancer research with the perspective of individualised treatment.

Most studies have been retrospective and included small numbers of highly selected patients. The risk of such studies being false positive is very high, and it has become evident that most biomarker studies have failed verification in new independent patient series (Locker *et al*, 2006). However, the present study included nearly all stage II patients in a population of 5 million people and can thus be considered unbiased with regard to selection.

The present study shows that increasing mean log(TB) (representing the relative miR-21 expression level) and mean log(TBR) (representing values normalised to the nuclear density) are significantly related to decreasing RF-CSS. These results thus confirm the prognostic importance of miR-21 independently from prognostic markers, proven to be inadequate, for example, T-category, malignancy grade, tumour perforation, tumour fixation, invasion of nerves and invasion of veins. Our results are in agreement with the previous study by Nielsen *et al* (2011) reporting that high miR-21 levels determined by ISH in 130 cases of stage II colon cancer is correlated with poor disease-free survival. The findings were based on a sample cohort as part of the RANX study and contained patient samples collected from 1991 to 1993 (Nielsen *et al*, 2011). They also found a significant impact on OS. In contrast, we found no prognostic value of miR-21 in analyses of OS. At the cut-off point set to 1 January 2010, 116 patients had died from other causes than colon cancer, whereas 110 patients had experienced relapse or had died from colon cancer. This indicates that at least half of stage II colon cancer patients die from causes other than colon cancer. Hence, OS analyses will be diluted, calling for endpoint analyses focusing on recurrence of the disease.

Our results are also in keeping with previous studies using PCR to quantify miR-21 in CRC tissue. Schetter *et al* (2008) studied the profile of the miRNA expression in paired tumour and normal tissue samples from 84 patients with colon cancer (29 stage II patients) as a training set and paired samples from another 113 patients with colon cancer (37 stage II patients) as a validation set. Among the 37 miRNAs that were differentially expressed, miR-21 was selected for validation. They found that high expression of miR-21 was significantly associated with poor prognosis, independent of T-category, age, sex and tumour location (Schetter *et al*, 2008). Slaby *et al* (2007) also reported that miR-21 upregulation in CRC patients was associated with lymph node positivity and development of distant metastasis based on their study of 29 patients.

In this study, the majority of tumours expressed the miR-21 ISH signal in fibroblast-like stromal cells. However, miR-21-positive cancer cells were also found in a small fraction of the tumours. Previous studies using identical probes to visualise miR-21 report the same distribution (Nielsen *et al*, 2011; Rask *et al*, 2011), while other groups using different probes describe miR-21-positive tumour cells in the majority of the tumours (Schetter *et al*, 2008; Yamamichi *et al*, 2009). The reason for the discrepancies could be explained by cross-reaction of the probe to 'similar sequences' allowed under suboptimal hybridisation conditions as well as different reagents employed to detect the labelled probe. However, it can not be excluded that a different probe could influence the results. It is noteworthy that miR-21 demonstrates prognostic impact despite the fact that it is found in the stroma cells and not in the tumour cells. Explanations are speculative but it can not be excluded that signals from stroma to the tumour cells, including paracrine signalling, influence the behaviour of the tumour.

Because of the exclusion criterion that each slide should be evaluated by at least eight images, 41 patients were excluded. This is most likely explained by the fact that we collected the tumour block representing the invasive front from each patient. Therefore, some of the blocks had small tumour content and as the software did not allow image fields to overlap, fewer images were available for analysis.

Using image quantified ISH we were able to assess miR-21 on archival FFPE tissue in this unique population. The results showed that increasing mean log(TBR) is an independent prognostic marker of poor RF-CSS in a stage II colon cancer population consisting of nearly all patients diagnosed with this disease in Denmark in the year 2003. Our findings strongly suggest that miR-21 measured by ISH is a robust and valuable indicator of adverse prognosis in stage II colon cancer. The results call for evaluation together with other variables to generate a fully specified prognostic index, pointing out the individuals, in this group of patients, in need of adjuvant chemotherapy. Eventually, such an index should be tested in a prospective, randomised trial setting for conclusive evaluation of the clinical impact.

ACKNOWLEDGEMENTS

We are thankful for the initial work on the database conducted by the DCCG and for the help on the search in this database. We are also thankful for the technical assistance provided by Birgit Roed Sørensen and proof reading by Karin Larsen.

Conflict of interest

SJ and BSN held a full-time employment at the time of analysis for an entity (name of entity: Exiqon A/S) having a commercial interest in the subject matter under consideration in the manuscript. The remaining authors declare no conflict of interest.

REFERENCES

Asangani IA, Rasheed SA, Nikolova DA, Leupold JH, Colburn NH, Post S, Allgayer H (2008) MicroRNA-21 (miR-21) post-transcriptionally downregulates tumor suppressor Pdcd4 and stimulates invasion, intravasation and metastasis in colorectal cancer. *Oncogene* **27**: 2128–2136

Bandres E, Cubedo E, Agirre X, Malumbres R, Zarate R, Ramirez N, Abajo A, Navarro A, Moreno I, Monzo M, Garcia-Foncillas J (2006) Identification by Real-time PCR of 13 mature microRNAs differentially expressed in colorectal cancer and non-tumoral tissues. *Mol Cancer* **5**: 29

Bastos DA, Ribeiro SC, de FD, Hoff PM (2010) Combination therapy in high-risk stage II or stage III colon cancer: current practice and future prospects. *Ther Adv Med Oncol* **2**: 261–272

Benson III AB, Schrag D, Somerfield MR, Cohen AM, Figueredo AT, Flynn PJ, Krzyzanowska MK, Maroun J, McAllister P, Van CE, Brouwers M, Charette M, Haller DG (2004) American Society of Clinical Oncology recommendations on adjuvant chemotherapy for stage II colon cancer. *J Clin Oncol* **22**: 3408–3419

Carrington JC, Ambros V (2003) Role of microRNAs in plant and animal development. *Science* **301**: 336–338

Chan SH, Wu CW, Li AF, Chi CW, Lin WC (2008) MiR-21 microRNA expression in human gastric carcinomas and its clinical association. *Anticancer Res* **28**: 907–911

Ferdin J, Kunej T, Calin GA (2010) Non-coding RNAs: identification of cancer-associated microRNAs by gene profiling. *Technol Cancer Res Treat* **9**: 123–138

Figueredo A, Coombes ME, Mukherjee S (2008) Adjuvant therapy for completely resected stage II colon cancer. *Cochrane Database Syst Rev* **3**: CD005390

Gabriely G, Wurdinger T, Kesari S, Esau CC, Burchard J, Linsley PS, Krichevsky AM (2008) MicroRNA 21 promotes glioma invasion by targeting matrix metalloproteinase regulators. *Mol Cell Biol* **28**: 5369–5380

Gangadhar T, Schilsky RL (2010) Molecular markers to individualize adjuvant therapy for colon cancer. *Nat Rev Clin Oncol* **7**: 318–325

Gross CP, Andersen MS, Krumholz HM, McAvay GJ, Proctor D, Tinetti ME (2006) Relation between Medicare screening reimbursement and stage at diagnosis for older patients with colon cancer. *JAMA* **296**: 2815–2822

Kopetz S, Freitas D, Calabrich AF, Hoff PM (2008) Adjuvant chemotherapy for stage II colon cancer. *Oncology (Williston Park)* **22**: 260–270

Lim LP, Lau NC, Garrett-Engele P, Grimson A, Schelter JM, Castle J, Bartel DP, Linsley PS, Johnson JM (2005) Microarray analysis shows that some microRNAs downregulate large numbers of target mRNAs. *Nature* **433**: 769–773

Locker GY, Hamilton S, Harris J, Jessup JM, Kemeny N, Macdonald JS, Somerfield MR, Hayes DF, Bast Jr RC (2006) ASCO 2006 update of recommendations for the use of tumor markers in gastrointestinal cancer. *J Clin Oncol* **24**: 5313–5327

Lombardi L, Morelli F, Cinieri S, Santini D, Silvestris N, Fazio N, Orlando L, Tonini G, Colucci G, Maiello E (2010) Adjuvant colon cancer chemotherapy: where we are and where we'll go. *Cancer Treat Rev* **36**(Suppl 3): S34–S41

Markou A, Tsaroucha EG, Kaklamanis L, Fotinou M, Georgoulias V, Lianidou ES (2008) Prognostic value of mature microRNA-21 and microRNA-205 overexpression in non-small cell lung cancer by quantitative real-time RT-PCR. *Clin Chem* **54**: 1696–1704

Meng F, Henson R, Wehbe-Janek H, Ghoshal K, Jacob ST, Patel T (2007) MicroRNA-21 regulates expression of the PTEN tumor suppressor gene in human hepatocellular cancer. *Gastroenterology* **133**: 647–658

Nielsen BS (2012) MicroRNA in situ hybridization. *Methods Mol Biol* **822**: 67–84

Nielsen BS, Jorgensen S, Fog JU, Sokilde R, Christensen IJ, Hansen U, Brunner N, Baker A, Moller S, Nielsen HJ (2011) High levels of microRNA-21 in the stroma of colorectal cancers predict short disease-free survival in stage II colon cancer patients. *Clin Exp Metastasis* **28**: 27–38

O'Connell MJ (2004) Current status of adjuvant therapy for colorectal cancer. *Oncology (Williston Park)* **18**: 751–755

O'Connor ES, Greenblatt DY, Loconte NK, Gangnon RE, Liou JI, Heise CP, Smith MA (2011) Adjuvant chemotherapy for stage ii colon cancer with poor prognostic features. *J Clin Oncol* **29**(25): 3381–3388

Parkin DM, Bray F, Ferlay J, Pisani P (2005) Global cancer statistics, 2002. *CA Cancer J Clin* **55**: 74–108

Qian B, Katsaros D, Lu L, Preti M, Durando A, Arisio R, Mu L, Yu H (2009) High miR-21 expression in breast cancer associated with poor disease-free survival in early stage disease and high TGF-beta1. *Breast Cancer Res Treat* **117**: 131–140

Rask L, Balslev E, Jorgensen S, Eriksen J, Flyger H, Moller S, Hogdall E, Litman T, Nielsen BS (2011) High expression of miR-21 in tumor stroma correlates with increased cancer cell proliferation in human breast cancer. *APMIS* **119**: 663–673

Schetter AJ, Leung SY, Sohn JJ, Zanetti KA, Bowman ED, Yanaihara N, Yuen ST, Chan TL, Kwong DL, Au GK, Liu CG, Calin GA, Croce CM, Harris CC (2008) MicroRNA expression profiles associated with prognosis and therapeutic outcome in colon adenocarcinoma. *JAMA* **299**: 425–436

Slaby O, Svoboda M, Fabian P, Smerdova T, Knoflickova D, Bednarikova M, Nenutil R, Vyzula R (2007) Altered expression of miR-21, miR-31, miR-143 and miR-145 is related to clinicopathologic features of colorectal cancer. *Oncology* **72**: 397–402

Tournigand C, de Gramont A (2011) Chemotherapy: is adjuvant chemotherapy an option for stage II colon cancer? *Nat Rev Clin Oncol* **8**: 574–576

Yamamichi N, Shimomura R, Inada K, Sakurai K, Haraguchi T, Ozaki Y, Fujita S, Mizutani T, Furukawa C, Fujishiro M, Ichinose M, Shiogama K, Tsutsumi Y, Omata M, Iba H (2009) Locked nucleic acid in situ hybridization analysis of miR-21 expression during colorectal cancer development. *Clin Cancer Res* **15**: 4009–4016

Yan LX, Huang XF, Shao Q, Huang MY, Deng L, Wu QL, Zeng YX, Shao JY (2008) MicroRNA miR-21 overexpression in human breast cancer is associated with advanced clinical stage, lymph node metastasis and patient poor prognosis. *RNA* **14**: 2348–2360

Yao Q, Cao S, Li C, Mengesha A, Kong B, Wei M (2011) Micro-RNA-21 regulates TGF-beta-induced myofibroblast differentiation by targeting PDCD4 in tumor-stroma interaction. *Int J Cancer* **128**: 1783–1792

MicroRNA therapeutics for cardiovascular disease: opportunities and obstacles

Eva van Rooij[1] and Eric N. Olson[2]

Abstract | In recent years, prominent roles for microRNAs (miRNAs) have been uncovered in several cardiovascular disorders. The ability to therapeutically manipulate miRNA expression and function through systemic or local delivery of miRNA inhibitors, referred to as antimiRs, has triggered enthusiasm for miRNAs as novel therapeutic targets. Here, we focus on the pharmacokinetic and pharmacodynamic properties of current antimiR designs and their relevance to cardiovascular indications, and evaluate the opportunities and obstacles associated with this new therapeutic modality.

microRNAs
(miRNAs). Short, non-coding RNAs that suppress protein expression by most commonly binding to complementary sequences located within 3′ untranslated regions of target mRNAs.

Hepatitis C virus
(HCV). An infectious disease primarily affecting the liver.

[1]*miRagen Therapeutics, 6200 Lookout Rd, Boulder, Colorado 80301, USA.*
[2]*Department of Molecular Biology, University of Texas Southwestern Medical Center, 6000 Harry Hines Boulevard, Dallas, Texas 75390–79148, USA.*
Correspondence to E.N.O.
e-mail: eric.olson@utsouthwestern.edu
doi:10.1038/nrd3864
Published online 19 October 2012

Cardiovascular disease remains the primary cause of morbidity and mortality worldwide. Despite the therapeutic benefits of numerous treatment options, including statins, angiotensin-converting enzyme (ACE) inhibitors, beta blockers and other drugs, the prevalence of cardiovascular disease continues to increase, underscoring the need for new therapeutic strategies.

MicroRNAs (miRNAs) are short, single-stranded RNAs that anneal with complementary sequences in mRNAs, thereby suppressing protein expression. Individual miRNAs engage numerous mRNA targets, often encoding multiple components of complex intracellular networks. Thus, the manipulation of miRNA expression or function can have a profound impact on cellular phenotypes. Depending on the abundance of a miRNA and its targets, as well as the physiological state of a cell, a miRNA can act as a fine-tuner of gene expression or an on/off switch. The functions of miRNAs are heightened under conditions of pathophysiological stress and in disease, making them attractive candidates for therapeutic manipulation.

The first report implicating miRNAs in heart disease was published in 2006 (REF. 1), in which signature patterns of miRNA expression were shown to correlate with heart failure and cardiac hypertrophy in mice and humans. Since then, numerous follow-up studies have described changes in miRNA expression in diseased human hearts[2,3] and vascular tissues[4,5], and gain- and loss-of-function studies have uncovered prominent roles for miRNAs in cardiovascular disorders including myocardial infarction, cardiac hypertrophy, heart failure, angiogenesis, vascular stenosis and fibrosis[1–3,6–12]. These actions reflect the involvement of specific miRNAs in fundamental cellular processes, such as cell survival (miR-15)[13], extracellular matrix production (miR-21 and miR-29)[9,10] and hypoxia (miR-210)[14].

The ability to therapeutically manipulate miRNA expression and function through systemic or local delivery of miRNA inhibitors or mimics, and the recent success of the first-in-human clinical trial of a miRNA therapeutic for suppression of hepatitis C virus (HCV) replication (BOX 1), have both raised possibilities for a new class of disease-modifying therapeutics based on miRNA biology. miRNA-based therapeutics have not yet reached clinical trials for cardiovascular disorders, but the promising results in numerous animal models of related diseases such as heart failure, cardiac hypertrophy, fibrosis and hyperlipidaemias, as discussed below, suggest that clinical data will soon be available.

Here, we review the mechanistic basis of miRNA functions within the context of disease modification and consider the roles of representative miRNAs in cardiovascular disease. With this perspective, we evaluate miRNAs as potential therapeutic targets for cardiovascular disorders and consider the challenges associated with this potential new therapeutic modality.

miRNA biogenesis and mechanism of action

Mature miRNAs are ~22 nucleotides in length and are transcribed by RNA polymerase II as long precursor RNAs, called primary miRNAs (pri-miRNAs), which are sequentially processed in the nucleus and cytoplasm. The RNase III Drosha associates with DiGeorge syndrome critical region 8 (DGCR8) and other cofactors

Box 1 | **Clinical trials of antimiR-122 in the treatment of HCV**

AntimiR therapeutics (inhibitors of microRNAs) recently became a reality when Santaris Pharma reported both the safety and efficacy of its antimiR against the microRNA miR-122, miravirsen, in humans. Data from a Phase I trial showed that either a single dose (up to 12 mg per kg) or multiple ascending doses (up to five doses of 5 mg per kg) of miravirsen are well tolerated in healthy volunteers. These studies indicated that miravirsen has an attractive pharmacokinetic profile and a clear dose-dependent pharmacology, without having dose-limiting toxicities at the doses used in these studies.

A follow-up Phase IIa trial (see the 3 October 2011 press release on the Santaris Pharma website) indicated that miravirsen was well tolerated and provided continuous and prolonged antiviral activity that extended well beyond the end of active therapy in patients infected with hepatitis C virus (HCV). In this multiple-ascending-dose study, patients were enrolled sequentially to one of three cohorts (nine active: three placebo per cohort) and miravirsen was administered at doses of 3, 5 or 7 mg per kg with a total of five weekly subcutaneous injections over 29 days. Treatment with miravirsen provided robust, dose-dependent antiviral activity that was maintained for more than 4 weeks after the last dose. Notably, in four out of nine patients treated at the highest dose (7 mg per kg), HCV RNA became undetectable during the study. No serious adverse events were observed and only mild and infrequent adverse events such as headaches, coryza and diarrhoea were reported. Furthermore, there were no clinically significant changes in safety tests, vital signs or electrocardiograms. Taken together, these data indicate that miravirsen, given as a 4-week monotherapy to patients with HCV, provides long-lasting suppression of viraemia and provides a strong barrier to viral infection.

Additional Phase II studies of miravirsen are planned in combination with direct-acting antivirals and as a single agent.

to crop pri-miRNAs in the nucleus, yielding hairpin-shaped pre-miRNAs (~70 nucleotides in length) that are further shortened in the cytoplasm by Dicer to give rise to the mature miRNA[15]. In the cytoplasm, miRNAs associate with mRNAs within a multiprotein complex of Argonaute proteins, known as the RNA-induced silencing complex (RISC), which facilitates and stabilizes miRNA–mRNA interactions. miRNAs anneal via Watson–Crick base pairing, with sequences most commonly located in 3′ untranslated regions (UTRs) of mRNA[15], although there are some examples of miRNA interactions within mRNA coding regions, intron–exon junctions and 5′ UTRs[16,17]. The primary determinant of mRNA target regulation by miRNAs is perfect pairing between the sequence of nucleotides 2–7 at the 5′ end of the mature miRNA (referred to as the 'seed region') and the target mRNA, but other nucleotides also contribute to the interactions[15]. Association of a miRNA with its mRNA target results in degradation of the mRNA as well as inhibition of translation (FIG. 1). Currently, it is believed that the vast majority of the gene-regulatory effects of miRNAs occur though mRNA decay rather than translational repression[18]. Recently, pseudogenes have also been implicated in regulating miRNA activity. Pseudogene transcripts containing conserved miRNA binding sites, referred to as competing endogenous RNAs (ceRNAs), act as decoys or sponges by sequestering miRNAs and preventing them from binding to their mRNA targets[19,20].

An especially puzzling feature of miRNA biology has been the minimal effects of miRNA-mediated loss of function. Although lin-4, the first miRNA to be discovered, was identified on the basis of its strong loss-of-function phenotype in nematodes, systematic genetic deletions of miRNAs in this organism have revealed grossly abnormal phenotypes in less than 10% of miRNA-mutant animals[21]. Similarly, genetic analyses of miRNAs in mice have revealed relatively minor functions under conditions of homeostasis in controlled laboratory settings[22]. The lack of strong loss-of-function miRNA phenotypes might be explained by compensatory mechanisms that allow for re-balancing of protein networks when the expression of individual components is subtly altered as a consequence of the absence of a miRNA.

Redundancy among homologous miRNAs within families or the targeting of individual mRNAs by several miRNAs can also diminish the consequences of the loss of individual miRNAs. However, a general theme seems to be that the actions of miRNAs become pronounced under conditions of injury or stress. Thus, the elimination of some miRNAs sensitizes cells to stress, resulting in exacerbated pathology, whereas the absence of other miRNAs can confer resistance to stress. Stress signalling impinges on numerous points in the pathway of miRNA biogenesis and function (FIG. 1). There are many examples in which miRNA abundance increases or decreases in response to stress, and changes in the expression of specific miRNAs have been shown to be diagnostic for disease progression in cardiovascular disorders[23]. The heightened function of a miRNA during stress can also be explained by changes in the abundance of its mRNA targets or differences in miRNA activity under stress[24]. For example, a stress-induced reduction in the level of expression of a miRNA can have a disease-modifying effect by increasing the levels of downstream mRNA targets, whereas a stress-induced increase in miRNA expression will result in a decrease in levels of downstream targets. Conversely, changes in the expression of mRNA targets under disease conditions can influence the effect of the miRNA on the mRNA. Although the influence of stress is likely to be miRNA- and trigger-dependent, changes in miRNA expression and functionality under disease conditions imply the existence of an active mechanism for differential miRNA activity under stress.

Therapeutic inhibition of miRNAs

Genetic gain- and loss-of-function approaches, as well as pharmacological modulation of individual miRNAs or miRNA families in animal models of disease, point to miRNAs as key regulators of many disorders, including cardiovascular disease[23]. Their pathological roles, along with their pharmacological properties, have catalysed efforts to develop miRNA therapeutics. In principle, miRNA mimics can be used to elevate the expression of beneficial miRNAs in disease settings, whereas miRNA inhibitors can be delivered to block the activity of miRNAs that drive disease progression[25]. miRNA mimicry has lagged behind the development of antimiR chemistries owing to substantial challenges in their delivery and design. Currently, the most effective means of enhancing miRNA function or replacing miRNAs that are lost or downregulated in disease is through adeno-associated viruses (AAVs). The availability of numerous different AAV serotypes allows for potential tissue enrichment as a result of the natural tropism of each individual AAV

RNA-induced silencing complex
(RISC). A multiprotein complex that incorporates a microRNA to recognize complementary sequences in mRNAs and block protein expression.

Pseudogenes
Non-coding transcripts that are often conserved across species and contain conserved microRNA binding sites that can act as decoys to interfere with microRNA activity.

AntimiRs
Antisense oligonucleotides designed to target specific microRNAs.

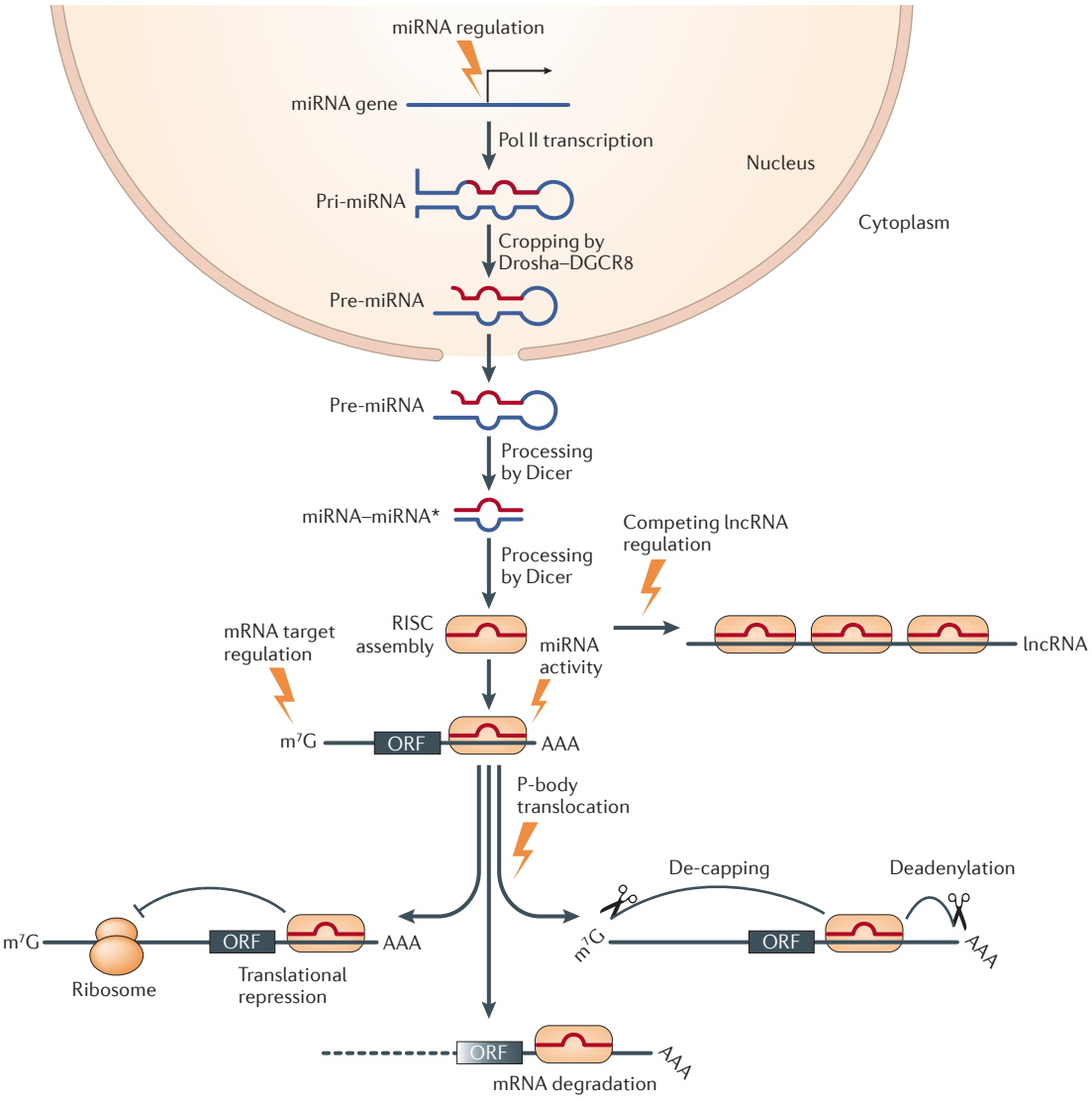

Figure 1 | **MicroRNA biogenesis and mechanism of action.** MicroRNA (miRNA) genes are usually transcribed by RNA polymerase II (Pol II) to form a capped and polyadenylated transcript. The miRNA precursor, termed primary miRNA (pri-miRNA), forms a hairpin-shaped loop structure that is cleaved by the RNase III Drosha and DiGeorge syndrome critical region 8 (DGCR8), yielding a hairpin-shaped precursor miRNA (pre-miRNA) that is ~70 nucleotides in length. The pre-miRNA is exported from the nucleus into the cytoplasm, where it is further cleaved by the RNase III enzyme Dicer, yielding an imperfect miRNA–miRNA* duplex that is about 22 nucleotides in length. Although either strand of the duplex may potentially act as a functional miRNA, only one strand is usually incorporated into the RNA-induced silencing complex (RISC). miRNAs incorporated in the RISC often recognize their targets — nucleotides 2–7 of miRNA (known as the 'seed region'). Association of a miRNA with its mRNA target results in degradation of the mRNA as well as translational inhibition. Recently, pseudogenes have also been implicated in regulating miRNA activity. Pseudogene transcripts are often conserved across species and many contain conserved miRNA binding sites, referred to as competing endogenous RNAs (ceRNAs), which act as decoys or sponges by sequestering miRNAs and preventing them from binding to their mRNA targets. Stress conditions can influence miRNA biogenesis at multiple levels (indicated on the figure by lightening bolts). lncRNA, long non-coding RNA; m^7G, 7-methylguanosine (a modified form of guanosine attached to the 5′ ends of mRNAs); ORF, open reading frame.

Pharmacokinetic
In the context of antimiR (microRNA inhibitor) designs, this refers to the potency of an antimiR in binding to and inhibiting a microRNA *in vivo*.

Pharmacodynamic
In the context of antimiR (microRNA inhibitor) designs, this refers to mRNA de-repression of direct microRNA targets in response to treatment with an antimiR.

serotype towards different organs, as well as the different cellular receptors with which each AAV serotype interacts[26,27]. AAV type 6 and type 9, for example, display preferential tropism for skeletal muscle and heart, respectively, when delivered systemically in rodents[28–30]. Here, we focus on the pharmacokinetic and pharmacodynamic properties of current antimiR designs.

AntimiR chemistries. miRNAs possess several features as potential drug targets that distinguish them from other therapeutic modalities. In contrast to small-molecule inhibitors identified in cell-based screens, in which target identification can pose substantial challenges, antimiRs act through complementary base pairing with miRNAs, so their direct target sequence in mRNAs is known — at

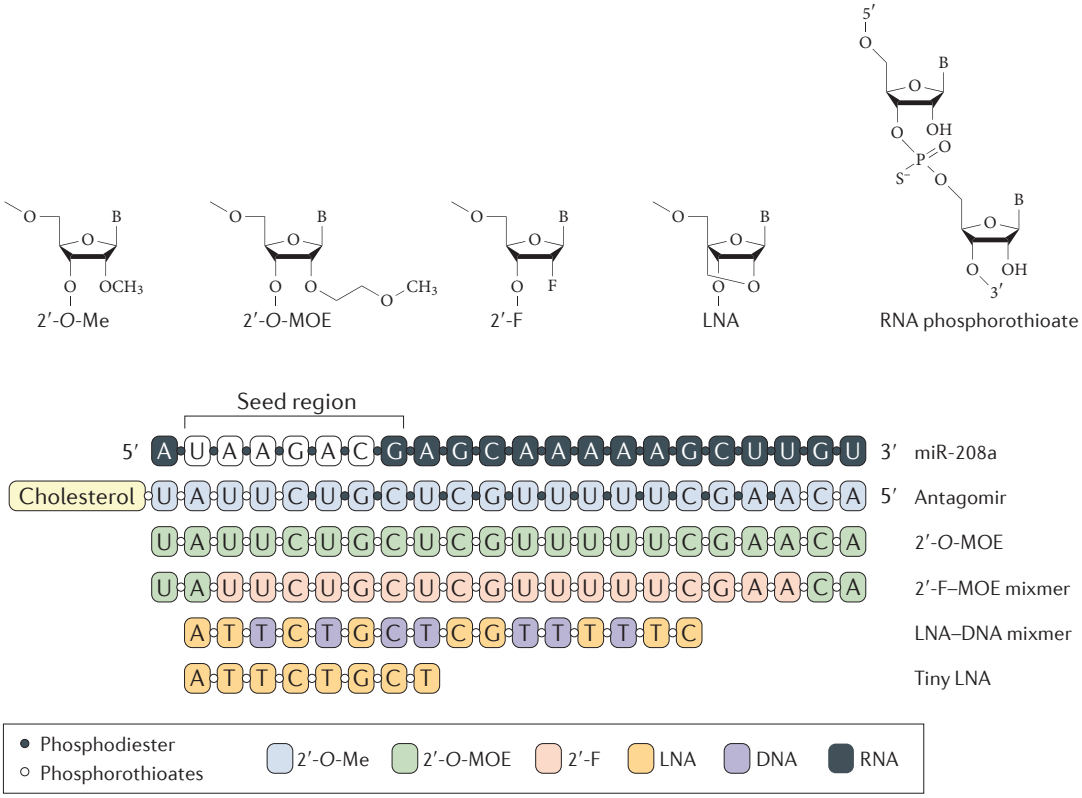

Figure 2 | **AntimiR chemistries.** AntimiR (inhibitor of microRNA (miRNA)) chemistries currently use various high-affinity 2′ sugar modifications such as conformationally restricted nucleotides with 2′-*O*-methyl (2′-*O*-Me), 2′-*O*-methoxyethyl (2′-MOE), 2′-fluoro (2′-F) or locked nucleic acid (LNA) modifications. To increase nuclease resistance, most antimiR chemistries to date harbour phosphorothioate backbone linkages, whereby a sulphur atom replaces one of the non-bridging oxygen atoms in the phosphate group. AntimiRs containing cholesterol, conjugated via a 2′-*O*-Me linkage, named antagomirs, are fully complementary to the mature miRNA sequence and contain several phosphorothioate moieties to increase their stability. Several unconjugated phosphorothioate antisense molecules with various high-affinity 2′ sugar modifications (such as 2′-MOE, 2′-F or LNA) are currently also being used. Although all of these modifications improve nuclease resistance and increase duplex melting temperature, the high duplex melting temperature of LNA-modified oligonucleotides enables efficient miRNA inhibition with shorter antimiRs.

Phosphorothioate
Backbone linkage in which a sulphur atom replaces one of the non-bridging oxygen atoms in the phosphate group of oligonucleotides to increase nuclease resistance.

Antagomir
A cholesterol-conjugated antimiR (microRNA inhibitor) chemistry that is complementary to the full-length sequence of the target microRNA, consisting of 2′-*O*-methyl (2′-*O*-Me) linkages and containing several phosphorothioate moieties to increase stability.

2′ sugar modifications
High-affinity 2′ sugar modifications such as 2′-*O*-methyl (2′-*O*-Me), 2′-*O*-methoxyethyl (2′-MOE), 2′-fluoro (2′-F) or locked nucleic acid; used in oligonucleotide chemistries to improve nuclease resistance and increase duplex melting temperature (T_m).

Locked nucleic acid
(LNA). A 2′ sugar modification in which the ribose is locked in a C3′-endo conformation by the introduction of a 2′-*O*-,4′-C methylene bridge that strongly increases the affinity for complementary RNA and increases the duplex melting temperature (T_m) by +2 °C to +8 °C per introduced LNA modification.

Duplex melting temperature
(T_m). The temperature at which half of a particular duplex dissociates and becomes single-stranded; in this case the temperature at which an antimiR (a microRNA inhibitor) will dissociate from complementary RNA.

least theoretically. However, it should also be emphasized that there is substantial ambiguity in miRNA target identification, in that sequences outside the miRNA 'seed region' — as well as the secondary structure of the mRNA target and the association of mRNAs with RNA-binding proteins — can influence target engagement[31]. Thus, it is essential to experimentally document the regulation of specific targets in response to changes in miRNA abundance in order to firmly establish their contributions to miRNA functions.

Several oligonucleotide chemistries allow for high-affinity interaction of antisense oligonucleotides with miRNAs, preventing their interaction with — and repression of — target mRNAs. To achieve effective pharmacological inhibition of disease-associated miRNAs, antimiR chemistries should contain chemical modifications to enhance binding affinity, confer nuclease resistance and facilitate cellular uptake. To increase nuclease resistance, most antimiR chemistries to date harbour phosphorothioate backbone linkages (FIG. 2). In addition to increasing stability, the phosphorothioate backbone modifications promote plasma protein binding, thereby reducing clearance of the antimiRs by glomerular filtration and urinary excretion, which facilitates tissue delivery of antimiRs *in vivo*[32–34]. AntimiRs containing cholesterol, conjugated via a 2′-*O*-methyl (2′-*O*-Me) linkage, named antagomirs, are fully complementary to the mature miRNA sequence and contain several phosphorothioate moieties to increase stability (FIG. 2). Cholesterol is thought to enhance cellular uptake and *in vivo* stability[32,33], as well as promote hepatic uptake of the antimiR while lowering delivery to other tissue types.

The antagomir chemistry has been especially useful as an experimental tool; however, all antimiR chemistries currently in development use unconjugated phosphorothioate antisense molecules with various additional high-affinity 2′ sugar modifications such as 2′-*O*-methoxyethyl (2′-MOE) and 2′-fluoro (2′-F) or locked nucleic acid (LNA) and LNA-like conformationally restricted nucleotides (FIG. 2). Although all of these modifications improve nuclease resistance and increase duplex melting temperature (T_m)[35], LNAs possess the highest affinity, with an increase

in T_m of +2 °C to +8 °C per introduced LNA modification against complementary RNA. A 2′-MOE-modified antimiR-122 has shown efficacy in mice[36], and an LNA-modified antimiR-122 has been shown to be efficacious in non-human primates[37]. Moreover, LNA-modified antimiR-122 was recently shown to be efficacious in humans (see the ClinicalTrials.gov website). A 2′-F- and 2′-MOE-modified antimiR-33 was recently shown to be efficacious in reducing atherosclerosis in non-human primates[38].

The high T_m of LNA-modified oligonucleotides enables efficient miRNA inhibition with truncated antimiRs. Several studies have reported efficient miRNA inhibition *in vivo*, using high-affinity 15–16-nucleotide-long LNA–DNA mixmers targeting the 5′ region of mature miRNA. The high binding affinity of seed region-targeting tiny 8-mer LNA-modified antimiRs with a complete phosphorothioate backbone allows for *in vivo* delivery and silences miRNAs without the need for additional conjugation or formulation chemistries[13,39–41] (FIG. 2). Microarray analysis indicated that 8-mers and 15-mers evoked comparable changes in miR-122 targets in the liver and induced similar physiological responses[39]. However, as many miRNAs belong to families that differ by only a few bases in the 3′ regions, antimiRs that are complementary to the full-length miRNA sequence may have greater specificity towards individual miRNA family members than shorter antimiRs that are directed against 5′ regions of miRNAs.

Potential sources of toxicity after the administration of a miRNA inhibitor include unwanted gene changes or the effects of the antimiR on off-target, non-diseased tissues; the chemistry of the antimiR is also a common source of toxicity for oligonucleotide therapeutics. Phosphorothioate oligonucleotides, for example, can inhibit the tenase complex in the intrinsic clotting cascade[42], activate the alternative pathway of the complement cascade[43] and activate innate immunity. Additionally, although LNA-containing oligonucleotides have an increased potency for reducing the levels of mRNA targets, some signs of hepatotoxicity (determined by measuring serum levels of transaminases, liver weight and body weight) have been observed with LNA-modified antisense oligonucleotides directed against mRNAs. Histopathological evaluation of tissues from LNA-treated animals confirmed the hepatocellular involvement, suggesting that although LNA-modified antisense oligonucleotides have the potential to improve potency, they potentially create a risk of developing hepatotoxicity[44]. However, contrary to this report, no hepatotoxicity was observed in mice treated with LNA-modified antimiRs (at a dose of 75 mg per kg; three doses of 25 mg per kg per day), as shown by unaltered levels of the serum transaminases alanine aminotransferase and aspartate aminotransferase 24 hours after treatment (compared to saline controls) and by the absence of histological changes in liver sections from LNA-treated animals[45]. Further toxicity studies of chemically modified miRNA inhibitors will be required to establish safety parameters for the different antimiR chemistries. Different oligonucleotide sequences are also likely to display differences in toxicity, tissue distribution and efficacy.

Pharmacokinetic properties of antimiR chemistries. The antimiR molecules that are currently being used to target miRNAs *in vivo* are highly water-soluble and have molecular masses of several kDa. Their size and charge limit intestinal absorption, thereby preventing them from becoming good candidates for oral administration. Thus far, successful delivery of chemically modified oligonucleotide antimiRs has been dependent on parenteral administration via intravenous (i.v.), intraperitoneal (i.p.) or subcutaneous (s.c.) injection. Unlike typical (low-molecular-mass) drugs, plasma levels of antimiR chemistries are largely cleared within hours after administration as a result of their uptake into tissues[34,46], except for a low level of antimiR that remains detectable in the circulation for several weeks[13,39]. The persistent presence of the antimiR in the circulation probably reflects its association with circulating plasma proteins and/or the gradual release of antimiRs trapped in extracellular spaces.

Studies using northern blotting, enzyme-linked immunosorbent assay (ELISA)-based detection methods or fluorescently labelled oligonucleotides have shown that antimiRs containing the typical nucleic acid ribose sugar backbone with 2′ modifications are distributed broadly to most tissues but tend to accumulate in the kidney and liver[13,32,33,45,47]. However, it is becoming apparent that oligonucleotide sequence, length and chemical modifications affect cellular distribution and functionality, thus strongly influencing the pharmacokinetic and pharmacodynamic properties of each molecule[32,33,36,39].

Currently, relatively little is known about the mechanisms of cellular uptake, storage and mode of action of the different antimiR chemistries. Once inside cells, many modified antimiRs are extremely stable and have half-lives in the order of weeks[48]. Additionally, although systemically delivered antagomirs appear to accumulate in a cytoplasmic compartment distinct from P-bodies and induce miRNA degradation by an RNA interference (RNAi)-independent pathway[32,33], LNA-modified antimiRs seem to inhibit miRNA function by sequestering the mature miRNA[45,47], which implies that the different antimiR chemistries have different modes of action.

In the context of this Review, although it is clear that oligonucleotide chemistries directed against miRNAs are taken up by, or at least reach, cardiac and vascular cell populations, it will be interesting to determine whether some cell types are more efficiently targeted and whether stress plays a part in cellular uptake. Another question that remains unanswered is where within the cell the antimiRs reside and whether all antimiRs are actually functional. Currently used doses provide a vast excess of antimiR copies relative to miRNA, and the long-lasting duration of effects suggests that there is a cellular reservoir that — over time — enables antimiRs to inhibit newly formed miRNAs, but it is unknown how the release of antimiRs from such cellular depots is controlled. Subcellular sites of antimiR storage, as well as the kinetics of release, may vary depending on the chemical modifications to the oligonucleotide.

Tiny
A locked nucleic acid (LNA)-containing 8-mer antimiR (microRNA inhibitor) with a complete phosphorothioate backbone targeting the seed region of a microRNA or microRNA family.

P-bodies
Cytoplasmic sites of mRNA turnover. Also referred to as stress granules.

Efficacy of antimiRs. Although antimiR detection studies indicate that there is a rapid uptake of antimiR chemistries in many tissues, unless the antimiR is located within the appropriate cellular compartment, these assays can be deceptive as the *in vivo* activity of an antimiR is determined by its cellular distribution. Processing of tissue during experimental analysis can potentially introduce artificial binding between the antimiR and miRNA, which does not actually occur within the intact cell, leading to an overestimation of antimiR function and binding.

The impact of a miRNA on its target depends on the relative ratio of a miRNA to its target. miRNAs display a range of intracellular concentrations, with the most abundant miRNAs being expressed at up to tens of thousands of copies per cell[49]. Strategies to inhibit miRNA function and thereby de-repress expression of their targets are based on the presumption that relatively modest increases in the expression of targets are sufficient to evoke substantial therapeutic benefits. In this regard, the mRNA targets of miRNAs have been shown to display threshold effects such that the mRNA can be efficiently repressed when it is present at relatively low levels compared to the miRNA, but when the mRNA reaches such a level that the miRNA is not able to inhibit it, the biological impact of the miRNA becomes diminished[50].

In order to demonstrate the efficacy of target engagement by antimiRs *in vivo*, it is necessary to measure target de-repression. This task is burdened by the fact that target regulation in general is modest, ranging — on average — from a 20% to 50% change in mRNA expression, making it difficult to determine significant changes above naturally occurring variations in gene expression[18,51]. Additionally, proteomic studies in response to miRNA modulation have reported that the average changes in protein levels of miRNA targets are less than twofold following miRNA inhibition[52,53]. Target de-repression is often dependent on stress conditions, whereby both the severity and the type of cellular stress influence whether an mRNA is regulated by a miRNA. This is probably due to an abundance of mRNA targets and the expression of cofactors regulating the activity of miRNAs (FIG. 1).

The time course and nature of the pharmacological effects (or pharmacodynamics) of antimiRs are often complicated by the fact that the pharmacology is the summation of the de-repression of gene families and downstream events caused by the de-repression of multiple target genes controlled by that particular miRNA. Thus, the onset of the functional efficacy of antimiRs can be delayed by days or weeks following initial administration of the drug, as reported for the miR-122 inhibitor and its effects on serum cholesterol levels[9]. Delays in pharmacodynamic effects are atypical for most low-molecular-mass drugs and are more akin to so-called disease-modifying agents wherein it is established that pharmacological activity is related to the sum of pharmacological effects over time that cause a change in the disease phenotype. The delayed actions of at least some antimiRs suggest that this class of potential drugs may be better suited for chronic rather than acute disease indications. It should be noted that in these same studies it was shown that the downstream effect of antimiR treatment appeared to be reversible[45,47].

miRNA targets in cardiovascular disease

Although a long-standing dogma in the small interfering RNA (siRNA) field has been that the heart is resistant to oligonucleotide uptake, it has been well established that the heart effectively takes up exogenous DNA[54]. Indeed, several studies have demonstrated effective cardiac delivery and miRNA inhibition using antimiR chemistries and have indicated the potent effects of miRNA inhibition under disease conditions. Below, we present some recent representative examples of the therapeutic effects of antimiRs in the cardiovascular system (TABLE 1).

Control of pathological cardiac remodelling and obesity by miR-208. Myosin heavy chain protein (encoded by *MYH* genes) is the major contractile protein of striated muscles, and myosin 6 (encoded by *MYH6*; also known as MyHC-α) is the predominant myosin isoform expressed in the adult rodent heart. An intron of this gene encodes miR-208a, which — like the host gene — is expressed specifically in the heart[55,56]. Two related miRNAs, miR-208b and miR-499, are encoded by introns of the *MYH7* (encoding myosin 7; also known as MyHC-β) and *MYH7B* genes, respectively, which are expressed specifically in cardiac and slow skeletal muscle[57]. Knockout mice lacking each of these miRNAs (referred to as myomiRs) are viable, but miR-208b–miR-499 double-knockout mice display a reduction in slow myofibres and a corresponding increase in fast myofibres, which is consistent with a role for these miRNAs in the regulation of myofibre switching[57].

Most relevant to cardiac disease is the finding that miR-208a-knockout mice display reduced fibrosis and hypertrophy in response to cardiac stress, and fail to upregulate myosin 7 expression, which is a sensitive marker of pathological cardiac remodelling[56]. These findings initially suggested that therapeutic inhibition of miR-208a might evoke similar benefits in settings of heart disease. Indeed, Montgomery *et al.*[48] showed that subcutaneous delivery of an LNA-modified oligonucleotide inhibitor directed against miR-208a induced potent and functional inhibition of the cardiomyocyte-specific miR-208a. Inhibition of miR-208a suppresses fibrosis, diminishes myosin 7 expression and improves survival in Dahl salt-sensitive rats, which are susceptible to diastolic dysfunction when maintained on a high-salt diet[48]. These findings provide proof-of-concept support for the potential therapeutic benefit of antimiR-208a agents in the setting of heart disease. This study also showed that the antimiR was detectable in the heart for up to 6 weeks following i.v., s.c. or i.p. delivery (whereas higher levels of the antimiR were detected in the kidney and liver) and that a low level of the antimiR remained detectable in the plasma for a comparable period[48]. Interestingly, the downregulation of myosin 7 expression in the heart in response to antimiR-208a was delayed[48], which mirrors the delay in cholesterol lowering after miR-122 inhibition. Whether oligonucleotide inhibition of miR-208a

MyomiRs
The collection of microRNAs co-expressed with three different myosin heavy chain (*MYH*) genes: *MYH6* (miR-208a), *MYH7* (miR-208b) and *MYH7B* (miR-499).

Table 1 | **Therapeutic targeting of cardiovascular miRNAs***

miRNA	Indication	Chemistry	Therapeutic effect	Refs
miR-15 family	Post-MI remodelling	Tiny LNA	Reduces infarct size by increasing the number of viable myocytes after ischaemic injury, resulting in improved cardiac function	13
miR-15 family	Cardiac regeneration	LNA–DNA mixmer	Increases the number of mitotic cardiomyocytes	74
miR-21	Cardiac fibrosis	Antagomir	Inhibits and reverses cardiac fibrosis, leading to enhanced cardiac function in response to pressure overload	9
miR-23 and miR-27	Retinal angiogenesis	LNA–DNA mixmer	Represses neovascularization in the choroid in response to laser injury	99
miR-24	Post-MI remodelling	Antagomir	Reduces infarct size by increasing capillary density, resulting in improved cardiac function after MI	100
miR-33	Atherosclerosis	LNA–DNA mixmer	Increases plasma HDL in mice	104,105
miR-33	Atherosclerosis	2′-F–2′-MOE mixmer	Increases plasma HDL and decreases VLDL in non-human primates on a high-fat diet	38
miR-29	Aneurysms	LNA–DNA mixmer	Increases collagen expression, resulting in a significant reduction in vascular dilation and aneurysm progression	7,88
miR-92a	Neoangiogenesis	Antagomir	Enhances blood vessel growth and functional improvement of damaged tissue in models of hindlimb ischaemia and MI	6
miR-145	Pulmonary hypertension	LNA–DNA mixmer	Reduces systolic right ventricular pressure during pulmonary hypertension	8
miR-155	Viral myocarditis	LNA–DNA mixmer	Lowers myocardial damage and increases survival in response to viral myocarditis	97
miR-199b	Cardiac hypertrophy	Antagomir	Inhibits cardiomyocyte hypertrophy and fibrosis, resulting in improved cardiac function in different models of heart disease	106
miR-208a	Pathological cardiac remodelling	LNA–DNA mixmer	Blocks cardiac remodelling and improves cardiac function and survival in hypertension-induced heart failure	48
miR-208a	Metabolic disease	LNA–DNA mixmer	Reduces weight gain and improves glucose handling and plasma lipid levels in response to a high-fat diet	58
miR-320	Post-MI remodelling	Antagomir	Reduces infarct size in response to ischaemic injury	107

2′-F, 2′-fluoro; 2′-MOE, 2′-*O*-methoxyethyl; antimiR, microRNA inhibitor; HDL, high-density lipoprotein; LNA, locked nucleic acid; MI, myocardial infarction; miRNA, microRNA; VLDL, very-low-density lipoprotein. *Preclinical rodent and large animal studies have shown that antimiR-mediated inhibition of specific miRNAs has therapeutic potential in different aspects of cardiovascular disease.

confers cardiac benefits in forms of heart disease beyond diastolic dysfunction remains to be determined.

Gene profiling studies have shown that the expression of a cohort of predicted mRNA targets is elevated in response to miR-208a inhibition *in vivo*, and many of these mRNA targets have unknown functions in the heart[48]. Although such genes serve as sensitive biomarkers of antimiR efficacy, their unknown functions underscore the challenges associated with establishing the mechanistic basis of the therapeutic efficacy of antimiR-208a.

Unexpectedly, mice treated with antimiR-208a display resistance to obesity, especially when on a high-fat diet[58]. This effect occurs in the absence of detectable toxicity and suggests that the heart has a role in systemic metabolic homeostasis and energy expenditure via a miR-208a-dependent mechanism. Among the strongest predicted and validated targets of miR-208a is mediator of RNA polymerase II transcription subunit 13 (MED13; also known as THRAP1), a component of the mediator complex, which interconnects RNA polymerase II at gene promoters with distal enhancers. Other mediator components have been shown to associate with numerous nuclear hormone receptors and to have key roles in metabolic control[59–61]. It is especially intriguing, in this regard, that cardiac-specific overexpression of MED13 confers resistance to obesity, as observed with miR-208a inhibition. Conversely, cardiac-specific deletion of MED13 results in obesity. These findings raise the possibility of developing antimiRs against miR-208a as therapeutic modifiers of metabolic syndrome (FIG. 3). In this regard, other miRNAs, including miR-103, miR-107, miR-33 and let-7, have been implicated in systemic metabolic control in mice[38,62–64].

MED13
Mediator of RNA polymerase II transcription subunit 13 (also known as THRAP1); a component of the mediator complex that can associate with numerous nuclear hormone receptors and have key roles in metabolic control. MED13 is regulated by the microRNA miR-208.

Control of cardiac hypertrophy and fibrosis by miR-21. Studies of miR-21 in heart disease illustrate the potential disease-modifying actions, as well as the many unknown responses, associated with therapeutic targeting of miRNAs. miR-21 is upregulated in cardiac fibroblasts in response to pathological stresses that promote cardiac fibrosis. Systemic delivery of cholesterol-modified antagomirs directed against miR-21 has been reported to prevent fibrosis and cardiac hypertrophy while preserving cardiac contractility under conditions of pressure overload. Remarkably, miR-21 antagomirs can apparently also cause regression of fibrosis and restore function in severely injured hearts. These salutary effects of miR-21 inhibition have been attributed to the regulation of a single target, Sprouty 1 (SPRY1); SPRY1 acts as an inhibitor of mitogen-activated protein kinase (MAPK) signalling, which is a driver of cardiac dysfunction[9]. According to this model, upregulation of miR-21 in response to stress would be predicted to inhibit SPRY1 expression, thereby promoting MAPK signalling, whereas inhibition of miR-21 would have the opposite effect[9].

There is also mounting evidence for the involvement of miR-21 in fibrosis of other tissues[65–68] as well as in cancer[69]. Systemic delivery of miR-21 inhibitors, for example, has shown efficacy in suppressing extracellular matrix production in settings of muscular dystrophy, renal fibrosis and pulmonary fibrosis, suggesting that miR-21 occupies a central node in pathways of pathological fibrosis. The suppression of tumorigenesis by miR-21 inhibitors[69] appears to result from the regulation of different mRNA targets and exemplifies the ability of individual miRNAs to modulate distinct cellular processes depending on the physiological status of the cell and the abundance and availability of targets.

In contrast to these findings, mice with genetic deletion of miR-21 show no diminution in fibrosis in response to multiple cardiac stresses, indicating that miR-21 does not have an obligatory role in this pathological process[41]. Additionally, different antimiR chemistries show different functional outcomes with respect to miR-21 inhibition[41,70]. For example, a 22-mer antimiR-21 modified by cholesterol, 2′-F or 2′-MOE prevented cardiac fibrosis and loss of cardiac contractility in mice subjected to thoracic aortic banding (TAB), whereas an 8-mer tiny LNA-modified antimiR-21 oligonucleotide showed no efficacy in suppressing fibrosis or preventing cardiac dysfunction following TAB in mice, despite forming a stable heteroduplex with the miR-21 target miRNA and inducing downstream target de-repression[41,70]. The basis for the seemingly contradictory conclusions regarding the role of miR-21 in fibrosis has not been resolved, but there are several potential explanations. It is conceivable, for example, that genetic deletion of miR-21 throughout embryonic and postnatal stages allows for compensatory mechanisms that substitute for miR-21 function, and such mechanisms are not deployed under conditions of acute miR-21 inhibition with antagomirs. Alternatively, or in addition, individual antimiR-21 chemistries might have a different mode of action, hence resulting in a different outcome.

Studies by Care *et al.*[71] and Liu *et al.*[72] further document the discrepancies in phenotypic outcomes resulting from oligonucleotide-based miRNA inhibition versus genetic deletion of a miRNA. In this case, antagomir-mediated inhibition of miR-133 induced cardiac hypertrophy in mice[71], whereas genetic deletion of miR-133 resulted in partial lethality and a dilated cardiomyopathy in the survivors[72].

Control of cardiomyocyte apoptosis and regeneration by the miR-15 family. Members of the miR-15 family, which includes miR-15a, miR-15b, miR-16-1, miR-16-2, miR-195 and miR-497, have been implicated in cell cycle arrest and cell survival in several cell types, by regulating many anti-apoptotic and cell cycle genes[73]. Members of this miRNA family are upregulated in the heart in response to cardiac stress and myocardial infarction, which cause death of cardiomyocytes and loss of pump function[10]. Moreover, forced overexpression of miR-195 in the heart is sufficient to cause myocyte loss and heart failure, indicating that this miRNA family is a crucial component of heart disease pathogenesis[1]. The multiplicity of miR-15 family members exemplifies one of the challenges associated with miRNA inhibition as a therapeutic strategy, as sequence divergence among different members of miRNA families prevents their collective inhibition by the delivery of a single antisense oligonucleotide inhibitor.

One approach to potentially overcome such miRNA redundancy is the use of tiny 8-mer LNA-modified inhibitors, which target the conserved seed regions of miRNAs and thereby enable inhibition of co-expressed miRNA family members that may have redundant biological functions (FIG. 2). A recent report showed that an 8-mer directed against the seed region of the miR-15 family was able to target mutiple members of the miR-15 family, which all contain a similar seed region but different 3′ regions[13]. In comparison with an LNA-modified 16-mer preferentially targeting miR-15b, the 8-mer was more efficacious in eliciting downstream target de-repression, whereas both chemistries were equally distributed to cardiac tissue in mice and pigs. Mouse efficacy studies, using a model of ischaemia reperfusion, showed that inhibition of the miR-15 family reduced infarct size and improved cardiac function 2 weeks after ischaemic damage[13].

Interestingly, miR-15 family members are also upregulated in the heart during the first few days after birth[74]. Recent studies have shown that the neonatal mouse heart is capable of complete regeneration following amputation of the apex or ischaemic injury during the period before miR-15 family upregulation[75], and precocious upregulation of miR-195 in the heart suppresses this neonatal regenerative response. The inhibitory influence of miR-195 on heart muscle regeneration appears to be attributable to the inhibition of a cohort of pro-proliferative proteins[74]. Thus, antimiR-mediated inhibition of miR-15 family members represents an intriguing strategy to enhance cardiac repair following injury.

Control of stress-induced neoangiogenesis by miR-92a. AntimiR strategies have also been effective in targeting miRNAs that are preferentially expressed in endothelial

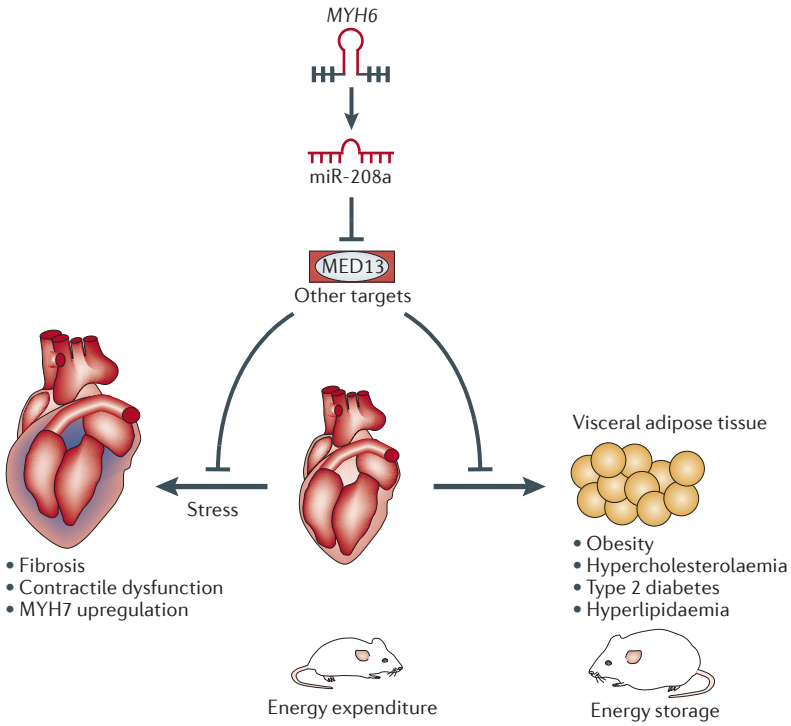

Figure 3 | **Multiple functions of miR-208 in the heart.** The microRNA miR-208a is encoded by an intron of the gene encoding myosin 6 (*MYH6*). miR-208a is required for the upregulation of myosin 7 (*MYH7*) and cardiac fibrosis in response to stress. miR-208a inhibits mediator of RNA polymerase II transcription subunit 13 (MED13), a component of the mediator complex, which regulates metabolic genes and additional targets. Inhibition of miR-208a with an antimiR (a miRNA inhibitor) inhibits cardiac remodelling and enhances systemic energy metabolism, resulting in beneficial effects in the settings of obesity and diabetes.

and smooth muscle cells. miR-92a, a member of the miR-17–miR-92 cluster, has been implicated in neoangiogenesis following ischaemic injury[6]. Intravenous administration of a miR-92a antagomir showed efficacious inhibition of the miRNA, and resulted in enhanced blood vessel growth as well as functional improvement of damaged tissue in models of hindlimb ischaemia and myocardial infarction[6]. The neoangiogenic effect of inhibiting miR-92a *in vivo* was attributed to the derepression of several pro-angiogenic factors, including integrin α5 — a direct target of miR-92a. Although the pro-angiogenic effect of miR-92a inhibition is currently being explored as a potential therapeutic approach in diseases such as ischaemic heart disease or peripheral artery disease, additional studies have shown that miR-92a regulates the atheroprotective transcription factors Krüppel-like factor 2 (KLF2) and KLF4 (REFS 76,77). KLF2 and KLF4 regulate gene networks that confer atheroprotective properties to the endothelium through an anti-inflammatory and anticoagulant effect[78] and, as such, antimiR-92a might exert comparable properties.

Control of extracellular matrix deposition by the miR-29 family. A fibroblast-enriched miRNA family, miR-29, has shown strong coordinate effects by directly regulating the expression of at least 16 confirmed extracellular matrix genes[79]. The miR-29 family consists of miR-29a, miR-29b and miR-29c, which are expressed as two bicistronic clusters (miR-29a–miR-29b1 and miR-29b2–miR-29c) and are largely homologous in sequence, with several mismatches between the different members in the 3′ regions of the mature miRNA[10]. Members of the miR-29 family are downregulated in response to myocardial infarction in mice, specifically in the infarcted region, and their downregulation correlates with increased expression of extracellular matrix-related genes required for infarct healing[10]. Members of this miRNA family are also downregulated during pathological cardiac remodelling[1]. A cholesterol-conjugated miR-29 antagomir was detected in several tissues after delivery by i.v. injection in mice, which resulted in de-repression of several direct target genes[10]. The presence in the genome of four different copies of this miRNA with a comparable set of predicted targets, in combination with the fact that many of these verified targets are involved in extracellular matrix deposition, strongly supports a potent influence of miR-29 on fibrosis (FIG. 4). miR-29 mimicry or overexpression could have therapeutic benefit in different forms of tissue fibrosis by inducing a subsequent decrease in the expression of fibrosis-related genes, as has been shown for heart[10], kidney[80–82], liver[83–85], lung[86] and systemic sclerosis[87].

The obvious importance of this miRNA family was further demonstrated by recent reports on miR-29 inhibition for vascular indications. Levels of miR-29 were found to be upregulated in two animal models of aortic dilation as well as in biopsy samples of human thoracic aneurysms, which correlated with a profound downregulation of numerous extracellular matrix components[7,88]. LNA-modified oligonucleotides against miR-29 were able to abrogate aortic dilation induced by angiotensin II in mice, which suggests that miR-29 inhibition could have a role in maintaining vascular integrity during aneurysm formation[7]. These data were confirmed by studies in two additional models of aortic aneurysms, showing that antimiR-29 induced an increase in collagen expression, resulting in a significant reduction in abdominal aneurysm progression[88]. The concept of miR-29 inhibition leading to enhanced vascular integrity was further supported by data showing that miR-29 has a role in early aneurysm formation in a mouse model of Marfan syndrome[89]. Finally, inhibition of miR-29 can dramatically increase elastin expression in cells from patients with elastin haploinsufficiencies, such as Williams–Beuren syndrome, which is characterized by aortic stenosis[90]. Combined, these data support miR-29 inhibition as a therapeutic approach in various vascular indications such as aneurysm formation; however, even though short-term treatment with antimiR-29 does not appear to result in liver or kidney fibrosis[7], adverse effects of stimulating extracellular matrix deposition should be considered in more chronic treatment regimens.

Control of viral myocarditis by miR-155. miR-155 is processed from an exon of a non-coding RNA transcribed from the B cell integration cluster (BIC), which is highly expressed in activated B and T cells as well as in monocytes

Aneurysm
An abnormal widening or ballooning of a portion of an artery resulting from weakness in the wall of the blood vessel.

Marfan syndrome
A systemic connective tissue disorder in which aortic aneurysm formation is the leading cause of death.

and macrophages[91]. miR-155 levels change dynamically during both haematopoietic lineage differentiation and the course of the immune response, and to date miR-155 has been implicated in several diseases, including cancer, cardiovascular disease and viral infections[92,93]. With regard to cardiovascular disease, it was discovered that a single nucleotide polymorphism (+1166A/C) in the human angiotensin II type 1 receptor (AT1), the receptor through which angiotensin II exerts most of its actions, is associated with hypertension, cardiac hypertrophy and myocardial infarction, and disrupts a miR-155 binding site so it can no longer reduce AT1 expression[94]. Additional data suggesting that miR-155 might be involved in regulating blood pressure came from a study on homozygous twins discordant for trisomy 21. The participants of this study expressed elevated levels of miR-155 (located on chromosome 21), which correlated with a lower level of AT1 expression and low blood pressure[95].

Although it has been well established that miR-155 regulates myeloid and lymphoid immune cell function[96], it has recently been shown that miR-155 is also upregulated during the acute inflammatory phase of viral myocarditis[97]. Acute viral myocarditis is an important cause of heart failure, resulting from infection of the heart by cardiotrophic viruses. *In situ* hybridization of heart tissue suffering from acute viral myocarditis indicates that the increase in miR-155 expression is induced by haematopoietic cells and all leukocyte subtypes, including macrophages and T cells. Therapeutic treatment with an antimiR against miR-155 elicited an increase in levels of miR-155 targets, and detection of 6-carboxyfluorescein (FAM)-labelled antimiR indicated a distribution of miR-155 to cardiomyocytes, endothelial borders as well as circulating monocytes, lymphocytes and neutrophils. Moreover, antimiR-155 treatment resulted in reduced myocardial damage and increased survival in response to viral myocarditis. This effect is likely to be immune-cell-autonomous as miR-155 inhibition did not affect viral load, myocyte viability or cytokine signalling in unstressed hearts before their infiltration by immune cells[97]. Although the authors did not observe an effect of antimiR treatment on cardiac fibrosis through a potential de-repression of AT1, this will have to be taken into account when considering antimiR-155 as a therapy for viral myocarditis.

Control of angiogenesis and vascular stability by miR-23, miR-27 and miR-24. Another miRNA cluster with prominent roles in vascular indications is the cluster composed of miR-23, miR-27 and miR-24. The human genome contains two versions of this cluster, both of which are enriched in endothelial cells[98,99]. Members of this cluster are involved in cell cycle control as well as proliferation and differentiation of various cell types, and have important functions during angiogenesis[98,99].

Choroidal neovascularization, which is characterized by abnormal vascular growth in the back of the eye, is a hallmark of age-related macular degeneration. A recent study by Zhou *et al.*[99] showed that miR-23 and miR-27 are upregulated during normal retinal vascular development and in response to laser-induced choroidal neovascularization. *In vivo* studies using LNA-modified antimiRs against both miR-23 and miR-27 demonstrated that inhibition of both miRNAs resulted in increased levels of SPRY2, semaphorin 6A and semaphorin 6D, which repressed neovascularization in the choroid in response to laser injury[99]. Interestingly, *in vitro* inhibition of either miR-23 or miR-27 in human umbilical vein endothelial cells caused a corresponding increase in miR-27 or miR-23 levels, respectively. *In vivo* inhibition of both miR-23 and miR-27 resulted in an increase in miR-24 levels. These effects are probably biological rather than chemical, as a scrambled oligonucleotide control with a comparable chemical composition did not induce this effect. Although this study did not present *in vivo* data after inhibition of either miR-23 or miR-27 alone, the *in vitro* data — based on target de-repression — seem to suggest that miR-27 is the major player. From a therapeutic standpoint, it would be a developmental challenge to investigate two compounds in parallel, and targeting two separate miRNAs could increase the risk of off-target effects.

The third member of the cluster, miR-24, was recently implicated in cardiac angiogenesis after myocardial infarction[100]. Cardiac ischaemia was shown to increase miR-24 levels in endothelial cells, and antagomir-based inhibition of miR-24 in endothelial cells reduced infarct size by preventing apoptosis and enhancing vascularity, probably through direct regulation of the transcription factors GATA2 and p21-activated kinase 4 (PAK4). Interestingly, in tracing the cellular fate of the antagomir by Cy labelling, the authors found that at a high dose (80 mg per kg) the antagomir was taken up by both cardiomyocytes and endothelial cells, whereas at a lower dose (5 mg per kg) the antagomir was preferentially taken up by endothelial cells[100]. This might be relevant as it was previously shown that increased levels of miR-24 might have a cardioprotective effect in myocytes during an ischaemic event by decreasing the expression of the pro-apoptotic protein BIM (BCL-2 interacting mediator of cell death)[101]. These findings further highlight the potential functional differences of miRNAs in individual cell types, which should be taken into account when considering miR-24 as a therapeutic target.

Control of pulmonary hypertension by miR-145. Vascular smooth muscle cell (VSMC)-enriched miR-145 is expressed as part of the miR-143–miR-145 cluster[102]. Genetic deletion of this cluster showed that these miRNAs are essential for VSMC contractility[12,102,103]. Although miR-143 and miR-145 have distinct sequences, they coordinately regulate overlapping genes but also target different genes with regulatory functions in actin remodelling. Individual deletion of the miRNAs in mice indicated a prominent and distinct role for miR-145 in VSMC contractility, as this miRNA appeared to be mainly responsible for the thinning of the VSMC layer. Blood pressure analysis in these genetic models showed that removal of the cluster induced arterial hypotension at the baseline and reduced the increase in systolic pressure in response to angiotensin II[12,102].

In lung samples of patients with both idiopathic and heritable pulmonary hypertension, miR-145 levels are upregulated in comparison with unaffected controls.

Angiotensin II type 1 receptor
(AT1). The receptor through which angiotensin II exerts most of its cardiac actions. This receptor has been associated with hypertension, cardiac hypertrophy and myocardial infarction, and is a direct target of the microRNA miR-155.

Viral myocarditis
Inflammation of the heart that can lead to cardiomyopathy.

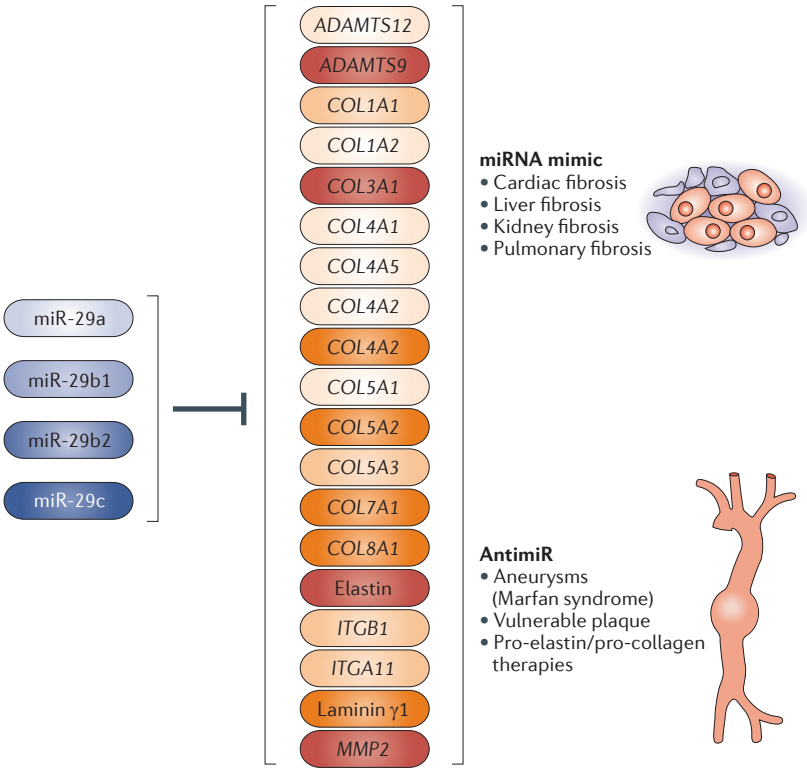

Figure 4 | **MicroRNAs often regulate related target genes.** Members of the miR-29 family exemplify the influence of microRNAs (miRNAs) on targets involved in common cellular processes. In this case, miR-29 coordinately inhibits the expression of numerous extracellular matrix proteins, such that the downregulation of this miRNA family under conditions of cardiovascular stress leads to vascular remodelling and fibrosis. ADAMTS, a disintegrin and metalloproteinase with thrombospondin motifs; COL1A1, collagen type 1 α1; ITGA11, integrin α11; MMP2, matrix metalloproteinase 2.

Using chronic hypoxia as a model for pulmonary arterial hypertension in mice showed that antimiR-mediated inhibition of miR-145 reduced systolic right ventricular pressure[8]. Histological analysis supported these findings by showing that antimiR-145 reduced pulmonary vascular remodelling in response to hypoxia[8]. Although these initial data are encouraging and suggest that miR-145 inhibition has therapeutic potential in the setting of pulmonary arterial hypertension, genetic deletion of miR-145 resulted in a more pronounced phenotype as it reduced both blood pressure and right ventricular remodelling, which might indicate that the timing and incidence of dosing requires optimization. Additionally, as genetic deletion of the miRNA cluster indicates a more supportive function of this cluster in maintaining a normal VSMC phenotype and regulating normal contractility of arteries[12], caution should be taken when applying antimiR strategies to more chronic diseases, and local delivery options should be contemplated.

Challenges in clinical development

The preclinical studies discussed above indicate that all cardiovascular cell types can be targeted by miRNA inhibitors, and inhibition of miRNAs can have profound effects on cardiovascular function, supporting enthusiasm for further exploration of miRNAs as novel drug candidates. However, numerous challenges and questions remain in the path towards the development of miRNA-based therapeutics in general. In most of the animal studies to date, the phenotypic effects of miRNA inhibition have only been studied in the target tissue of interest, which might overlook off-target effects in additional tissues. Moreover, the doses used in most studies are unlikely to be therapeutically feasible. Follow-up preclinical studies will have to guide appropriate dosing regimens in order to establish the lowest possible efficacious doses while attempting to prevent unacceptable side effects.

The identification and validation of miRNA targets is especially relevant to the development of miRNA-based therapeutics in general. In contrast to many other therapeutic modalities, antimiR drugs are designed with the understanding that they will affect all genes that are under the control of the target miRNA. Although miRNAs often target many related genes involved in cellular processes, which are intended to be manipulated by the antimiR therapeutic (FIG. 4), a single miRNA will probably also target unrelated genes and possibly produce unexpected (and sometimes undesired) changes in gene expression. An excellent example of the diverse, and potentially unanticipated, actions of miRNAs was provided by the finding that antimiR therapeutics directed against the cardiac-specific miR-208a prevented obesity and metabolic syndrome in mice maintained on a high-fat diet[58]. Before these findings, miR-208a was thought to function primarily to modulate myosin switching in striated muscle cells[55–57]. However, mechanistic follow-up of the metabolic effects of miR-208a inhibitors revealed a fascinating function of this miRNA in the regulation of a network of transcription factors that are involved in metabolic control and energy homeostasis. The potential pleiotropy of miRNA actions contrasts with the mechanistic basis of most classical drugs, which act with maximal specificity against single cellular targets. Additional ambiguity derives from the relatively modest inhibitory effects of individual miRNAs on mRNA targets, as revealed in miRNA loss-of-function studies. It is not uncommon, for example, for miRNA inhibition to result in minimal increases (<1.5-fold) in the expression of mRNA targets, suggesting that it is the cumulative impact of small changes in the expression of myriad targets — rather than pronounced changes in single targets — that mediates the biological actions of miRNAs on disease processes. Thus, it is often difficult or impossible to ascribe the effects of a miRNA to the regulation of a specific mRNA target. The multiplicity of miRNA targets also raises crucial issues with respect to possible off-target effects of miRNA inhibitors in different tissues and opposing actions of miRNAs on different phenotypic readouts. For example, if a miRNA displays broad tissue distribution, its systemic inhibition may have multiple effects in different tissues, thus confounding the interpretation of the responses to miRNA-based therapeutics. In addition, a miRNA may exert counterbalancing actions on cellular pathways such that the inhibition of

Miravirsen
Pharmacological name for antimiR-122 (a microRNA inhibitor targeting miR-122), which has shown therapeutic efficacy in clinical trials by providing long-lasting suppression of viraemia.

a miRNA could, in principle, have both beneficial and deleterious consequences in the same or different tissues. Because miRNAs often control multiple components of complex regulatory networks, modulation of a specific miRNA — either up- or downregulation — can result in re-balancing of the network. In this respect, the multiplicity of miRNA targets can minimize bypass or desensitization mechanisms that can diminish the efficacy of certain drugs directed against single targets.

Despite these potential challenges, antimiR therapeutics have recently become a reality, following the successful Phase I and Phase II clinical trials of Santaris Pharma's antimiR against miR-122, miravirsen, which is currently in development for the treatment of HCV (BOX 1). It is hoped that these promising findings will accelerate the development of miRNA-targeting therapeutics into additional disease areas such as cardiovascular disease.

miRNAs have also been found in plasma and blood samples and have emerged as potential biomarkers for disease. However, many questions remain regarding the basis for the altered expression of such biomarkers, their relationship to disease progression and their power for predicting disease progression and clinical outcome.

In conclusion, the obvious relevance and importance of miRNAs during disease, in addition to the success of the first clinical data showing the safety and efficacy of an antimiR, support enthusiasm for the continued exploration of miRNAs as a new class of drug targets.

1. van Rooij, E. *et al.* A signature pattern of stress-responsive microRNAs that can evoke cardiac hypertrophy and heart failure. *Proc. Natl Acad. Sci. USA* **103**, 18255–18260 (2006).
This is the first description of changes in miRNA levels in murine and human heart disorders, and provides evidence for the relevance of miRNAs in heart disease.
2. Ikeda, S. *et al.* Altered microRNA expression in human heart disease. *Physiol. Genomics* **31**, 367–373 (2007).
This study describes unique miRNA signature patterns for different forms of human heart disease.
3. Thum, T. *et al.* MicroRNAs in the human heart: a clue to fetal gene reprogramming in heart failure. *Circulation* **116**, 258–267 (2007).
This study suggests a relationship between changes in miRNAs and the expression of fetal genes in human heart disease.
4. Bonauer, A., Boon, R. A. & Dimmeler, S. Vascular microRNAs. *Curr. Drug Targets* **11**, 943–949 (2010).
5. Zampetaki, A. & Mayr, M. MicroRNAs in vascular and metabolic disease. *Circ. Res.* **110**, 508–522 (2012).
6. Bonauer, A. *et al.* MicroRNA-92a controls angiogenesis and functional recovery of ischemic tissues in mice. *Science* **324**, 1710–1713 (2009).
7. Boon, R. A. *et al.* MicroRNA-29 in aortic dilation: implications for aneurysm formation. *Circ. Res.* **109**, 1115–1119 (2011).
8. Caruso, P. *et al.* A role for miR-145 in pulmonary arterial hypertension. *Circ. Res.* **111**, 290–300 (2012).
9. Thum, T. *et al.* MicroRNA-21 contributes to myocardial disease by stimulating MAP kinase signalling in fibroblasts. *Nature* **456**, 980–984 (2008).
10. van Rooij, E. *et al.* Dysregulation of microRNAs after myocardial infarction reveals a role of miR-29 in cardiac fibrosis. *Proc. Natl Acad. Sci. USA* **105**, 13027–13032 (2008).
11. Wang, S. *et al.* The endothelial-specific microRNA miR-126 governs vascular integrity and angiogenesis. *Dev. Cell* **15**, 261–271 (2008).
12. Xin, M. *et al.* MicroRNAs miR-143 and miR-145 modulate cytoskeletal dynamics and responsiveness of smooth muscle cells to injury. *Genes Dev.* **23**, 2166–2178 (2009).
13. Hullinger, T. G. *et al.* Inhibition of miR-15 protects against cardiac ischemic injury. *Circ. Res.* **110**, 71–81 (2012).
14. Mutharasan, R. K., Nagpal, V., Ichikawa, Y. & Ardehali, H. microRNA-210 is upregulated in hypoxic cardiomyocytes through Akt- and p53-dependent pathways and exerts cytoprotective effects. *Am. J. Physiol. Heart Circ. Physiol.* **301**, H1519–H1530 (2011).
15. Bartel, D. P. MicroRNAs: target recognition and regulatory functions. *Cell* **136**, 215–233 (2009).
This is a key review explaining miRNA biogenesis and function.
16. Orom, U. A., Nielsen, F. C. & Lund, A. H. MicroRNA-10a binds the 5'UTR of ribosomal protein mRNAs and enhances their translation. *Mol. Cell* **30**, 460–471 (2008).
17. Tay, Y., Zhang, J., Thomson, A. M., Lim, B. & Rigoutsos, I. MicroRNAs to Nanog, Oct4 and Sox2 coding regions modulate embryonic stem cell differentiation. *Nature* **455**, 1124–1128 (2008).
18. Guo, H., Ingolia, N. T., Weissman, J. S. & Bartel, D. P. Mammalian microRNAs predominantly act to decrease target mRNA levels. *Nature* **466**, 835–840 (2010).
19. Salmena, L., Poliseno, L., Tay, Y., Kats, L. & Pandolfi, P. P. A ceRNA hypothesis: the Rosetta Stone of a hidden RNA language? *Cell* **146**, 353–358 (2011).
20. Tay, Y. *et al.* Coding-independent regulation of the tumor suppressor PTEN by competing endogenous mRNAs. *Cell* **147**, 344–357 (2011).
21. Miska, E. A. *et al.* Most *Caenorhabditis elegans* microRNAs are individually not essential for development or viability. *PLoS Genet.* **3**, e215 (2007).
22. Park, C. Y., Choi, Y. S. & McManus, M. T. Analysis of microRNA knockouts in mice. *Hum. Mol. Genet.* **19**, R169–R175 (2010).
23. Small, E. M., Frost, R. J. & Olson, E. N. MicroRNAs add a new dimension to cardiovascular disease. *Circulation* **121**, 1022–1032 (2010).
24. Leung, A. K. & Sharp, P. A. MicroRNA functions in stress responses. *Mol. Cell* **40**, 205–215 (2010).
25. Stenvang, J., Petri, A., Lindow, M., Obad, S. & Kauppinen, S. Inhibition of microRNA function by antimiR oligonucleotides. *Silence* **3**, 1 (2012).
26. Kota, J. *et al.* Therapeutic microRNA delivery suppresses tumorigenesis in a murine liver cancer model. *Cell* **137**, 1005–1017 (2009).
27. Miyazaki, Y. *et al.* Viral delivery of miR-196a ameliorates the SBMA phenotype via the silencing of CELF2. *Nature Med.* **18**, 1136–1141 (2012).
28. Bish, L. T. *et al.* Adeno-associated virus (AAV) serotype 9 provides global cardiac gene transfer superior to AAV1, AAV6, AAV7, and AAV8 in the mouse and rat. *Hum. Gene Ther.* **19**, 1359–1368 (2008).
29. Gao, G. *et al.* Adenovirus-based vaccines generate cytotoxic T lymphocytes to epitopes of NS1 from dengue virus that are present in all major serotypes. *Hum. Gene Ther.* **19**, 927–936 (2008).
30. Zincarelli, C., Soltys, S., Rengo, G. & Rabinowitz, J. E. Analysis of AAV serotypes 1–9 mediated gene expression and tropism in mice after systemic injection. *Mol. Ther.* **16**, 1073–1080 (2008).
31. Pasquinelli, A. E. MicroRNAs and their targets: recognition, regulation and an emerging reciprocal relationship. *Nature Rev. Genet.* **13**, 271–282 (2012).
This paper reviews the different influences of stress on miRNA function.
32. Krutzfeldt, J. *et al.* Specificity, duplex degradation and subcellular localization of antagomirs. *Nucleic Acids Res.* **35**, 2885–2892 (2007).
33. Krutzfeldt, J. *et al.* Silencing of microRNAs *in vivo* with 'antagomirs'. *Nature* **438**, 685–689 (2005).
This is the first study to show that antimiRs can be used to silence miRNAs *in vivo* using antagomirs.
34. Levin, A. A. A review of the issues in the pharmacokinetics and toxicology of phosphorothioate antisense oligonucleotides. *Biochim. Biophys. Acta* **1489**, 69–84 (1999).
35. van Rooij, E., Purcell, A. L. & Levin, A. A. Developing microRNA therapeutics. *Circ. Res.* **110**, 496–507 (2012).
36. Esau, C. *et al.* miR-122 regulation of lipid metabolism revealed by *in vivo* antisense targeting. *Cell Metab.* **3**, 87–98 (2006).
37. Lanford, R. E. *et al.* Therapeutic silencing of microRNA-122 in primates with chronic hepatitis C virus infection. *Science* **327**, 198–201 (2010).
This paper describes the therapeutic efficacy of antimiR-based inhibition of miR-122 in primates infected with HCV.
38. Rayner, K. J. *et al.* Inhibition of miR-33a/b in non-human primates raises plasma HDL and lowers VLDL triglycerides. *Nature* **478**, 404–407 (2011).
This study shows the therapeutic benefit of antimiR-mediated inhibition of miR-33 in non-human primates in increasing plasma levels of high-density lipoprotein (HDL) and lowering very-low-density lipoprotein (VLDL) triglycerides.
39. Obad, S. *et al.* Silencing of microRNA families by seed-targeting tiny LNAs. *Nature Genet.* **43**, 371–378 (2011).
40. Garchow, B. G. *et al.* Silencing of microRNA-21 *in vivo* ameliorates autoimmune splenomegaly in lupus mice. *EMBO Mol. Med.* **3**, 605–615 (2011).
41. Patrick, D. M. *et al.* Stress-dependent cardiac remodeling occurs in the absence of microRNA-21 in mice. *J. Clin. Invest.* **120**, 3912–3916 (2010).
42. Sheehan, J. P. & Phan, T. M. Phosphorothioate oligonucleotides inhibit the intrinsic tenase complex by an allosteric mechanism. *Biochemistry* **40**, 4980–4989 (2001).
43. Henry, S. P. *et al.* Complement activation is responsible for acute toxicities in rhesus monkeys treated with a phosphorothioate oligodeoxynucleotide. *Int. Immunopharmacol.* **2**, 1657–1666 (2002).
44. Swayze, E. E. *et al.* Antisense oligonucleotides containing locked nucleic acid improve potency but cause significant hepatotoxicity in animals. *Nucleic Acids Res.* **35**, 687–700 (2007).
45. Elmen, J. *et al.* Antagonism of microRNA-122 in mice by systemically administered LNA-antimiR leads to up-regulation of a large set of predicted target mRNAs in the liver. *Nucleic Acids Res.* **36**, 1153–1162 (2008).
46. Geary, R. S., Yu, R. Z. & Levin, A. A. Pharmacokinetics of phosphorothioate antisense oligodeoxynucleotides. *Curr. Opin. Investig. Drugs* **2**, 562–573 (2001).
47. Elmen, J. *et al.* LNA-mediated microRNA silencing in non-human primates. *Nature* **452**, 896–899 (2008).
48. Montgomery, R. L. *et al.* Therapeutic inhibition of miR-208a improves cardiac function and survival during heart failure. *Circulation* **124**, 1537–1547 (2011).
49. Chang, J. *et al.* miR-122, a mammalian liver-specific microRNA, is processed from hcr mRNA and may downregulate the high affinity cationic amino acid transporter CAT-1. *RNA Biol.* **1**, 106–113 (2004).
50. Mukherji, S. *et al.* MicroRNAs can generate thresholds in target gene expression. *Nature Genet.* **43**, 854–859 (2011).
51. Hendrickson, D. G. *et al.* Concordant regulation of translation and mRNA abundance for hundreds of targets of a human microRNA. *PLoS Biol.* **7**, e1000238 (2009).

52. Baek, D. *et al.* The impact of microRNAs on protein output. *Nature* **455**, 64–71 (2008).
53. Selbach, M. *et al.* Widespread changes in protein synthesis induced by microRNAs. *Nature* **455**, 58–63 (2008).
References 52 and 53 show that a single miRNA can repress the production of hundreds of proteins but this repression is typically relatively mild. Furthermore, although direct repression of translation occurs, mRNA destabilization is the major driver of gene repression.
54. Wolff, J. A. & Budker, V. The mechanism of naked DNA uptake and expression. *Adv. Genet.* **54**, 3–20 (2005).
55. Callis, T. E. *et al.* MicroRNA-208a is a regulator of cardiac hypertrophy and conduction in mice. *J. Clin. Invest.* **119**, 2772–2786 (2009).
56. van Rooij, E. *et al.* Control of stress-dependent cardiac growth and gene expression by a microRNA. *Science* **316**, 575–579 (2007).
This study describes the first genetic deletion by a miRNA, miR-208, which is a cardiomyocyte-specific miRNA involved in cardiac remodelling during stress.
57. van Rooij, E. *et al.* A family of microRNAs encoded by myosin genes governs myosin expression and muscle performance. *Dev. Cell* **17**, 662–673 (2009).
58. Grueter, C. E. *et al.* A cardiac microRNA governs systemic energy homeostasis by regulation of MED13. *Cell* **149**, 671–683 (2012).
This paper describes how inhibition of a cardiac-specific miRNA, miR-208, can have an effect on total body metabolism by regulation of downstream cardiac targets.
59. Taubert, S., Van Gilst, M. R., Hansen, M. & Yamamoto, K. R. A mediator subunit, MDT-15, integrates regulation of fatty acid metabolism by NHR-49-dependent and -independent pathways in *C. elegans*. *Genes Dev.* **20**, 1137–1149 (2006).
60. Wang, W. *et al.* Mediator MED23 links insulin signaling to the adipogenesis transcription cascade. *Dev. Cell* **16**, 764–771 (2009).
61. Yang, F. *et al.* An ARC/mediator subunit required for SREBP control of cholesterol and lipid homeostasis. *Nature* **442**, 700–704 (2006).
62. Frost, R. J. & Olson, E. N. Control of glucose homeostasis and insulin sensitivity by the Let-7 family of microRNAs. *Proc. Natl Acad. Sci. USA* **108**, 21075–21080 (2011).
63. Trajkovski, M. *et al.* MicroRNAs 103 and 107 regulate insulin sensitivity. *Nature* **474**, 649–653 (2011).
64. Zhu, H. *et al.* The Lin28/let-7 axis regulates glucose metabolism. *Cell* **147**, 81–94 (2011).
65. Ardite, E. *et al.* PAI-1-regulated miR-21 defines a novel age-associated fibrogenic pathway in muscular dystrophy. *J. Cell Biol.* **196**, 163–175 (2012).
66. Liu, G. *et al.* miR-21 mediates fibrogenic activation of pulmonary fibroblasts and lung fibrosis. *J. Exp. Med.* **207**, 1589–1597 (2010).
67. Zarjou, A., Yang, S., Abraham, E., Agarwal, A. & Liu, G. Identification of a microRNA signature in renal fibrosis: role of miR-21. *Am. J. Physiol. Renal Physiol.* **301**, F793–F801 (2011).
68. Zhong, X., Chung, A. C., Chen, H. Y., Meng, X. M. & Lan, H. Y. Smad3-mediated upregulation of miR-21 promotes renal fibrosis. *J. Am. Soc. Nephrol.* **22**, 1668–1681 (2011).
69. Hatley, M. E. *et al.* Modulation of K-Ras-dependent lung tumorigenesis by microRNA-21. *Cancer Cell* **18**, 282–293 (2010).
70. Thum, T. *et al.* Comparison of different miR-21 inhibitor chemistries in a cardiac disease model. *J. Clin. Invest.* **121**, 461–462; author reply 462–463 (2011).
71. Care, A. *et al.* MicroRNA-133 controls cardiac hypertrophy. *Nature Med.* **13**, 613–618 (2007).
72. Liu, N. *et al.* microRNA-133a regulates cardiomyocyte proliferation and suppresses smooth muscle gene expression in the heart. *Genes Dev.* **22**, 3242–3254 (2008).
73. He, J. F., Luo, Y. M., Wan, X. H. & Jiang, D. Biogenesis of miRNA-195 and its role in biogenesis, the cell cycle, and apoptosis. *J. Biochem. Mol. Toxicol.* **25**, 404–408 (2011).
74. Porrello, E. R. *et al.* MiR-15 family regulates postnatal mitotic arrest of cardiomyocytes. *Circ. Res.* **109**, 670–679 (2011).
75. Porrello, E. R. *et al.* Transient regenerative potential of the neonatal mouse heart. *Science* **331**, 1078–1080 (2011).
76. Fang, Y. & Davies, P. F. Site-specific microRNA-92a regulation of Kruppel-like factors 4 and 2 in atherosusceptible endothelium. *Arterioscler. Thromb. Vasc. Biol.* **32**, 979–987 (2012).
77. Wu, W. *et al.* Flow-dependent regulation of Kruppel-like factor 2 is mediated by microRNA-92a. *Circulation* **124**, 633–641 (2011).
78. Parmar, K. M. *et al.* Integration of flow-dependent endothelial phenotypes by Kruppel-like factor 2. *J. Clin. Invest.* **116**, 49–58 (2006).
79. Kriegel, A. J., Liu, Y., Fang, Y., Ding, X. & Liang, M. The miR-29 family: genomics, cell biology, and relevance to renal and cardiovascular injury. *Physiol. Genom.* **44**, 237–244 (2012).
80. Qin, W. *et al.* TGF-β/Smad3 signaling promotes renal fibrosis by inhibiting miR-29. *J. Am. Soc. Nephrol.* **22**, 1462–1474 (2011).
81. Wang, B. *et al.* Suppression of microRNA-29 expression by TGF-β1 promotes collagen expression and renal fibrosis. *J. Am. Soc. Nephrol.* **23**, 252–265 (2012).
82. Xiao, J. *et al.* miR-29 inhibits bleomycin-induced pulmonary fibrosis in mice. *Mol. Ther.* **20**, 1251–1260 (2012).
83. Roderburg, C. *et al.* Micro-RNA profiling reveals a role for miR-29 in human and murine liver fibrosis. *Hepatology* **53**, 209–218 (2011).
84. Sekiya, Y., Ogawa, T., Yoshizato, K., Ikeda, K. & Kawada, N. Suppression of hepatic stellate cell activation by microRNA-29b. *Biochem. Biophys. Res. Commun.* **412**, 74–79 (2011).
85. Zhang, Y. *et al.* Protective role of estrogen-induced miRNA-29 expression in carbon tetrachloride-induced mouse liver injury. *J. Biol. Chem.* **287**, 14851–14862 (2012).
86. Cushing, L. *et al.* miR-29 is a major regulator of genes associated with pulmonary fibrosis. *Am. J. Respir. Cell Mol. Biol.* **45**, 287–294 (2011).
87. Maurer, B. *et al.* MicroRNA-29, a key regulator of collagen expression in systemic sclerosis. *Arthritis Rheum.* **62**, 1733–1743 (2010).
88. Maegdefessel, L. *et al.* Inhibition of microRNA-29b reduces murine abdominal aortic aneurysm development. *J. Clin. Invest.* **122**, 497–506 (2012).
89. Merk, D. R. *et al.* miR-29b participates in early aneurysm development in Marfan syndrome. *Circ. Res.* **110**, 312–324 (2012).
90. Zhang, P. *et al.* Inhibition of microRNA-29 enhances elastin levels in cells haploinsufficient for elastin and in bioengineered vessels — brief report. *Arterioscler. Thromb. Vasc. Biol.* **32**, 756–759 (2012).
91. Turner, M. & Vigorito, E. Regulation of B- and T-cell differentiation by a single microRNA. *Biochem. Soc. Trans.* **36**, 531–533 (2008).
92. Faraoni, I., Antonetti, F. R., Cardone, J. & Bonmassar, E. miR-155 gene: a typical multifunctional microRNA. *Biochim. Biophys. Acta* **1792**, 497–505 (2009).
93. Tili, E., Croce, C. M. & Michaille, J. J. miR-155: on the crosstalk between inflammation and cancer. *Int. Rev. Immunol.* **28**, 264–284 (2009).
94. Martin, M. M. *et al.* The human angiotensin II type 1 receptor +1166 A/C polymorphism attenuates microRNA-155 binding. *J. Biol. Chem.* **282**, 24262–24269 (2007).
95. Sethupathy, P. *et al.* Human microRNA-155 on chromosome 21 differentially interacts with its polymorphic target in the AGTR1 3′ untranslated region: a mechanism for functional single-nucleotide polymorphisms related to phenotypes. *Am. J. Hum. Genet.* **81**, 405–413 (2007).
96. Thai, T. H. *et al.* Regulation of the germinal center response by microRNA-155. *Science* **316**, 604–608 (2007).
97. Corsten, M. F. *et al.* MicroRNA profiling identifies microRNA-155 as an adverse mediator of cardiac injury and dysfunction during acute viral myocarditis. *Circ. Res.* **111**, 415–425 (2012).
98. Bang, C., Fiedler, J. & Thum, T. Cardiovascular importance of the microRNA-23/27/24 family. *Microcirculation* **19**, 208–214 (2012).
99. Zhou, Q. *et al.* Regulation of angiogenesis and choroidal neovascularization by members of microRNA-23 ~ 27 ~ 24 clusters. *Proc. Natl Acad. Sci. USA* **108**, 8287–8292 (2011).
100. Fiedler, J. *et al.* MicroRNA-24 regulates vascularity after myocardial infarction. *Circulation* **124**, 720–730 (2011).
101. Qian, L. *et al.* miR-24 inhibits apoptosis and represses Bim in mouse cardiomyocytes. *J. Exp. Med.* **208**, 549–560 (2011).
102. Boettger, T. *et al.* Acquisition of the contractile phenotype by murine arterial smooth muscle cells depends on the mir143/145 gene cluster. *J. Clin. Invest.* **119**, 2634–2647 (2009).
103. Elia, L. *et al.* The knockout of miR-143 and -145 alters smooth muscle cell maintenance and vascular homeostasis in mice: correlates with human disease. *Cell Death Differ.* **16**, 1590–1598 (2009).
104. Marquart, T. J., Allen, R. M., Ory, D. S. & Baldan, A. miR-33 links SREBP-2 induction to repression of sterol transporters. *Proc. Natl Acad. Sci. USA* **107**, 12228–12232 (2010).
105. Najafi-Shoushtari, S. H. *et al.* MicroRNA-33 and the SREBP host genes cooperate to control cholesterol homeostasis. *Science* **328**, 1566–1569 (2010).
106. da Costa Martins, P. A. *et al.* MicroRNA-199b targets the nuclear kinase Dyrk1a in an auto-amplification loop promoting calcineurin/NFAT signalling. *Nature Cell Biol.* **12**, 1220–1227 (2010).
107. Ren, X. P. *et al.* MicroRNA-320 is involved in the regulation of cardiac ischemia/reperfusion injury by targeting heat-shock protein 20. *Circulation* **119**, 2357–2366 (2009).

Acknowledgements
We gratefully acknowledge J. Cabrera for graphics.

Competing interests statement
The authors declare competing financial interests: see Web version for details.

FURTHER INFORMATION
ClinicalTrials.gov website: http://clinicaltrials.gov
Santaris Pharma website — 3 October 2011 press release: http://www.santaris.com/news/2011/10/03/santaris-pharma-report-new-clinical-data-miravirsen-phase-2a-study-treat-hepatitis-c

ALL LINKS ARE ACTIVE IN THE ONLINE PDF

LETTER

doi:10.1038/nature11793

Obesity-induced overexpression of miR-802 impairs glucose metabolism through silencing of *Hnf1b*

Jan-Wilhelm Kornfeld[1,2,3], Catherina Baitzel[1,2,3], A. Christine Könner[1,2,3], Hayley T. Nicholls[1,2,3], Merly C. Vogt[1,2,3], Karolin Herrmanns[4], Ludger Scheja[5], Cécile Haumaitre[6,7], Anna M. Wolf[8], Uwe Knippschild[8], Jost Seibler[9], Silvia Cereghini[6,7], Joerg Heeren[5], Markus Stoffel[4] & Jens C. Brüning[1,2,3]

Insulin resistance represents a hallmark during the development of type 2 diabetes mellitus and in the pathogenesis of obesity-associated disturbances of glucose and lipid metabolism[1–3]. MicroRNA (miRNA)-dependent post-transcriptional gene silencing has been recognized recently to control gene expression in disease development and progression, including that of insulin-resistant type 2 diabetes. The deregulation of miRNAs miR-143 (ref. 4), miR-181 (ref. 5), and miR-103 and miR-107 (ref. 6) alters hepatic insulin sensitivity. Here we report that the expression of miR-802 is increased in the liver of two obese mouse models and obese human subjects. Inducible transgenic overexpression of miR-802 in mice causes impaired glucose tolerance and attenuates insulin sensitivity, whereas reduction of miR-802 expression improves glucose tolerance and insulin action. We identify *Hnf1b* (also known as *Tcf2*) as a target of miR-802-dependent silencing, and show that short hairpin RNA (shRNA)-mediated reduction of Hnf1b in liver causes glucose intolerance, impairs insulin signalling and promotes hepatic gluconeogenesis. In turn, hepatic overexpression of Hnf1b improves insulin sensitivity in $Lepr^{db/db}$ mice. Thus, this study defines a critical role for deregulated expression of miR-802 in the development of obesity-associated impairment of glucose metabolism through targeting of *Hnf1b*, and assigns Hnf1b an unexpected role in the control of hepatic insulin sensitivity.

To identify novel miRNAs that are deregulated during obesity development and that may contribute to the development of obesity-associated insulin resistance and type 2 diabetes, we carried out 'miRNome' expression profiling using miRNA microarrays on RNA isolated from liver of two mouse models of obesity and insulin resistance: (1) high fat diet (HFD)-fed mice compared to normal chow diet fed mice, and (2) mice homozygous for the diabetes *db* mutation of the leptin receptor ($Lepr^{db/db}$) compared to wild-type controls. Out of 769 miRNA-specific probe sets, 334 (43.4%) and 311 (40.4%) miRNAs were detectable in liver of normal chow diet/HFD and control/$Lepr^{db/db}$ livers, respectively (Supplementary Fig. 1a, b). In the liver of HFD-fed mice, expression of 66 miRNAs was significantly changed compared to miRNAs in normal chow diet controls, of which 90.1% were increased and 9.9% decreased (Supplementary Table 1). In $Lepr^{db/db}$ livers, 156 miRNAs were significantly changed, the vast majority (99%) were upregulated in $Lepr^{db/db}$ mice compared to controls (Supplementary Table 2). This screen confirmed an increased expression of miRNAs previously associated with obesity-induced insulin resistance, such as miR-103 and miR-107(ref. 6), miR-143 (ref. 4) and miR-335 (ref. 7). In addition to these reported changes in obesity-associated miRNA expression, our screen revealed an even more pronounced overexpression of miR-802 in the liver of HFD and $Lepr^{db/db}$ mice compared to controls (Supplementary Tables 1 and 2). Increased miR-802 expression in obese mouse models was further confirmed by quantitative real-time PCR with reverse transcription (qRT–PCR) analyses, which revealed a 5.5-fold upregulation of miR-802 expression in the liver of HFD-fed mice and a 30-fold increase of miR-802 expression in the liver of $Lepr^{db/db}$ mice (Fig. 1a). Northern blot analyses confirmed miR-802 expression in the liver of control mice, and hepatic overexpression in HFD and $Lepr^{db/db}$ mice (Fig. 1a and Supplementary Fig. 1c). In addition, our analysis revealed that murine miR-802 expression is highly enriched in the liver of lean mice (Supplementary Fig. 1d). Moreover, we compared miR-802 expression in primary hepatocytes versus non-hepatocytes isolated from control mice, revealing that miR-802 expression was tenfold higher in hepatocytes versus non-hepatocytes, indicating that liver parenchymal cells represent the main source of miR-802 expression in this tissue (Supplementary Fig. 1e). miR-802 expression was also increased in other tissues of obese mice, such as in kidney, pancreatic islets, skeletal muscle, white adipose tissue (WAT) and the brain, particularly in $Lepr^{db/db}$ mice (Fig. 1a), although to a lesser extent than the overexpression observed in the liver. Next, we quantified miR-802 expression in liver of a cohort of human individuals. miR-802 levels were significantly increased in overweight (body mass index (BMI) >25) compared with lean individuals (Fig. 1b) and hepatic miR-802 expression significantly correlated with the BMI of these subjects (Fig. 1c). Taken together, hepatic expression of miR-802 is increased in dietary and genetic mouse models of obesity as well as in overweight human subjects.

To address whether increased miR-802 expression may contribute to the development of insulin resistance, we overexpressed miR-802 in the murine hepatoma cell line Hepa1-6 (Supplementary Fig. 2a). This resulted in a diminished ability of insulin to phosphorylate Akt, a central signalling node of insulin action (Fig. 2a). To further address potential mechanisms leading to insulin resistance upon miR-802 overexpression, we investigated the messenger RNA expression of insulin signalling mediators and known inducers of insulin resistance in the presence of miR-802 overexpression. This analysis revealed unaltered expression of mRNAs for *Akt1*, *Igf1r*, *Insr* and *Irs1* (Supplementary Fig. 2c), but showed significantly increased mRNA expression of suppressor of cytokine signalling *Socs1* and *Socs3* upon miR-802 overexpression (Fig. 2b). Because deregulation of hepatic glucose production represents a key step in the development of type 2 diabetes, we assessed the effect of miR-802 expression on the transcriptional regulation of glucose 6 phosphatase (*G6pc*) and phosphoenolpyruvate carboxykinase 1 (*Pck1*). This analysis revealed that in addition to inducing insulin resistance, overexpression of miR-802 enhanced both basal and forskolin-induced expression of *G6pc* (Fig. 2c), but not *Pck1* (Supplementary Fig. 2b).

[1]Max-Planck-Institute for Neurological Research, Gleueler Strasse 50a, 50931 Cologne, Germany. [2]Cologne Excellence Cluster on Cellular Stress Responses in Aging Associated Diseases (CECAD), Zülpicher Strasse 47a, 50674 Cologne, Germany. [3]Department of Mouse Genetics and Metabolism, Institute for Genetics, University of Cologne, Center for Endocrinology, Diabetes and Preventive Medicine (CEDP), University Hospital Cologne and Center for Molecular Medicine Cologne, Zülpicher Strasse 47a, 50674 Cologne, Germany. [4]Swiss Federal Institute of Technology (ETH Zurich), Institute of Molecular Health Science, Schafmattstrasse 22, 8093 Zurich, Switzerland. [5]Department of Biochemistry and Molecular Cell Biology, University Hospital Hamburg-Eppendorf, Martinistrasse 52, 20246 Hamburg, Germany. [6]INSERM U 969, 9 Quai Saint Bernard, 75005 Paris, France. [7]CNRS Université Pierre et Marie Curie UMR7622, 9 Quai Saint Bernard, 75005 Paris, France. [8]Department of General and Visceral Surgery, University Hospital of Ulm, Albert-Einstein-Allee 23, 89081 Ulm, Germany. [9]TaconicArtemis GmbH, Neurather Ring 1, 51063 Cologne, Germany.

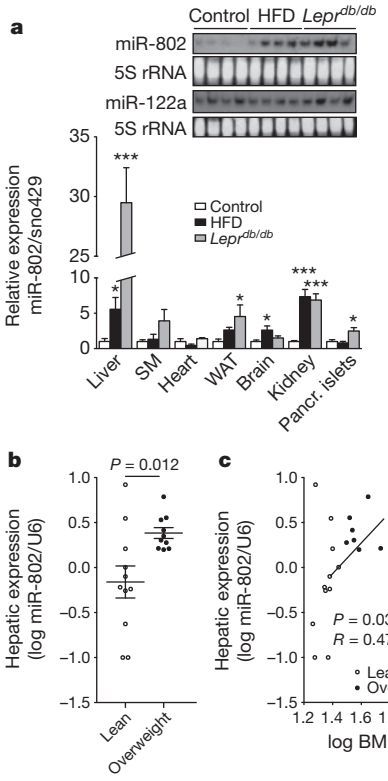

Figure 1 | miR-802 expression is increased in obese mice and humans. **a**, Comparative qRT–PCR analysis (bottom) of miR-802 expression in high fat diet (HFD)-fed mice (liver, $n = 6$; skeletal muscle (SM), $n = 8$; heart, $n = 6$; white adipose tissue (WAT), $n = 8$; brain, $n = 8$; kidney, $n = 7$; pancreatic islets, $n = 7$), *Lepr*$^{db/db}$ (liver, $n = 6$; SM, $n = 8$; heart, $n = 6$; WAT, $n = 7$; brain, $n = 8$; kidney, $n = 6$; pancreatic islets, $n = 5$) and chow-fed control mice (liver, $n = 6$; SM, $n = 8$; heart, $n = 7$; WAT, $n = 7$; brain, $n = 8$; kidney, $n = 14$; pancreatic islets, $n = 12$). Northern blot analysis (top) of miR-802 expression in liver of control, HFD-fed and *Lepr*$^{db/db}$ mice ($n = 4$ in each group). **b**, qRT–PCR quantification of human miR-802 expression in liver of lean ($n = 11$) and obese ($n = 10$) individuals. **c**, Correlation between hepatic miR-802 levels and BMI ($n = 21$) in lean ($n=11$) and obese ($n=10$) individuals. Expression was normalized to *sno429* in mice and to *U6* in humans; all error bars indicate mean ± s.e.m.; and $*P < 0.05$, $***P < 0.001$.

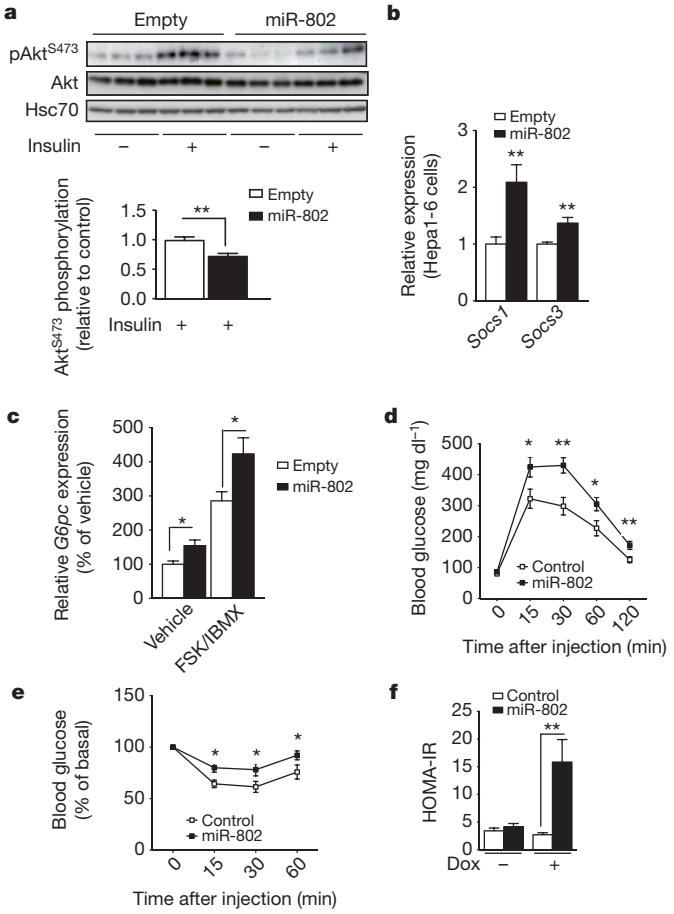

Figure 2 | Overexpression of miR-802 impairs insulin action and glucose metabolism. **a**, Immunoblot analysis (top) and quantification (bottom) of insulin-stimulated Akt Serine 473 phosphorylation versus total Akt protein levels in Hepa1-6 cells in the absence (empty vector) or presence of miR-802 overexpression. For quantification, the mean value for insulin-stimulated intensity of cells transfected with empty vector was set to 1. The results were obtained from three independent experiments, each performed in triplicate and a representative immunoblot is shown. Hsc70 is also known as Hspa8. **b**, qRT–PCR analysis of *Socs1* and *Socs3* expression in Hepa1-6 cells upon transfection with control or miR-802 expression vector. **c**, qRT–PCR analysis of *G6pc* expression in Hepa1-6 cells upon transfection with empty vector or miR-802 expression vector following stimulation with vehicle or forskolin (FSK) and 3-isobutyl-1-methylxanthine (IBMX). **d**, Glucose tolerance tests of miR-802 ($n = 11$) and control mice ($n = 11$) treated with doxycycline. **e**, Insulin tolerance tests of miR-802 ($n = 10$) and control mice ($n = 9$) after doxycycline administration. **f**, HOMA-IR of miR-802 ($n = 11$) and control littermates ($n = 11$). Dox, doxycycline. In all panels error bars indicate mean ± s.e.m.; $*P < 0.05$, $**P < 0.01$.

To verify whether overexpression of miR-802 also causes insulin resistance and impairs glucose metabolism *in vivo*, we aimed to mimic the obesity-associated increase of miR-802 expression via transgenic overexpression of miR-802 in lean mice. To do this we generated mice with the capacity for doxycycline (Dox)-induced overexpression of miR-802 (hereafter referred to as miR-802 mice, Supplementary Fig. 2d–f). Insertion of the transgenic miR-802 expression cassette in the absence of Dox stimulation did not alter body weight, glucose tolerance or insulin tolerance (Supplementary Fig. 2g–i). Upon Dox administration, we observed an increase of miR-802 expression in the liver, skeletal muscle, white adipose tissue, pancreatic islets and kidney of transgenic compared to control animals (Supplementary Fig. 2j). Profiling of global miRNA-expression of Dox-treated control and transgenic mice revealed no major differences in global miRNA-expression between both groups, indicating that transgenic overexpression of miR-802 does not interfere with transcription and processing of small RNAs in a non-specific manner (Supplementary Fig. 2k). Thus, transgenic overexpression of miR-802 mimicked the miR-802 expression observed in obese mice, with the exception of a higher degree of miR-802 expression in skeletal muscle and white adipose tissue compared to the obese state. Although we detected no differences in blood glucose concentrations (Supplementary Fig. 2l), transgenic mice developed glucose intolerance and insulin resistance upon miR-802 overexpression (Fig. 2d, e). Furthermore, homeostatic model assessment of insulin resistance (HOMA-IR) indices of mice overexpressing miR-802 were significantly increased (Fig. 2f). Collectively, overexpression of miR-802 in mice impairs glucose homeostasis *in vivo*.

Next, we assessed the functional contribution of increased miR-802 expression to the development of insulin resistance by reducing miR-802 expression in obese mice. We synthesized locked nucleic acids (LNA) specifically targeting the seed sequence of miR-802, as well as appropriate control LNA in which four nucleotides of the seed sequence were mutated. C57BL/6 mice, which had been receiving a HFD for 12 weeks, were injected with either anti-miR-802 or control LNA. We observed an 80% reduction of hepatic miR-802 expression in mice that had received the anti-miR-802 LNA compared to those receiving control LNA (Fig. 3a). Although anti-miR-802 treatment also efficiently reduced miR-802 expression in the kidney of obese mice, it only slightly reduced miR-802 expression in skeletal

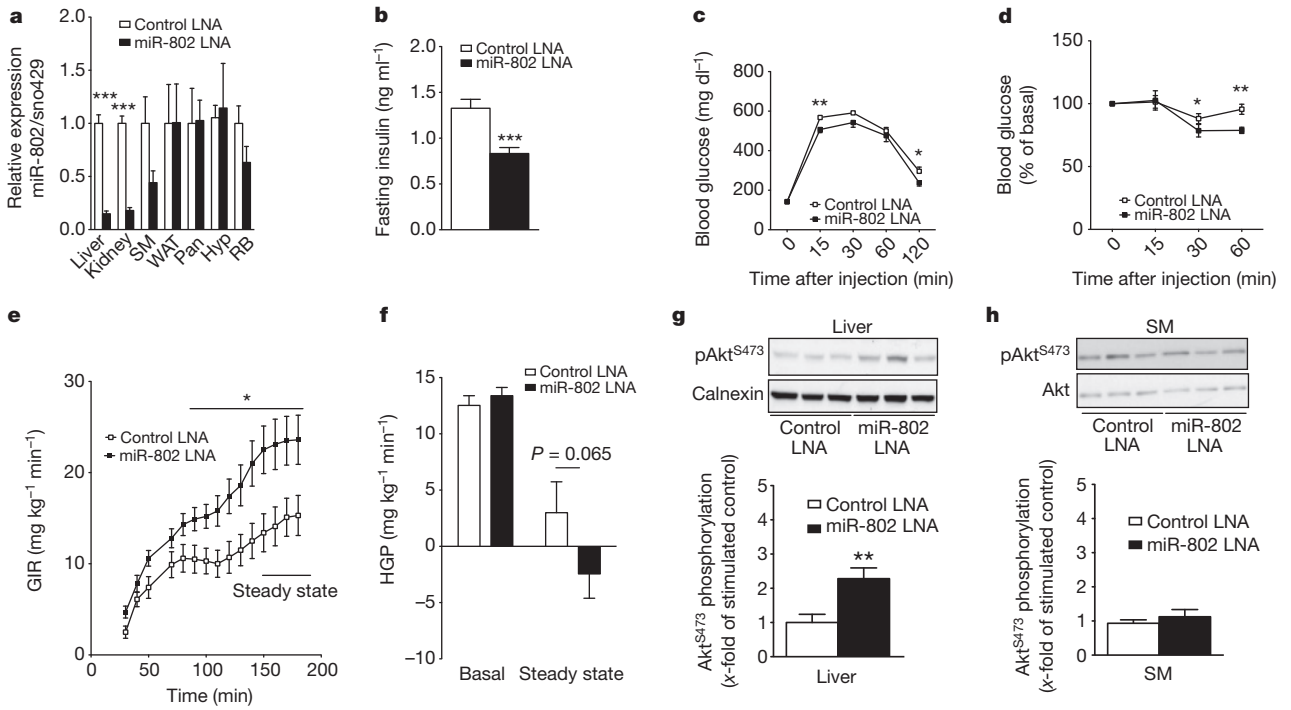

Figure 3 | Suppression of miR-802 expression improves obesity-associated insulin resistance and glucose intolerance. **a**, miR-802 expression after intravenous injection of HFD-fed mice with miR-802 locked nucleic acids (LNA) (liver, $n = 9$; kidney, $n = 10$; SM, $n = 6$; WAT, $n = 6$; pancreatic islets, $n = 3$; hypothalamus (Hyp), $n = 10$; rest of brain (minus the hypothalamus) (RB), $n = 9$) or control LNA (liver, $n = 7$; kidney, $n = 8$; skeletal muscle, $n = 6$; WAT, $n = 6$; Pan, $n = 4$; Hyp, $n = 7$; RB, $n = 6$). **b**, Serum insulin levels of HFD-fed mice treated with miR-802 LNA ($n = 8$) or control LNA ($n = 8$). **c**, Glucose tolerance tests of HFD-fed mice administered with miR-802 LNA ($n = 19$) or control LNA ($n = 17$). **d**, Insulin tolerance tests of HFD-fed mice treated with miR-802 LNA ($n = 14$) or control LNA ($n = 16$). **e**, Glucose infusion rates (GIR) during euglycaemic–hyperinsulinaemic clamps in HFD-fed mice treated with control LNA ($n = 9$) or miR-802 LNA ($n = 12$). **f**, Hepatic glucose production (HGP) of HFD-fed mice treated with control LNA ($n = 9$) or miR-802 LNA ($n = 12$) before (basal) and during (steady state) euglycaemic–hyperinsulinaemic clamp analysis. $P = 0.065$ in unpaired one-tailed (based on the improved insulin sensitivity of miR-802 LNA treated mice) Student's t-test. **g**, **h**, Immunoblot analysis of insulin-stimulated Akt^{S473} phosphorylation in liver (**g**) and skeletal muscle (**h**) of HFD-fed mice treated with control and miR-802 LNA (top). Densitometric quantification of Akt phosphorylation in liver (**g**) and skeletal muscle (**h**) of control ($n = 9$) or miR-802-LNA-treated mice ($n = 12$) (bottom). In all panels error bars indicate mean ± s.e.m.; $^*P < 0.05$, $^{**}P < 0.01$, $^{***}P < 0.001$.

muscle and did not affect miR-802 expression in the pancreas, WAT, hypothalamus or other brain areas (Fig. 3a). Anti-miR-802 treatment had no effect on body weight, body fat content or circulating serum leptin concentrations (Supplementary Fig. 3a–c) as well as no effect on adipocyte size or gene expression of pro-inflammatory mediators in WAT (Supplementary Fig. 3d–f). On the other hand, the obesity-associated rise in serum insulin concentrations was diminished in HFD animals treated with miR-802 LNA (Fig. 3b). In accordance with this, glucose tolerance tests revealed an improvement of glucose tolerance upon miR-802 inhibition (Fig. 3c). Moreover, insulin sensitivity was also improved upon inhibition of miR-802 (Fig. 3d). To further examine the exact mechanisms and cell type through which reducing miR-802 expression improves glucose metabolism, we performed euglycaemic–hyperinsulinaemic clamps in HFD-fed mice, which had received either control or anti-miR-802 LNA. Reduction of miR-802 expression significantly increased glucose infusion rate by 1.5-fold during the clamp (Fig. 3e and Supplementary Fig. 4a), whereas analysis of insulin-stimulated glucose uptake in skeletal muscle and WAT did not reveal any differences between mice receiving control or anti-miR-802 LNA (Supplementary Fig. 4b). By contrast, the ability of insulin to suppress glucose production was enhanced in mice receiving anti-miR-802 compared to those receiving control LNA, although this effect did not reach statistical significance (Fig. 3f). Moreover, the ability of insulin to inhibit *G6pc* expression in the liver as well as *G6pc* and *Pck1* expression in the kidney was enhanced upon inhibition of miR-802 expression (Supplementary Fig. 4c). Consistent with improved hepatic insulin sensitivity, insulin-stimulated Akt phosphorylation was enhanced in the liver (Fig. 3g), but not in the skeletal muscle of anti-miR-802 treated animals during the clamp (Fig. 3h). Taken together, the findings show that reduction of miR-802 expression in diet-induced obese mice results in improvement of insulin sensitivity predominantly by increasing insulin action in the liver.

We aimed to identify those mRNA(s) that are targeted by miR-802 and serve as its molecular effector(s) in disease progression. Using a stringent bioinformatics approach, we identified 26 putative murine miR-802 target genes (Supplementary Fig. 5a), among which the gene encoding hepatocyte nuclear factor 1 beta (*Hnf1b*; also known as transcription factor 2, *Tcf2*) harboured a miR-802 binding site, which is also conserved in the human *HNF1B* gene (Supplementary Fig. 5b). HNF1B has been causally linked to the development of maturity onset diabetes of the young (MODY) type 5 (ref. 8) and variants in *HNF1B* have also been linked to predisposition for type 2 diabetes[9]. Inclusion of the *Hnf1b* 3′ untranslated region (UTR) into a luciferase reporter construct reduced luciferase activity compared to a reporter lacking the *Hnf1b* 3′ UTR upon transfection into Hepa1-6 cells (Fig. 4a and Supplementary Fig. 5c). Overexpression of miR-802 led to a further reduction of luciferase activity when the reporter construct contained the *Hnf1b* 3′ UTR (Fig. 4a). In contrast, mutation of the conserved miR-802 binding motif abrogated reduced luciferase expression (Fig. 4a). Moreover, overexpression of miR-802 in Hepa1-6 cells led to reduced Hnf1b protein expression (Supplementary Fig. 5d). *In vivo*, hepatic Hnf1b protein expression was reduced by 50% in $Lepr^{db/db}$ mice, which exhibit increased miR-802 expression compared to controls (Fig. 4b), whereas hepatic Hnf1b protein expression was significantly increased in mice that had been treated with anti-miR-802 LNA

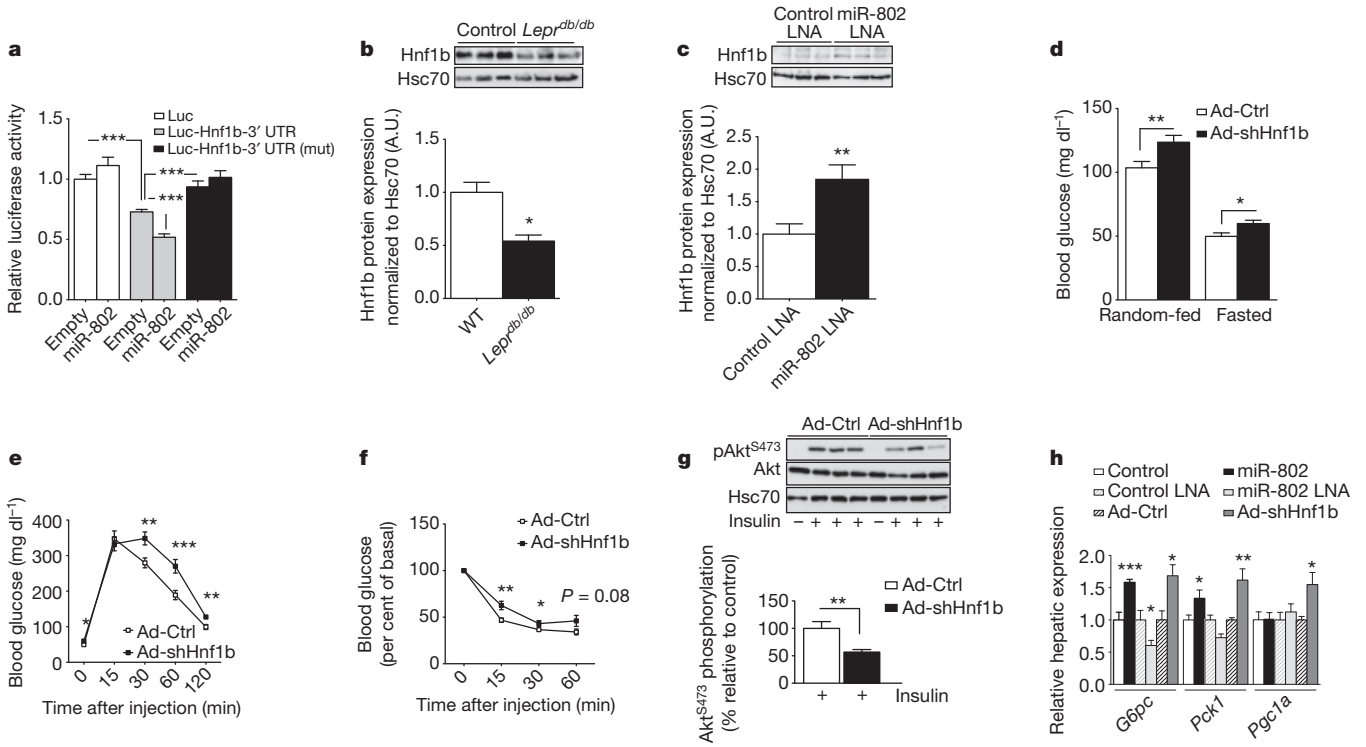

Figure 4 | Silencing of the miR-802 target *Hnf1b* impairs insulin action and glucose metabolism. **a**, Relative luciferase activity of the firefly reporter constructs containing either the wild-type or mutated 3′ UTR of the murine *Hnf1b* gene. Firefly luciferase activity was normalized to the activity of *Renilla* luciferase. Luciferase activity of the luciferase-only containing construct was set to 1. One-way ANOVA was carried out followed by Bonferroni post-hoc analysis, $*P < 0.05$, $**P < 0.01$, $***P < 0.001$. **b**, Immunoblot analysis (top) and densitometry quantification (bottom) of hepatic Hnf1b expression in the liver of $Lepr^{db/db}$ ($n = 3$) and control mice ($n = 3$). **c**, Representative immunoblot analysis (top) and densitometric quantification (bottom) of hepatic Hnf1b expression in HFD-fed control LNA treated mice ($n = 10$) and miR-802 LNA treated mice ($n = 9$). **d**, Blood glucose concentrations of random-fed and overnight-fasted mice treated with Ad-shHnf1b ($n = 20$) or Ad-Ctrl ($n = 20$). **e**, Glucose-tolerance tests of mice treated with Ad-shHnf1b ($n = 20$) or Ad-Ctrl ($n = 20$). **f**, Insulin tolerance tests of mice administered Ad-shHnf1b ($n = 20$) or Ad-Ctrl ($n = 20$). **g**, Representative immunoblot analysis (top) and quantification (bottom) of insulin-stimulated Akt Serine 473 phosphorylation versus total Akt protein levels in liver of mice delivered Ad-shHnf1b ($n = 7$) or Ad-Ctrl ($n = 7$). For quantification, the mean value for insulin-stimulated intensity of control animals was set to 100%. **h**, qRT–PCR analysis of *G6pc*, *Pck1* and *Pgc1a* mRNA expression in liver of Dox-treated miR-802 transgenic ($n = 6$) versus control animals ($n = 6$); HFD-fed mice treated with miR-802 LNA ($n = 9$) and control LNA ($n = 7$); and wild-type mice treated with Ad-shHnf1b ($n = 9$) and Ad-Ctrl ($n = 9$). In all panels error bars indicate mean ± s.e.m.; $*P < 0.05$, $**P < 0.01$, $***P < 0.001$.

(Fig. 4c). Functionally, shRNA-mediated silencing of *Hnf1b* in Hepa1-6 cells led to enhancement of basal and forskolin-induced *G6pc* and *Pck1* expression (Supplementary Fig. 6a) and to increased expression of *Socs1* and *Socs3* (Supplementary Fig. 6b), similar to what was observed upon miR-802 overexpression. Taken together, these experiments define *Hnf1b* as a target of miR-802-dependent post-transcriptional silencing in liver *in vitro* and *in vivo*.

To gain further insights into how partial reduction of Hnf1b expression affects glucose metabolism, we performed glucose and insulin tolerance tests in heterozygous *Hnf1b*-deficient mice ($Hnf1b^{+/-}$) and control littermates[10]. However, these analyses revealed no differences in glucose or insulin tolerance between these groups of mice (Supplementary Fig. 7a, b). Surprisingly, analysis of *Hnf1b* mRNA and protein expression revealed only a negligible reduction of *Hnf1b* mRNA and unaltered protein expression in liver (Supplementary Fig. 7c, d) and kidney of $Hnf1b^{+/-}$ mice (Supplementary Fig. 7e, f). Interestingly, $Hnf1b^{+/-}$ mice exhibited reduced hepatic miR-802 expression (Supplementary Fig. 7g), potentially contributing to unaltered Hnf1b protein expression in these animals. Thus, we next aimed to acutely and efficiently reduce hepatic Hnf1b expression through generation of adenoviruses expressing shRNA targeting *Hnf1b* (Ad-shHnf1b) and control viruses (Ad-Ctrl). When administered intravenously to the control mice, injection of Ad-shHnf1b led to a significant, 40% reduction of hepatic *Hnf1b* mRNA expression (Supplementary Fig. 8a). Importantly, analysis of global miRNA expression in these animals revealed that pol-III-dependent expression of the Hnf1b-shRNA did not generally interfere with expression and processing of small RNA molecules (Supplementary Fig. 9). Ad-shHnf1b-mediated reduction of hepatic Hnf1b protein expression had no effect on body weight, fat mass, adipocyte size or WAT inflammation (Supplementary Fig. 8b–e), whereas it resulted in significantly increased blood glucose concentrations (Fig. 4d). Moreover, glucose and insulin tolerance tests (GTT and ITT, respectively) revealed a profound reduction in glucose tolerance and insulin sensitivity in Ad-shHnf1b-treated animals (Fig. 4e, f), and insulin-evoked phosphorylation of Akt was significantly impaired in these mice (Fig. 4g). In addition, microarray gene expression profiling of mRNAs isolated from liver of Ad-shHnf1b- and Ad-Ctrl-treated mice revealed the coordinate induction of key catabolic, fasting-associated gene ontology (GO) pathways such as gluconeogenesis, beta-oxidation of fatty acids, oxidative phosphorylation and the tricarbon acid cycle upon reduction of Hnf1b expression (Supplementary Fig. 10 a–d). qRT–PCR analyses confirmed the significant induction of *Pgc1a* and its gluconeogenic target genes *Pck1* and *G6pc* upon reduction of Hnf1b protein expression (Fig. 4h). Conversely, expression of *G6pc* and *Pck1* mRNA was reduced in anti-miR-802 LNA treated HFD mice and increased in the liver of mice with conditional overexpression of miR-802 (Fig. 4h).

We next investigated whether adenoviral overexpression of Hnf1b can affect the increased *G6pc* expression observed upon miR-802 overexpression in Hepa1-6 cells. Indeed, a 1.5-fold increase in *Hnf1b* expression reversed the increased *G6pc* mRNA expression upon concomitant miR-802 overexpression (Supplementary Fig. 11 a, b). Next,

we aimed to restore hepatic Hnf1b expression via adenovirus-mediated overexpression of Hnf1b in liver of $Lepr^{db/db}$ mice. Injection of a *Hnf1b*-expressing adenovirus resulted in a ninefold increase in hepatic *Hnf1b* expression compared to $Lepr^{db/db}$ mice, which had been injected with a GFP-expressing control vector (Supplementary Fig. 11c). Increasing hepatic Hnf1b expression lead to an improvement of insulin sensitivity in $Lepr^{db/db}$ mice and to a reduction of HOMA-IR indices (Supplementary Fig. 11d, e), supporting the model that miR-802-mediated reduction of hepatic Hnf1b expression contributes to the metabolic impairment observed upon development of obesity.

Our study reveals an important role for obesity-induced overexpression of miR-802 in the development of obesity-associated insulin resistance. Interestingly, the degree of increased hepatic expression of miR-802 in $Lepr^{db/db}$ mice exceeded that of miRNAs, whose upregulation has been described so far in the context of obesity-associated insulin resistance. The observation that overexpression of miR-802 causes insulin resistance and impairs glucose tolerance, whereas reducing miR-802 expression in obese mice improves these metabolic parameters, clearly indicates a functional role for increased miR-802 expression in the development of obesity-associated insulin resistance. Importantly, increased miR-802 expression is not restricted to murine obesity models, but is also detected in obese humans, thus characterizing miR-802 and its target gene(s) as potential new targets for the treatment of obesity-associated insulin resistance and type 2 diabetes. Among these potential target genes, we have functionally validated *Hnf1b* as a bona fide miR-802 target both *in vitro* and *in vivo*. Hnf1b constitutes a member of the homeodomain-containing superfamily of liver-enriched transcription factors, and truncated or loss-of-function *HNF1B* alleles cause MODY type 5 in humans[8,11]. In addition, some genome-wide association studies revealed an association between *HNF1B* variants with the susceptibility to develop type 2 diabetes, whereas others failed to observe this effect in different populations[12]. Although the functional consequences of dysfunctional *HNF1B* alleles are well understood for the development of MODY type 5 in humans, as they affect not only pancreatic β-cell function but also cause insulin resistance[13,14], surprisingly few studies have addressed the role of Hnf1b in liver. Our experiments clearly reveal an important role for Hnf1b in control of hepatic insulin sensitivity and glucose metabolism *in vivo*. We demonstrate that both overexpression of miR-802 or knockdown of *Hnf1b* leads to upregulation of hepatic *Socs1* and *Socs3* expression. These findings are consistent with earlier reports that Hnf1b represses *Socs3* expression and in turn enhances hepatocyte growth factor signalling in kidney[15]. Because both *Socs1* and *Socs3* are characterized mediators of insulin resistance *in vitro* and *in vivo*[16,17], miR-802-evoked, Hnf1b-dependent derepression of *Socs* transcription represents a candidate pathway to cause insulin resistance. Although the mechanism(s) of how Hnf1b controls hepatic glucose metabolism clearly requires further investigation, our study reveals an important role for miR-802- and Hnf1b-dependent regulation of insulin sensitivity and glucose metabolism *in vivo*.

METHODS SUMMARY

LNA synthesis and administration. Custom-made miRCURY locked nucleic acids (LNA) for *in vivo* application were designed and synthesized as unconjugated and fully phosphorothiolated oligonucleotides by Exiqon. The sequence of the LNA targeting miR-802 was fully complementary to the mature miRNA sequence: 5′-AATCTTTGTTACTG-3′ (miR-802 LNA); the appropriate mismatch LNA control was mutated in four nucleotide positions: 5′-TATGTTACTTACTG-3′ (control LNA). LNA were intravenously delivered to HFD-fed mice at a concentration of 25 mg kg^{-1} body weight in 1×PBS. Mice were injected on two consecutive days and killed two weeks after LNA administration.

Received 16 May; accepted 15 November 2012.

1. Saltiel, A. R. & Kahn, C. R. Insulin signalling and the regulation of glucose and lipid metabolism. *Nature* **414,** 799–806 (2001).
2. Gregor, M. F. & Hotamisligil, G. S. Inflammatory mechanisms in obesity. *Annu. Rev. Immunol.* **29,** 415–445 (2011).
3. Glass, C. K. & Olefsky, J. M. Inflammation and lipid signaling in the etiology of insulin resistance. *Cell Metab.* **15,** 635–645 (2012).
4. Jordan, S. D. *et al.* Obesity-induced overexpression of miRNA-143 inhibits insulin-stimulated AKT activation and impairs glucose metabolism. *Nature Cell Biol.* **13,** 434–446 (2011).
5. Zhou, B. *et al.* Downregulation of *miR-181a* upregulates sirtuin-1 (SIRT1) and improves hepatic insulin sensitivity. *Diabetologia* **55,** 2032–2043.
6. Trajkovski, M. *et al.* MicroRNAs 103 and 107 regulate insulin sensitivity. *Nature* **474,** 649–653 (2011).
7. Nakanishi, N. *et al.* The up-regulation of microRNA-335 is associated with lipid metabolism in liver and white adipose tissue of genetically obese mice. *Biochem. Biophys. Res. Commun.* **385,** 492–496 (2009).
8. Horikawa, Y. *et al.* Mutation in hepatocyte nuclear factor-1β gene (*TCF2*) associated with MODY. *Nature Genet.* **17,** 384–385 (1997).
9. Han, X. *et al.* Implication of genetic variants near *SLC30A8*, *HHEX*, *CDKAL1*, *CDKN2A/B*, *IGF2BP2*, *FTO*, *TCF2*, *KCNQ1*, and *WFS1* in type 2 diabetes in a Chinese population. *BMC Med. Genet.* **11,** 81 (2010).
10. Barbacci, E. *et al.* Variant hepatocyte nuclear factor 1 is required for visceral endoderm specification. *Development* **126,** 4795–4805 (1999).
11. Lindner, T. H. *et al.* A novel syndrome of diabetes mellitus, renal dysfunction and genital malformation associated with a partial deletion of the pseudo-POU domain of hepatocyte nuclear factor-1β. *Hum. Mol. Genet.* **8,** 2001–2008 (1999).
12. Wen, J. *et al.* Investigation of type 2 diabetes risk alleles support *CDKN2A/B*, *CDKAL1*, and *TCF7L2* as susceptibility genes in a Han Chinese cohort. *PLoS ONE* **5,** e9153 (2010).
13. Haumaitre, C. *et al.* Severe pancreas hypoplasia and multicystic renal dysplasia in two human fetuses carrying novel *HNF1β/MODY5* mutations. *Hum. Mol. Genet.* **15,** 2363–2375 (2006).
14. Bellanné-Chantelot, C. *et al.* Clinical spectrum associated with hepatocyte nuclear factor-1β mutations. *Ann. Intern. Med.* **140,** 510–517 (2004).
15. Ma, Z. *et al.* Mutations of HNF-1β inhibit epithelial morphogenesis through dysregulation of SOCS-3. *Proc. Natl Acad. Sci. USA* **104,** 20386–20391 (2007).
16. Howard, J. K. & Flier, J. S. Attenuation of leptin and insulin signaling by SOCS proteins. *Trends Endocrinol. Metab.* **17,** 365–371 (2006).
17. Ueki, K., Kondo, T., Tseng, Y. H. & Kahn, C. R. Central role of suppressors of cytokine signaling proteins in hepatic steatosis, insulin resistance, and the metabolic syndrome in the mouse. *Proc. Natl Acad. Sci. USA* **101,** 10422–10427 (2004).

Supplementary Information is available in the online version of the paper.

Acknowledgements J.-W.K. was supported by stipends from EMBO and CECAD. S.C. received funds from INSERM, CNRS and EU FP7 (Marie Curie Initial Training Network BOLD). This work was in part supported by ERC grant 'Metabolomirs' (to M.S.), by a grant to J.H. by the DFG (SFB 841) and DFG funding to J.C.B. (Br1492-7). We thank D. Wagner-Stippich, J. Alber, P. Scholl and B. Hampel for technical assistance.

Author Contributions J.C.B. and J.-W.K. conceived the study and wrote the manuscript. J.-W.K. and C.B. performed most experiments. A.C.K. performed the euglycaemic–hyperinsulinaemic clamp experiments. H.T.N. performed adenoviral treatments of mice. M.C.V. contributed to bioinformatical analyses. K.H. and M.S. analysed miR-802 expression in murine tissues. J.S. aided in the generation of miR-802 transgenic mice. C.H. and S.C. provided tissues and analysed glucose metabolism in $Hnf1b^{+/-}$ mice. A.M.W., U.K., L.S. and J.H. provided and analysed human liver explants for miR-802 expression. All authors approved the manuscript.

Author Information Gene expression data was deposited with Gene Expression Omnibus (GEO) under accession number GSE42188. Reprints and permissions information is available at www.nature.com/reprints. The authors declare no competing financial interests. Readers are welcome to comment on the online version of the paper. Correspondence and requests for materials should be addressed to J.C.B. (bruening@nf.mpg.de).

nature medicine

Silencing microRNA-134 produces neuroprotective and prolonged seizure-suppressive effects

Eva M Jimenez-Mateos[1], Tobias Engel[1], Paula Merino-Serrais[2], Ross C McKiernan[1], Katsuhiro Tanaka[1], Genshin Mouri[1], Takanori Sano[1], Colm O'Tuathaigh[3], John L Waddington[3], Suzanne Prenter[3], Norman Delanty[4], Michael A Farrell[5], Donncha F O'Brien[6], Ronán M Conroy[7], Raymond L Stallings[3,8], Javier DeFelipe[2] & David C Henshall[1]

Temporal lobe epilepsy is a common, chronic neurological disorder characterized by recurrent spontaneous seizures. MicroRNAs (miRNAs) are small, noncoding RNAs that regulate post-transcriptional expression of protein-coding mRNAs, which may have key roles in the pathogenesis of neurological disorders. In experimental models of prolonged, injurious seizures (status epilepticus) and in human epilepsy, we found upregulation of miR-134, a brain-specific, activity-regulated miRNA that has been implicated in the control of dendritic spine morphology. Silencing of miR-134 expression *in vivo* using antagomirs reduced hippocampal CA3 pyramidal neuron dendrite spine density by 21% and rendered mice refractory to seizures and hippocampal injury caused by status epilepticus. Depletion of miR-134 after status epilepticus in mice reduced the later occurrence of spontaneous seizures by over 90% and mitigated the attendant pathological features of temporal lobe epilepsy. Thus, silencing miR-134 exerts prolonged seizure-suppressant and neuroprotective actions; determining whether these are anticonvulsant effects or are truly antiepileptogenic effects requires additional experimentation.

Epilepsy is a serious, chronic neurological disorder characterized by recurrent spontaneous seizures that affects about 50 million people worldwide. Antiepileptic drugs typically control seizures in two-thirds of patients but probably do not alter the underlying pathophysiology[1]. The development of symptomatic epilepsy is thought to involve altered expression of ion channels, synaptic remodeling, inflammation, gliosis and neuronal death, among other factors[2–5]. However, few antiepileptogenic interventions targeting these processes have shown sufficient efficacy *in vivo*[1], and our understanding of the cell and molecular mechanisms of epileptogenesis is incomplete.

Evidence is emerging that miRNAs may be crucial to the pathogenesis of several neurological disorders[6,7], including epilepsy[8,9]. MiRNAs are a family of small (~22 nt), endogenously expressed noncoding RNAs that regulate mRNA translation by imperfect base-pairing interactions within the 3′ untranslated region[10,11]. Depending on the degree of sequence complementarity, miRNA binding, which occurs with the help of Argonaute proteins within the RNA-induced silencing complex (RISC), results in either cleavage of the target mRNA or a reduction in its translational efficiency[10,11].

MiR-134 is a brain-specific, activity-regulated miRNA that has been implicated in the control of neuronal microstructure[12,13]. Pyramidal cells are the most common neurons in the neocortex and hippocampus[2]. They are the major source of intrinsic excitatory cortical synapses, and their dendritic spines are the main postsynaptic target of excitatory synapses, with their spine size acting as an index of synaptic strength[14–16]. Spine remodeling occurs during learning and memory formation, as well as in the setting of neuropsychiatric disorders and pathological brain activity[17–21]. Spine collapse is mediated in part by the *N*-methyl-D-aspartate (NMDA)-receptor–dependent and calcium-dependent depolymerization of actin by cofilin[19,22,23]. LIM kinase-1 (Limk1) phosphorylates cofilin and inactivates the ability of cofilin to depolymerize actin, and loss of Limk1 results in abnormal spine morphology[24]. In hippocampal neurons, miR-134 targets *Limk1* mRNA, thereby preventing Limk1 protein translation[13]. Overexpression of miR-134 *in vitro* has been reported to reduce spine volume[13], whereas overexpression of miR-134 *in vivo* reduces total dendritic length[25] and abrogates long-term potentiation[26]. Mice haploinsufficient for the miRNA biogenesis component DiGeorge syndrome critical region gene 8 do not produce several mature miRNAs, including miR-134, and have lower hippocampal spine density compared to wild-type mice[27]. Spine loss may have divergent consequences according to context[28], promoting excitability[29] or uncoupling NMDA-receptor–driven currents in neurons and preventing excitotoxicity[30].

Here we investigated the role of miR-134 in epilepsy and explored the *in vivo* effect of inhibiting miR-134. We report that miR-134 is upregulated

[1]Department of Physiology and Medical Physics and Centre for the Study of Neurological Disorders, Royal College of Surgeons in Ireland, Dublin, Ireland. [2]Instituto Cajal (CSIC) and Laboratorio Cajal de Circuitos Corticales (Centro de Tecnología Biomédica), Universidad Politécnica de Madrid, Madrid, Spain. [3]Molecular and Cellular Therapeutics, Royal College of Surgeons in Ireland, Dublin, Ireland. [4]Department of Neurology, Beaumont Hospital, Dublin, Ireland. [5]Department of Pathology, Beaumont Hospital, Dublin, Ireland. [6]Department of Neurological Surgery, Beaumont Hospital, Dublin, Ireland. [7]Division of Population Health Sciences, Royal College of Surgeons in Ireland, Dublin, Ireland. [8]National Children's Research Centre, Our Lady's Children's Hospital, Dublin, Ireland. Correspondence should be addressed to D.C.H. (dhenshall@rcsi.ie).

Received 28 November 2011; accepted 15 May 2012; published online 10 June 2012; doi:10.1038/nm.2834

in experimental and human epilepsy and show that silencing miR-134 generates a seizure-refractory state and attenuates epileptic seizures and the pathophysiological features of temporal lobe epilepsy (TLE).

RESULTS

MiR-134 is regulated by status epilepticus and in epilepsy

We first investigated whether pathologic brain activity *in vivo* affects miR-134 levels. We triggered prolonged seizures (status epilepticus) in C57BL/6 mice by intra-amygdala microinjection of the glutamate receptor agonist kainic acid[31,32]. The resultant seizures caused neuronal damage mainly within the hippocampal CA3 subfield (**Fig. 1a**).

To identify the cell populations expressing miR-134 *in vivo*, we performed *in situ* hybridization on tissue sections from C57BL/6 control mice labeled with a probe specific for mature miR-134. We detected a strong signal in the soma of hippocampal pyramidal neurons and hilar interneurons, as well as in neurons in the neocortex and amygdala (**Fig. 1b** and **Supplementary Fig. 1**).

Real-time quantitative PCR (qPCR) analysis showed that status epilepticus resulted in an increase in mature miR-134 levels in the ipsilateral CA3 ($P = 0.016$) and CA1 ($P = 0.035$) subfields (**Fig. 1c**). The levels of mature miR-134 were not changed in the undamaged contralateral CA3 subfield (**Supplementary Fig. 2a**). Nonharmful, nonconvulsive seizures induced by a low dose of systemic kainic acid, a model of epileptic preconditioning[33] in which status epilepticus does not develop, did not alter miR-134 levels compared to vehicle controls in the CA3 ($P = 0.89$) or CA1 subfields ($P = 0.56$) ($n = 6$ mice per group; data not shown).

To determine whether miR-134 was functional, we measured its levels within the RISC, where targeting of miRNAs to mRNA occurs[34], in control mice and in mice after status epilepticus. We eluted Argonaute-2 from the CA3 subfield[35,36] and extracted miRNA. We detected a low level of miR-134 in the RISC in the controls, whereas the levels of Argonaute-2–bound miR-134 were higher ($P = 0.035$) in mice in which we induced status epilepticus (**Fig. 1d**). Protein concentrations of the miR-134 target, Limk1 (ref. 13), were lower ($P = 0.001$) in mice after status epilepticus than in the controls (**Fig. 1e**).

We next investigated whether miR-134 levels and the expression of Limk1 were altered in experimental epilepsy. Recurrent spontaneous

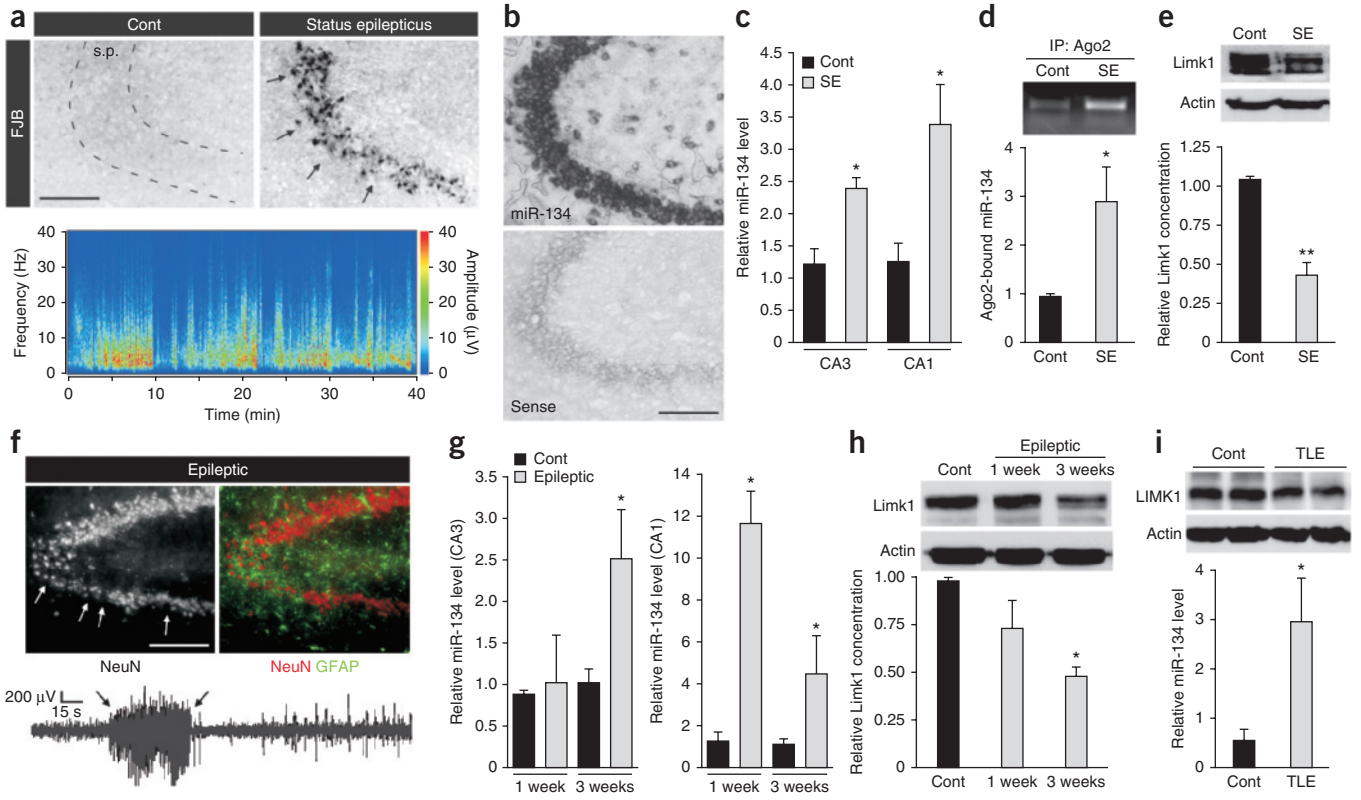

Figure 1 MiR-134 upregulation after status epilepticus and in epilepsy. (**a**) Photomicrographs show neuronal death (FJB) in the CA3 stratum pyramidale (s.p., within dashed lines in the top left image) 24 h after status epilepticus induced by intra-amygdala kainic acid compared to control (Cont) mouse. Arrows in the image on the top right point to damaged neurons. Below is a depiction of electrographic seizure frequency and amplitude during status epilepticus. Scale bar, 200 μm (**b**) *In situ* hybridization showing miR-134 in the soma of CA3 pyramidal neurons. Scale bar, 200 μm.'Sense' indicates the sense-labeled control section as a control for probe specificity. (**c**) Real-time qPCR measurement of miR-134 (normalized to RNU19) for the CA3 and CA1 24 h after status epilepticus (SE). $n = 5$ mice per group. $^*P < 0.05$ compared to Cont subfield by *t* test. (**d**) Argonaute-2 (Ago2)-immunoprecipitated (IP) miR-134 from control mice and mice 24 h after status epilepticus. $n = 3$ mice per group. $^*P < 0.05$ compared to Cont by *t* test. (**e**) Limk1 western blot and densitometry. Actin was used as the loading control. $n = 5$ mice per group. $^{**}P < 0.05$ compared to Cont by *t* test. (**f**) Photomicrographs showing loss of CA3 neurons (NeuN, arrows) and astrogliosis (glial fibrillary acidic protein, GFAP) in epileptic mice 14 d after status epilepticus (top) and a telemetry-recorded spontaneous seizure (bottom; denoted by arrows). Scale bar, 200 μm. (**g**) MiR-134 levels in the CA3 and CA1 subfields 1 and 3 weeks after status epilepticus. $n = 5$ mice per group. $^*P < 0.05$ compared to time-matched Cont by *t* test. (**h**) Western blot showing Limk1 concentrations 1 and 3 weeks after status epilepticus and densitometry. $n = 4$ mice per group. $^*P < 0.05$ compared to Cont by analysis of variance (ANOVA) followed by Bonferroni's *post hoc* test. (**i**) MiR-134 levels in surgically resected temporal lobe samples from individuals with TLE compared to autopsy controls (Cont). $n = 3$ samples per group. $^*P < 0.05$ compared to Cont by *t* test. Western blot (above) shows LIMK1 concentrations ($n = 1$ sample per lane). All data are mean ± s.e.m.

seizures emerge 3–4 d after status epilepticus in the model we used[31,33], and within 3 weeks, the mice show pathologic hallmarks of TLE, including neuron loss and astrogliosis (**Fig. 1f**). MiR-134 levels were elevated in the CA3 subfield 3 weeks after status epilepticus ($P = 0.049$) and 1 ($P = 0.003$) and 3 ($P = 0.008$) weeks after status epilepticus in the CA1 subfield compared to controls (**Fig. 1g**). Limk1 protein concentrations followed an opposite trend and were lower ($P = 0.028$) in epileptic mice than control mice (**Fig. 1h**). The concentrations of cAMP responsive element binding protein 1 (Creb1), another validated miR-134 target[26], were also lower in epileptic mice than control mice (**Supplementary Fig. 2b**).

We next analyzed surgically obtained temporal lobe material from individuals with pharmacoresistent TLE. We detected higher levels ($P = 0.029$) of mature miR-134 in the TLE specimens compared to autopsy control samples from people who died of causes unrelated to neurological disease (**Fig. 1i**). This difference was not an artifact of postmortem delay (**Supplementary Fig. 2c–e**). Protein concentrations of LIMK1 were lower ($P = 0.039$, *t* test) in individuals with TLE compared to the autopsy controls (**Fig. 1i**).

In vivo depletion of miR-134 using antagomirs

To explore the function of miR-134 *in vivo,* we injected mice with locked nucleic acid (LNA) 3′ cholesterol-conjugated oligonucleotides ('antagomirs')[36–39]. We injected antagomirs targeting miR-134 (Ant-134) (**Supplementary Fig. 3a**) or a nontargeting scrambled sequence (Scr) into the mouse ventricle (intracerebroventricularly, i.c.v.) (**Supplementary Fig. 3b**) and measured the miRNA levels 1, 4, 8 and 12 h later and then after 1, 3, 5 and 7 d and after 1 and 2 months. Knockdown of miR-134 was first evident 12 h after injection of 0.12 nmol Ant-134 (**Supplementary Fig. 4a–d**), and by 24 h after injection, the levels of miR-134 in the hippocampus of these mice were reduced by over 95% ($P = 0.005$) (**Fig. 2a**). This is similar to effects reported for antagomirs in other tissues[37]. Hippocampal levels of an unrelated miRNA, miR-19a, were not changed by injection of Ant-134 (**Fig. 2b**). Increasing the amount of Ant-134 injected to 1 nmol seemed to produce off-target knockdown of miRNAs (**Supplementary Fig. 4e,f**). The miR-134 levels began to recover by 7 d after Ant-134 injection, although they remained lower than the miR-134 levels in the mice injected with Scr at 1 month after injection ($P = 0.034$), which is consistent with other reports[37], and were no longer different from the levels in mice injected with Scr ($P = 0.469$) by 2 months after injection (**Fig. 2c**).

Brains from mice injected with the antagomirs had grossly normal anatomy (data not shown). We found no evidence of hippocampal neuronal death when we stained sections from the mice injected with antagomirs for Fluoro-Jade B (FJB), DNA fragmentation (terminal deoxynucleotidyl dUTP nick end labeling; TUNEL)[40] and the neuronal marker NeuN (**Fig. 2d,e** and data not shown).

To determine whether the reduction in the levels of miR-134 had any gross effects on mouse behavior, we performed ethological tests[41]. We injected mice with either Scr or Ant-134 and assessed them 24 h later. We found no differences in measures of animal exploratory activity including ambulatory counts, distance traveled or vertical counts between the two groups (**Fig. 2f**), suggesting that silencing of miR-134 does not alter normal exploratory activities.

MiR-134 antagomirs reduce pyramidal neuron spine density

Because *in vitro* and *in vivo* evidence supports a role for miR-134 in controlling dendritic spine morphology[13,25,27], we examined whether antagomirs caused changes to dendritic spines *in vivo*. We microinjected Lucifer yellow into individual CA3 pyramidal neurons in hippocampal slices from control mice 24 h after injection of 0.12 nmol Ant-134 or Scr and imaged them using confocal microscopy, as previously described[42,43] (**Fig. 3a,b**).

We analyzed 218 neurons in the Scr-injected mice ($n = 7$) and 181 neurons in the Ant-134–injected mice ($n = 7$). The structures of the basal dendritic trees were grossly normal in both groups, as were the distributions of spines (**Fig. 3c–e**). Dendrites from the Scr-injected mice had an average of 68 nodes (ramifications) compared to 72 nodes in the Ant-134–injected mice. The number of ramification points per µm was also similar in the two groups (0.0127 nodes per µm in the Scr-injected mice compared to 0.0131 nodes per µm in the Ant-134–injected mice). We then analyzed spine density, assessing a total length of 5,343.7 µm of dendrites in the Scr-injected mice (7,455 spines) and a similar length (5,477.5 µm) of dendrites in the Ant-134–injected mice (6,196 spines). Spine density in the Scr-injected mice was within the expected range[42] (**Fig. 3d–f**). Notably, spine density was 21% lower ($P = 0.037$) in Ant-134–injected mice than in the Scr-injected mice (**Fig. 3d–f**). Thus, injecting miR-134 antagomirs *in vivo* results in a reduction in spine density.

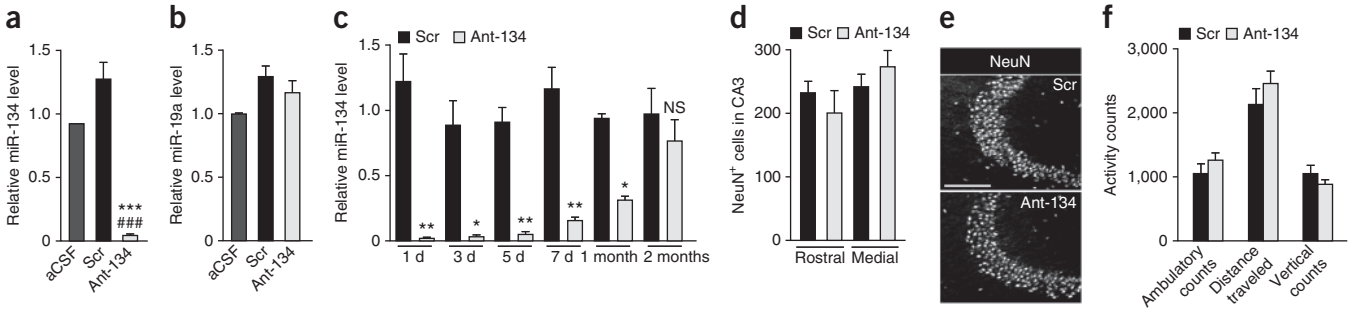

Figure 2 Antagomir-mediated silencing of miR-134 in mouse hippocampus. (**a**,**b**) Real-time qPCR measurement of miR-134 (**a**) and miR-19a (**b**) in mouse hippocampus 24 h after i.c.v. injection of Ant-134 or Scr. $n = 3$ mice per group. $^{***}P < 0.001$ compared to artificial cerebrospinal fluid (aCSF) and $^{###}P < 0.001$ compared to Scr by ANOVA followed by Bonferroni's *post hoc* test. (**c**) MiR-134 levels in hippocampus after injection of Ant-134 or Scr at 1 d, 3 d, 5 d, 7 d, 1 month and 2 months after injection. $n = 3$ or 4 mice per group. $^{*}P < 0.05$, $^{**}P < 0.01$ compared to Scr by ANOVA followed by Bonferroni's *post hoc* test. NS, not significant. (**d**) NeuN counts at two different levels of the dorsal hippocampus in mice 24 h after injection with either Scr or Ant-134. $n = 4$ mice per group. (**e**) NeuN staining of the CA3 subfield 24 h after injection of Scr or Ant-134. Scale bar, 200 µm. (**f**) Behavioral analysis of mice 24 h after injection with Scr or Ant-134. The graph shows indices of exploratory activity: total ambulatory counts; distance traveled (cm); and vertical counts. All data are mean ± s.e.m.

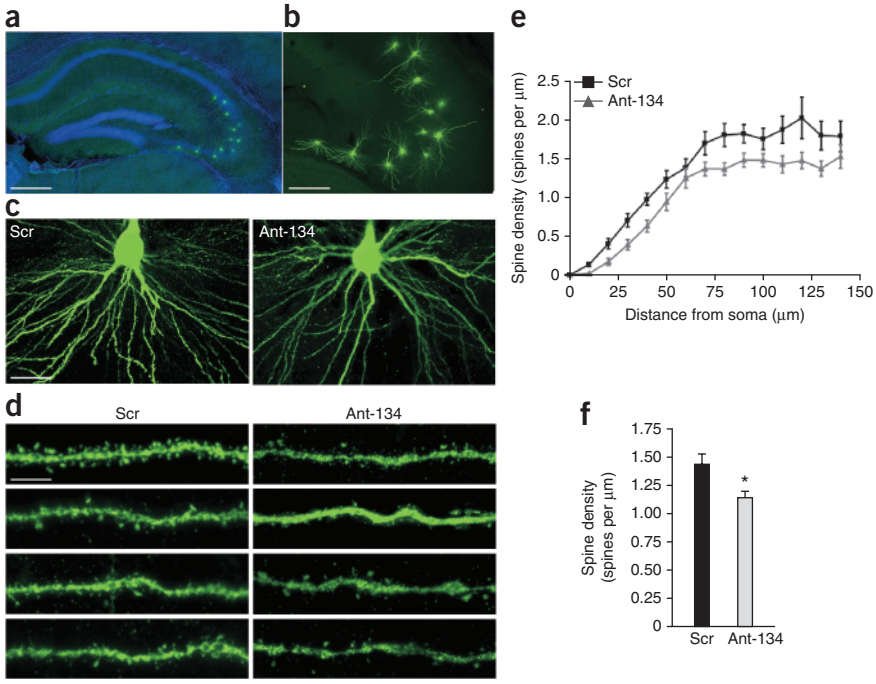

Figure 3 Antagomir silencing of miR-134 reduces hippocampal CA3 spine density *in vivo*. (**a**) Field view of a hippocampus showing Lucifer yellow–injected CA3 neurons (green) and nuclei (DAPI, blue). Scale bar, 500 µm. (**b**) Higher magnification of **a** showing the injected CA3 neurons. Scale bar, 100 µm. (**c**) Photomicrographs of the basal tree from Lucifer yellow–injected mice 24 h after injection with either Scr or Ant-134. Scale bar, 20 µm. (**d**) Representative images of individual dendrites from four mice injected with Scr (left) and four mice injected with Ant-134 (right). Scale bar, 12 µm. (**e**) Spine density as a function of the distance from the soma (by Sholl analysis) for Scr-injected and Ant-134–injected mice. (**f**) Spine density in Scr-injected and Ant-134–injected mice. $n = 7$ mice per group. $^{*}P < 0.05$ compared to Scr by *t* test. All data are mean ± s.e.m.

Silencing miR-134 reduces status epilepticus and neuronal death

To test the idea that antagomirs might influence pathologic brain activity *in vivo*, we compared seizures evoked by intra-amygdala microinjection of kainic acid in mice 24 h after injection with either Scr or Ant-134 (**Fig. 4** and **Supplementary Fig. 3c**). There was no difference in basal electroencephalography (EEG) measures between the two groups of mice (**Supplementary Fig. 5a**). Scr-injected mice experienced typical status epilepticus, comprising episodes of high-amplitude, high-frequency discharges (HAHFDs)[44] (**Fig. 4a–c**; compare **Fig. 4c** to **Fig. 1a**). An EEG analysis revealed that the duration of the HAHFDs ($P = 0.0051$), which are associated with damage-causing pathologic activity[45], and total EEG power ($P = 0.033$) were lower in Ant-134–injected mice compared to Scr-injected mice (**Fig. 4a–c**). This effect was qualitatively similar to the seizure suppression observed in mice given lorazepam 10 min before injection of kainic acid (compare **Fig. 4c** to **Supplementary Fig. 5b**).

MiR-134 levels were lower ($P = 0.0078$) in mice injected with Ant-134 before intra-amygdala injection of kainic acid compared to the mice injected with Scr (**Fig. 4d** and **Supplementary Fig. 6a**). Limk1 protein concentrations (**Fig. 4e**) and the concentrations of Creb1 (**Supplementary Fig. 6b**) were lower after status epilepticus in Scr-injected mice than in Ant-134–injected mice ($P = 0.018$), which had similar levels as nonseizure controls.

We next examined hippocampal damage in tissue sections from Scr-injected and Ant-134–injected mice. Scr-injected mice had typical CA3 lesions 24 h after status epilepticus, with extensive staining of neurons for FJB and TUNEL and a loss of NeuN staining (**Fig. 5a–f**). Mice injected with Ant-134 showed a marked

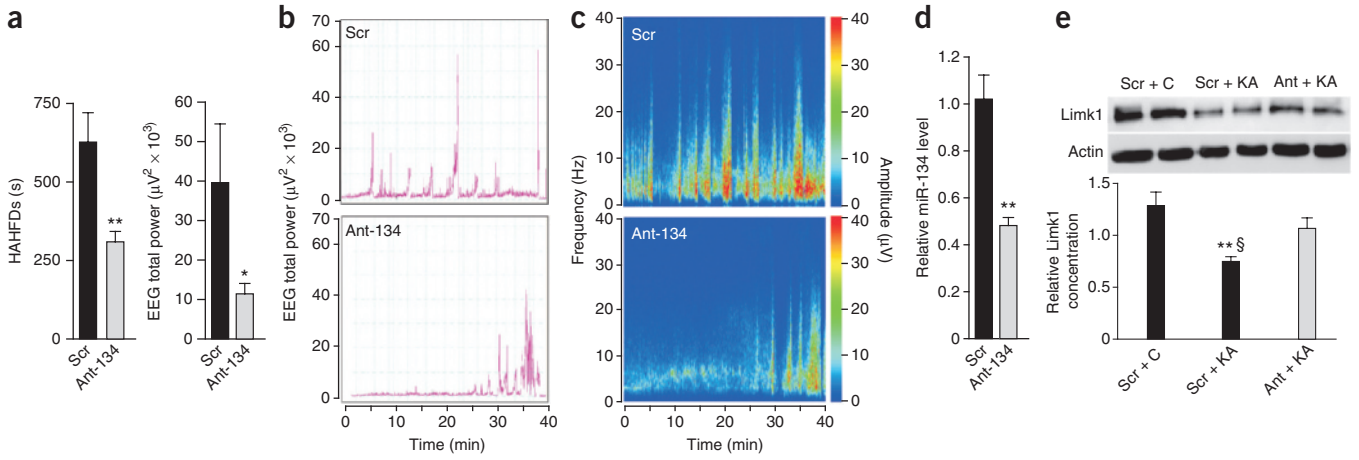

Figure 4 Antagomir silencing of miR-134 reduces seizure severity during status epilepticus. (**a**) Graphs show HAHFDs and total EEG power during status epilepticus in mice 24 h after injection with Scr or Ant-134. $n = 4$–8 mice per group. $^{*}P < 0.05$, $^{**}P < 0.01$ compared to Scr by *t* test. (**b**,**c**) Total EEG power (**b**) and the frequency and amplitude parameters (**c**) during status epilepticus in representative Scr-injected and Ant-134–injected mice covering the period between kainic acid injection and lorazepam administration. (**d**) MiR-134 levels in Scr- and Ant-134–injected mice 24 h after status epilepticus. $n = 4$ mice per group. $^{**}P < 0.01$ compared to Scr by *t* test. (**e**) Limk1 protein concentrations in Scr-injected mice without kainic-acid–induced status epilepticus (Scr + C) and after status epilepticus in mice given Scr (Scr + KA) or Ant-134 (Ant + KA). The graph shows Limk1 concentrations normalized to actin. $n = 4$ mice per group. $^{**}P < 0.01$ for Scr + KA compared to Scr + C; $^{\S}P < 0.05$ for Scr + KA compared to Ant + KA, by ANOVA with Bonferroni's *post hoc* test. All data are mean ± s.e.m.

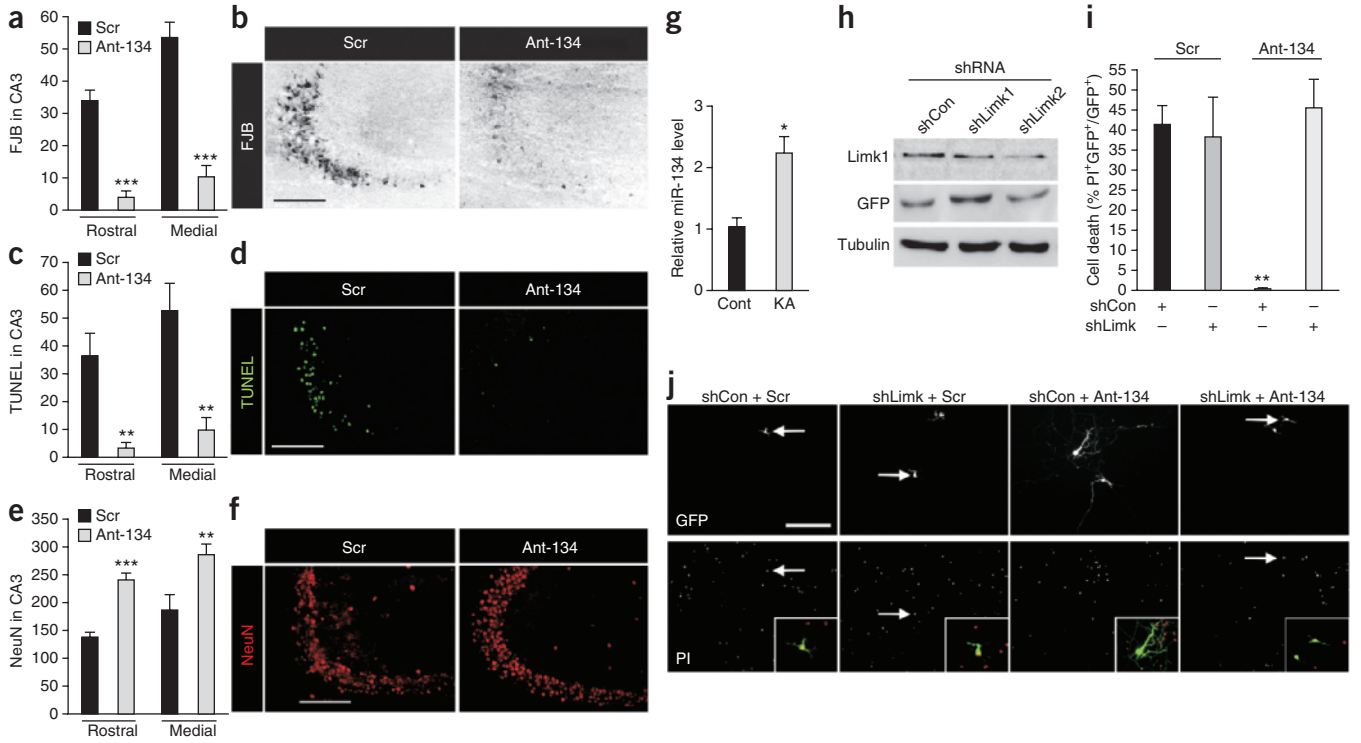

Figure 5 Antagomir silencing of miR-134 protects against status epilepticus *in vivo* and kainic acid toxicity *in vitro*. (**a**–**f**) *In vivo* studies. Graphs and representative photomicrographs from the dorsal hippocampus of mice 24 h after status epilepticus in mice treated beforehand with Scr or Ant-134 showing; FJB counts (**a**,**b**), TUNEL counts (**c**,**d**) and NeuN counts (**e**,**f**). $n = 4$–8 mice per group. $^{**}P < 0.01$, $^{***}P < 0.001$ compared to Scr by *t* test. Scale bars, 200 µm. (**g**–**j**) *In vitro* studies. (**g**) MiR-134 levels in primary hippocampal neurons 24 h after treatment with kainic acid. Data are from three independent experiments. $^{*}P < 0.05$ compared to Cont by *t* test. (**h**) Western blots showing Limk1 and GFP in SH-SY5Y cells transfected with control shRNA (shCon) or different shRNAs targeting Limk1 (shLimk1 and shLimk2). The shLimk2 reduced Limk1 concentrations by ~48% compared to shCon (average of two experiments). (**i**) Percentage of cell death induced by kainic acid treatment of hippocampal neurons (as the ratio of propidium iodide $(PI)^{+}GFP^{+}$ neurons over total GFP^{+} neurons) and the effect of Scr or Ant-134 in neurons cotransfected with either shCon or shLimk2 (shLimk). Results are from $n = 4$ independent experiments per group. $^{**}P < 0.01$ for shCon + Ant-134 compared to other groups by ANOVA with Bonferroni's *post hoc* test. (**j**) Photomicrographs of hippocampal neurons in each condition. Arrows indicate dead cells positive for both GFP (green) and PI (red), and the insets (40× lens) emphasize these regions. Scale bar, 50 µm. All data are mean ± s.e.m.

reduction in FJB and TUNEL staining and less of a loss of NeuN staining after status epilepticus (**Fig. 5a**–**f**).

To specifically link the neuroprotective effects of antagomirs to miR-134 and Limk1, we treated cultures of primary hippocampal neurons from C57BL/6 mice with kainic acid to model excitotoxic injury. Treatment of hippocampal neurons with kainic acid increased miR-134 levels ($P = 0.019$) (**Fig. 5g**). Next, neurons were co-transfected with shRNAs that targeted Limk1 (**Fig. 5h**), and either Scr or Ant-134, and then treated 48 h later with kainic acid. Ant-134 prevented kainic-acid–induced neurotoxicty in hippocampal neurons co-transfected with a non-targeting shRNA, and this protective effect was blocked in neurons cotransfected with shRNA targeting Limk1 (**Fig. 5i**,**j**).

Silencing miR-134 reduces spontaneous recurrent seizures

Based on our findings so far, we hypothesized that silencing miR-134 might also affect epilepsy. To avoid a confounding influence of shortened status epilepticus duration or neuroprotection on epileptogenesis[40,46], we injected antagomirs 1 h after triggering status epilepticus with intra-amygdala kainic acid. An analysis of EEG measures confirmed that when we injected antagomirs 1 h after kainic acid injection, there was no difference in duration of HAHFDs during status epilepticus between the Ant-134–injected and Scr-injected groups (**Fig. 6a**). In addition, CA3 damage assessed 24 h after triggering status epilepticus was similar between the Ant-134–injected and Scr-injected mice (**Fig. 6b**,**c**).

We then equipped groups of mice with EEG telemetry units[31] and undertook continuous EEG recording for 2 weeks after status epilepticus. In agreement with the normal course of epilepsy in this model[31], mice injected with Scr after status epilepticus experienced the first spontaneous seizures on the third day, and all mice were epileptic by the fourth day after status epilepticus (**Fig. 6d**,**e** and **Supplementary Fig. 6c**). The median epileptic seizure count during 14 d of monitoring of Scr-injected mice was 25 (range 8–79), with 200 epileptic seizures recorded in total for all the Scr-injected mice over this time period (**Fig. 6d** and **Supplementary Fig. 6c**). In contrast, only 60% of mice injected with Ant-134 had had a spontaneous seizure by the eleventh day after status epilepticus (**Fig. 6d** and **Supplementary Fig. 6c**); one mouse had only a single seizure on day 14 and another had no seizures in the 14 d after status epilepticus (**Fig. 6d**). Ant-134–injected mice had a median epileptic seizure count of 2 during the 14-d recording period (range 0–7), with just 16 epileptic seizures recorded in total for these mice during the 2 week recording period ($P = 0.0001$, compared to the Scr-injected group by two-way ANOVA) (**Fig. 6e**). The total amount of time spent in seizures also differed between the two groups, with Scr-injected mice spending more time in seizures then Ant-134–injected mice ($P < 0.001$ by two-way ANOVA; **Supplementary Fig. 6c**). The durations of the individual epileptic seizures were similar between the groups (**Supplementary Fig. 6d**).

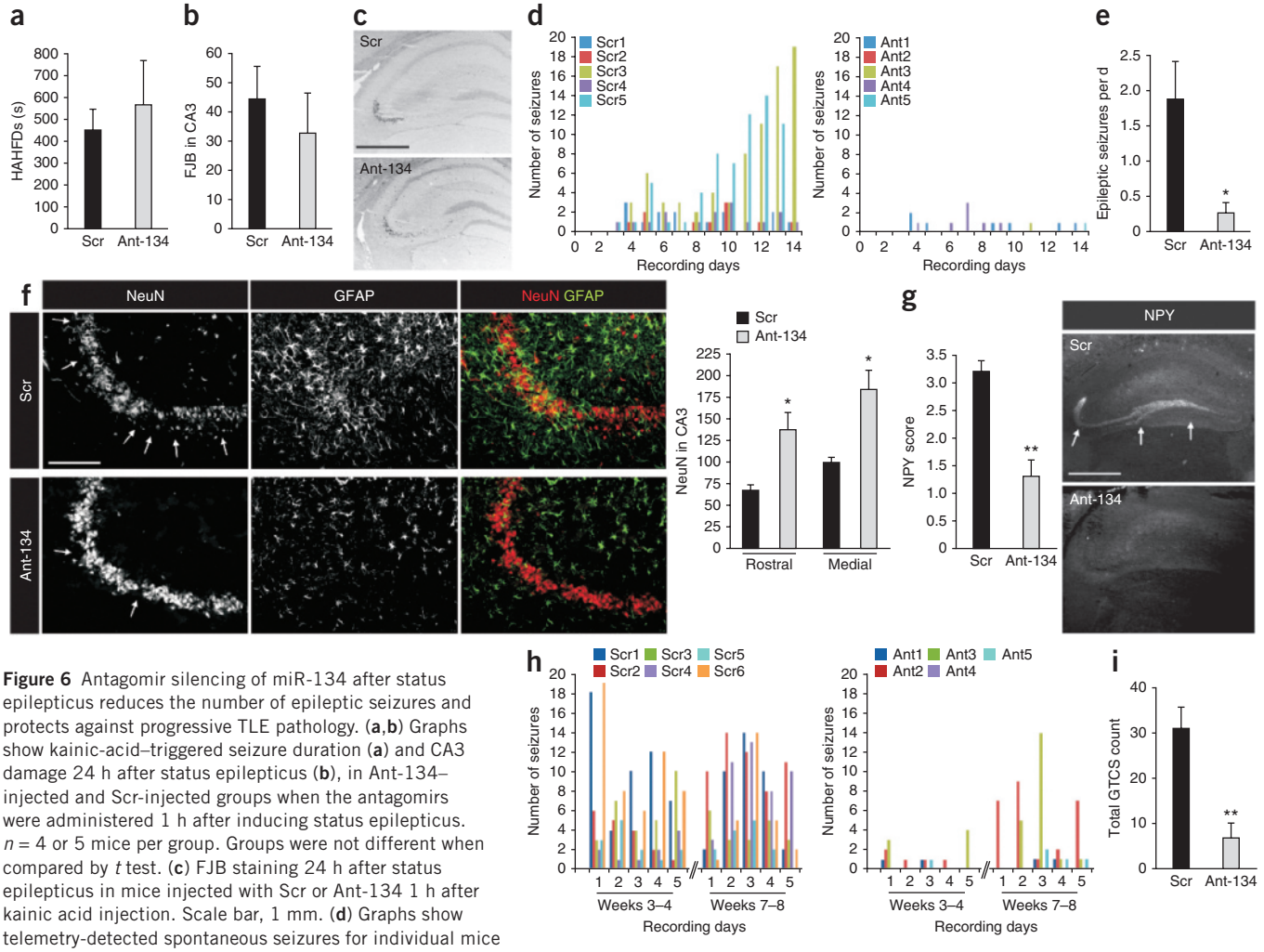

Figure 6 Antagomir silencing of miR-134 after status epilepticus reduces the number of epileptic seizures and protects against progressive TLE pathology. (**a**,**b**) Graphs show kainic-acid–triggered seizure duration (**a**) and CA3 damage 24 h after status epilepticus (**b**), in Ant-134–injected and Scr-injected groups when the antagomirs were administered 1 h after inducing status epilepticus. $n = 4$ or 5 mice per group. Groups were not different when compared by t test. (**c**) FJB staining 24 h after status epilepticus in mice injected with Scr or Ant-134 1 h after kainic acid injection. Scale bar, 1 mm. (**d**) Graphs show telemetry-detected spontaneous seizures for individual mice during the 2 weeks after status epilepticus for Scr-injected (left) and Ant-134–injected (right) mice. Scr1–Scr5, the five mice injected with Scr; Ant1–Ant5, the five mice injected with Ant-134. (**e**) Daily epileptic seizures in Scr-injected and Ant-134–injected mice. $n = 5$ mice per group. $^*P < 0.05$ compared to Scr by t test. (**f**) Hippocampal NeuN (arrows indicate areas of reduced NeuN staining) and GFAP (astrogliosis) staining in Scr-injected and Ant-134–injected mice after 2 weeks of epilepsy monitoring. The graph to the right shows NeuN counts in the dorsal hippocampus from the mice in each group. $^*P < 0.05$ compared to Scr group at rostral and $^*P < 0.05$ compared to Scr group at medial levels, by t test, $n = 5$ mice per group. Scale bar, 200 µm. (**g**) NPY scores in mice 14 d after status epilepticus (left) and representative NPY-stained sections from Scr-injected and Ant-134–injected mice (right). $^{**}P < 0.01$ compared to Scr by t test. Scale bar, 1 mm. $n = 5$ mice per group. (**h**) Graphs show the number of generalized tonic-clonic seizures (GTCS) each day for individual mice during two periods of 5 d of continuous video monitoring after status epilepticus for Scr-injected (left) and Ant-134–injected (right) mice. Scr1–Scr6, the six mice injected with Scr; Ant1–Ant5, the five mice injected with Ant-134. (**i**) Total GTCS counts averaged from the two monitoring periods. $n = 5$ or 6 mice per group. $^{**}P < 0.01$ compared to Scr by t test. All data are mean ± s.e.m.

Silencing miR-134 alters pathologic hallmarks of TLE

Progressive neuron loss, gliosis and rearrangement of mossy fibers are common pathological hallmarks of TLE[47,48]. We therefore examined whether Ant-134 altered the underlying pathology in the telemetry-equipped mice. Hippocampal CA3 neuron counts in the Ant-134–injected mice were higher than in the Scr-injected mice at the end of epilepsy monitoring, and astrogliosis was lower in the Ant-134–injected mice than in the Scr-injected mice (**Fig. 6f**). Neuropeptide Y (NPY) staining, an index of increasing reorganization of the hippocampus[33,49], in Scr-injected mice (**Fig. 6g**) was similar to the previously reported scores in epileptic mice[33], whereas the NPY scores in the Ant-134–injected mice were lower ($P = 0.008$) than in the Scr-injected mice (**Fig. 6g**).

To investigate whether the reduced epileptic seizure rates were the result of an antiepileptogenic effect or a prolonged anticonvulsant effect of Ant-134, we performed additional experiments. We first measured miR-134 levels in Ant-134–injected mice at the end of 14 d of telemetry recordings, which established that the miR-134 levels were ~55% of those in the Scr-injected mice (**Supplementary Fig. 7a**). Reducing miR-134 levels to ~55% of Scr in additional mice by injecting Ant-134 did not produce an anticonvulsant effect against kainic-acid–induced status epilepticus (**Supplementary Fig. 7b**,**c**). Likewise, mice subjected to kainic-acid–induced status epilepticus 14 d after i.c.v. injection with Ant-134, when levels of miR-134 are ~70% of those in Scr-injected mice (**Supplementary Fig. 7d**), were as sensitive to kainic-acid–induced status epilepticus as Scr-injected mice (**Supplementary Fig. 7e–h**), and mice were not protected against status epilepticus–induced hippocampal damage (**Supplementary Fig. 7i**,**j**).

Finally, longer-term video monitoring revealed that mice injected with Ant-134 after status epilepticus had fewer generalized tonic-clonic seizures and more seizure-free days at up to 2 months after

injection compared to Scr-injected mice, although the seizure rates did increase toward the rate of Scr-injected mice in three out of the 5 Ant-134–injected mice (**Fig. 6h**,**i** and **Supplementary Fig. 8**).

DISCUSSION

Our study shows that silencing miR-134 in mice using antagomirs suppresses evoked seizures, the occurrence of spontaneous seizures and the associated pathologic hallmarks of epilepsy. These are the first *in vivo* data, to our knowledge, to show that inhibition of a single mature miRNA can alter pathologic electrical activity in the brain, and they offer a new therapeutic target for the treatment of epilepsy.

An association between seizures and changes in miRNA expression has been suggested by recent profiling work[8,9,36,50] and by the phenotype of mice lacking Dicer[51], although our experiments are the first, to our knowledge, to link upregulation of miR-134 to evoked, harmful seizures and chronic epilepsy. Brief, nonharmful generalized seizures were insufficient to alter miR-134 expression. This suggests that *in vivo* regulation of miR-134 is not only a response to increased neuronal activity[13] but is also coupled to epileptic or pathogenic brain activity. Crucially, our miRNA silencing experiments support a role for miR-134 in facilitating pathologic neuronal activity *in vivo* because status epilepticus was potently suppressed in mice in which miR-134 was depleted by antagomirs. Notably, the seizure-suppressing effect of the antagomirs was nearly comparable to that of benzodiazepines[45,46,52]. Injecting antagomirs before status epilepticus also protected against seizure-induced hippocampal damage. This probably arises because of the resulting shortened seizure duration[46,52], but antagomirs also inhibited direct kainic acid toxicity *in vitro*. Our *in vitro* experiments also implicated Limk1 in the mechanism of protection, but rescuing Creb1 may also contribute[53], and our data are consistent with the neuroprotective effect of sirtuin 1, which negatively regulates miR-134 expression in brain[26].

Despite progress in understanding the pathogenesis of epilepsy, few studies targeting epileptogenic processes have shown sufficient efficacy at reducing the occurrence, course or severity of the disease[1,54]. A second major finding here was that silencing miR-134 after status epilepticus resulted in a substantial reduction in the number of epileptic seizures in mice. Epilepsy developed normally in Scr-injected mice[31], whereas spontaneous seizures seldom occurred in the Ant-134–injected mice. Thus, the effect of Ant-134 injection after status epilepticus was superior to that of neuroprotection by other means applied at the time of status epilepticus[40,55] and was comparable to or exceeded the performance of other experimental antiepileptogenic treatments[1]. Did the antagomirs interrupt epileptogenesis or simply prevent epileptic seizures from occurring as a result of a prolonged anticonvulsant effect, or did they work in a manner similar to antiepileptic drugs? We detected spontaneous seizures, albeit infrequently, in the mice treated with antagomirs, and the increase in seizure rates over extended monitoring in these mice supports the interpretation of a prolonged anticonvulsant or antiepileptic effect. Nevertheless, seizure rates in these mice never recovered to baseline, and seizure frequency 2 months after status epilepticus, a time when antagomir suppression of miR-134 was no longer occurring, was over 70% lower than baseline, so an antiepileptogenic effect is possible. Additional experiments examining seizure frequency at time points later than 2 months after antagomir administration will be required to distinguish between these possibilities.

The mechanism by which miR-134 antagomirs suppress seizures is unknown, but our study offers the possibility that the effect is through changes to dendritic spines. The finding that Ant-134 reduced hippocampal CA3 dendritic spine density *in vivo* was notable and contrasts with reports that spine size, not density, is controlled by miR-134 (ref. 13). Thus, a different phenotype results from miR-134 inhibition *in vivo*, which may be explained by the scale of miRNA suppression achieved, the distribution of the antagomir (somal compared to dendritic), the targets affected or the potency of LNA-modified antagomirs over 2′-O-methyl oligonucleotides[39]. Coincidently, a similar reduction in spine density was reported in mice lacking an miRNA biogenesis component in which the hippocampal levels of mature miR-134 were also reduced[27]. A key target of miR-134 is Limk1, which regulates dendritic spine dynamics[13]. Limk1 protein concentrations followed an opposite pattern as miR-134 expression, and miR-134 silencing prevented seizure-induced downregulation of Limk1, although other explanations for a decrease in spines are possible[15,56]. Could the reduction in spines account for the suppression of seizures? Dendritic spines are targets of excitatory axons in the brain[14,15]. Although spines have been suggested to operate as barriers against potentially harmful afferent input[28], our data are consistent with evidence showing that spine loss reduces excitatory responses[17,57] and transient spine reduction uncouples excitotoxic NMDA-mediated signaling[30]. The antagomirs seem to curtail pathologic activity in the brain without impairing tonic neuronal communication; an impairment would have been detected by the ethogram, and this result is consistent with reports that a ~20% reduction in the number of hippocampal pyramidal neuron spines does not alter basal neurotransmission[58]. Spine-localized synaptic signaling is also implicated in the pathogenesis of TLE[3], but whether a similar mechanism may account for the seizure-suppressive effects of miR-134 silencing is unknown. Loss of Limk1, which was countered with antagomirs, can result in increased hippocampal excitability[24]. However, other miR-134 targets with effects on excitability and seizure suppression are known, so we cannot exclude the involvement of these other targets in the effects we observed[26,53].

Although the therapeutic application of miR-134 antagomirs for status epilepticus is probably barred by a need for pretreatment, the longevity of the suppression after a single injection, consistent with antagomir data from mouse and primate experiments[37,39], suggests applications in refractory epilepsy or in disease modification in the wake of epilepsy-precipitating injuries. Alternate routes for antagomir delivery, such as an intranasal route, which has been considered for antiepileptic drug delivery[59], may avoid the blood-brain barrier exclusion of antagomirs *in vivo*[37] and may facilitate translation to the clinic for the treatment of epilepsy.

METHODS

Methods and any associated references are available in the online version of the paper.

Note: Supplementary information is available in the online version of the paper.

ACKNOWLEDGMENTS

We would like to thank J. Varley, J. Phillips and members of the Epilepsy Programme, Beaumont Hospital. We thank S. Miller-Delaney for assistance and N. Plesnila, J. Prehn and R. Simon for helpful suggestions on the manuscript. We thank the Brain and Tissue Bank for Developmental Disorders at the University of Maryland, Baltimore, Maryland. This work was supported by funding from Science Foundation Ireland awards 08/IN1/B1875 (D.C.H., E.M.J.-M., K.T., G.M. and T.S.), 11/TIDA/B1988 (D.C.H.) and 07/IN.1/B960 (J.W. and C.O.), US National Institute of Neurological Disorders and Stroke award R56 073714 (D.C.H.), an Irish Research Council for Science, Engineering and Technology postdoctoral fellowship (E.M.J.-M.), Irish Health Research Board grant PHD/2007/11 (R.C.M.) and the Spanish Ministry of Education, Science and Innovation grant SAF2009-09394 (J.D.).

AUTHOR CONTRIBUTIONS

E.M.J.-M. performed expression analyses, tissue culture, spine imaging, histology and epilepsy monitoring. T.E., K.T., G.M. and T.S. performed mouse modeling and telemetry. P.M.-S. and J.D. performed spine injections and data analysis. R.C.M. and S.P. performed expression studies. C.O. and J.L.W. conducted and analyzed the behavioral studies. N.D., D.F.O. and M.A.F. organized the human studies. R.M.C. performed statistical analyses. R.L.S. contributed to study design and analysis. D.C.H. and E.M.J.-M. conceived of the study, analyzed data and wrote the manuscript.

COMPETING FINANCIAL INTERESTS

The authors declare no competing financial interests.

Published online at http://www.nature.com/doifinder/10.1038/nm.2834.
Reprints and permissions information is available online at http://www.nature.com/reprints/index.html.

1. Pitkänen, A. & Lukasiuk, K. Mechanisms of epileptogenesis and potential treatment targets. *Lancet Neurol.* **10**, 173–186 (2011).
2. DeFelipe, J. Chandelier cells and epilepsy. *Brain* **122**, 1807–1822 (1999).
3. McNamara, J.O., Huang, Y.Z. & Leonard, A.S. Molecular signaling mechanisms underlying epileptogenesis. *Sci. STKE* **2006**, re12 (2006).
4. Wetherington, J., Serrano, G. & Dingledine, R. Astrocytes in the epileptic brain. *Neuron* **58**, 168–178 (2008).
5. Vezzani, A., French, J., Bartfai, T. & Baram, T.Z. The role of inflammation in epilepsy. *Nat. Rev. Neurol.* **7**, 31–40 (2011).
6. Eacker, S.M., Dawson, T.M. & Dawson, V.L. Understanding microRNAs in neurodegeneration. *Nat. Rev. Neurosci.* **10**, 837–841 (2009).
7. Saugstad, J.A. MicroRNAs as effectors of brain function with roles in ischemia and injury, neuroprotection, and neurodegeneration. *J. Cereb. Blood Flow Metab.* **30**, 1564–1576 (2010).
8. Aronica, E. *et al.* Expression pattern of miR-146a, an inflammation-associated microRNA, in experimental and human temporal lobe epilepsy. *Eur. J. Neurosci.* **31**, 1100–1107 (2010).
9. Song, Y.J. *et al.* Temporal lobe epilepsy induces differential expression of hippocampal miRNAs including let-7e and miR-23a/b. *Brain Res.* **1387**, 134–140 (2011).
10. Ambros, V. The functions of animal microRNAs. *Nature* **431**, 350–355 (2004).
11. Bartel, D.P. MicroRNAs: genomics, biogenesis, mechanism, and function. *Cell* **116**, 281–297 (2004).
12. Lagos-Quintana, M. *et al.* Identification of tissue-specific microRNAs from mouse. *Curr. Biol.* **12**, 735–739 (2002).
13. Schratt, G.M. *et al.* A brain-specific microRNA regulates dendritic spine development. *Nature* **439**, 283–289 (2006).
14. Matsuzaki, M., Honkura, N., Ellis-Davies, G.C. & Kasai, H. Structural basis of long-term potentiation in single dendritic spines. *Nature* **429**, 761–766 (2004).
15. Zhou, Q., Homma, K.J. & Poo, M.M. Shrinkage of dendritic spines associated with long-term depression of hippocampal synapses. *Neuron* **44**, 749–757 (2004).
16. Noguchi, J., Matsuzaki, M., Ellis-Davies, G.C. & Kasai, H. Spine-neck geometry determines NMDA receptor-dependent Ca^{2+} signaling in dendrites. *Neuron* **46**, 609–622 (2005).
17. Müller, M., Gahwiler, B.H., Rietschin, L. & Thompson, S.M. Reversible loss of dendritic spines and altered excitability after chronic epilepsy in hippocampal slice cultures. *Proc. Natl. Acad. Sci. USA* **90**, 257–261 (1993).
18. Rensing, N. *et al. In vivo* imaging of dendritic spines during electrographic seizures. *Ann. Neurol.* **58**, 888–898 (2005).
19. Zeng, L.H. *et al.* Kainate seizures cause acute dendritic injury and actin depolymerization *in vivo*. *J. Neurosci.* **27**, 11604–11613 (2007).
20. Penzes, P., Cahill, M.E., Jones, K.A., VanLeeuwen, J.E. & Woolfrey, K.M. Dendritic spine pathology in neuropsychiatric disorders. *Nat. Neurosci.* **14**, 285–293 (2011).
21. Bhatt, D.H., Zhang, S. & Gan, W.B. Dendritic spine dynamics. *Annu. Rev. Physiol.* **71**, 261–282 (2009).
22. Halpain, S., Hipolito, A. & Saffer, L. Regulation of F-actin stability in dendritic spines by glutamate receptors and calcineurin. *J. Neurosci.* **18**, 9835–9844 (1998).
23. Saneyoshi, T., Fortin, D.A. & Soderling, T.R. Regulation of spine and synapse formation by activity-dependent intracellular signaling pathways. *Curr. Opin. Neurobiol.* **20**, 108–115 (2010).
24. Meng, Y. *et al.* Abnormal spine morphology and enhanced LTP in LIMK-1 knockout mice. *Neuron* **35**, 121–133 (2002).
25. Christensen, M., Larsen, L.A., Kauppinen, S. & Schratt, G. Recombinant adeno-associated virus-mediated microRNA delivery into the postnatal mouse brain reveals a role for miR-134 in dendritogenesis *in vivo*. *Front Neural Circuits* **3**, 16 (2010).
26. Gao, J. *et al.* A novel pathway regulates memory and plasticity via SIRT1 and miR-134. *Nature* **466**, 1105–1109 (2010).
27. Stark, K.L. *et al.* Altered brain microRNA biogenesis contributes to phenotypic deficits in a 22q11-deletion mouse model. *Nat. Genet.* **40**, 751–760 (2008).
28. Segal, M. Dendritic spines, synaptic plasticity and neuronal survival: activity shapes dendritic spines to enhance neuronal viability. *Eur. J. Neurosci.* **31**, 2178–2184 (2010).
29. Sierra-Paredes, G., Oreiro-Garcia, T., Nunez-Rodriguez, A., Vazquez-Lopez, A. & Sierra-Marcuno, G. Seizures induced by *in vivo* latrunculin a and jasplakinolide microperfusion in the rat hippocampus. *J. Mol. Neurosci.* **28**, 151–160 (2006).
30. Meller, R. *et al.* Ubiquitin proteasome-mediated synaptic reorganization: a novel mechanism underlying rapid ischemic tolerance. *J. Neurosci.* **28**, 50–59 (2008).
31. Mouri, G. *et al.* Unilateral hippocampal CA3-predominant damage and short latency epileptogenesis after intra-amygdala microinjection of kainic acid in mice. *Brain Res.* **1213**, 140–151 (2008).
32. Murphy, B.M. *et al.* Contrasting patterns of Bim induction and neuroprotection in Bim-deficient mice between hippocampus and neocortex after status epilepticus. *Cell Death Differ.* **17**, 459–468 (2010).
33. Jimenez-Mateos, E.M., Mouri, G., Conroy, R.M. & Henshall, D.C. Epileptic tolerance is associated with enduring neuroprotection and uncoupling of the relationship between CA3 damage, neuropeptide Y rearrangement and spontaneous seizures following intra-amygdala kainic acid-induced status epilepticus in mice. *Neuroscience* **171**, 556–565 (2010).
34. Peters, L. & Meister, G. Argonaute proteins: mediators of RNA silencing. *Mol. Cell* **26**, 611–623 (2007).
35. Karginov, F.V. *et al.* A biochemical approach to identifying microRNA targets. *Proc. Natl. Acad. Sci. USA* **104**, 19291–19296 (2007).
36. Jimenez-Mateos, E.M. *et al.* MicroRNA expression profile after status epilepticus and hippocampal neuroprotection by targeting miR-132. *Am. J. Pathol.* **179**, 2519–2532 (2011).
37. Krützfeldt, J. *et al.* Silencing of microRNAs *in vivo* with 'antagomirs'. *Nature* **438**, 685–689 (2005).
38. Krützfeldt, J. *et al.* Specificity, duplex degradation and subcellular localization of antagomirs. *Nucleic Acids Res.* **35**, 2885–2892 (2007).
39. Elmén, J. *et al.* LNA-mediated microRNA silencing in non-human primates. *Nature* **452**, 896–899 (2008).
40. Engel, T. *et al.* Reduced hippocampal damage and epileptic seizures after status epilepticus in mice lacking proapoptotic Puma. *FASEB J.* **24**, 853–861 (2010).
41. O'Tuathaigh, C.M. *et al.* Phenotypic characterization of spatial cognition and social behavior in mice with 'knockout' of the schizophrenia risk gene neuregulin 1. *Neuroscience* **147**, 18–27 (2007).
42. Merino-Serrais, P., Knafo, S., Alonso-Nanclares, L., Fernaud-Espinosa, I. & Defelipe, J. Layer-specific alterations to CA1 dendritic spines in a mouse model of Alzheimer's disease. *Hippocampus* **21**, 1037–1044 (2011).
43. Ballesteros-Yáñez, I., Benavides-Piccione, R., Bourgeois, J.P., Changeux, J.P. & DeFelipe, J. Alterations of cortical pyramidal neurons in mice lacking high-affinity nicotinic receptors. *Proc. Natl. Acad. Sci. USA* **107**, 11567–11572 (2010).
44. Engel, T. *et al.* Loss of p53 results in protracted electrographic seizures and development of an aggravated epileptic phenotype following status epilepticus. *Cell Death Dis.* **1**, e79 (2010).
45. Shinoda, S. *et al.* Development of a model of seizure-induced hippocampal injury with features of programmed cell death in the BALB/c mouse. *J. Neurosci. Res.* **76**, 121–128 (2004).
46. Pitkänen, A., Kharatishvili, I., Narkilahti, S., Lukasiuk, K. & Nissinen, J. Administration of diazepam during status epilepticus reduces development and severity of epilepsy in rat. *Epilepsy Res.* **63**, 27–42 (2005).
47. Nairismägi, J. *et al.* Progression of brain damage after status epilepticus and its association with epileptogenesis: a quantitative MRI study in a rat model of temporal lobe epilepsy. *Epilepsia* **45**, 1024–1034 (2004).
48. Mathern, G.W., Babb, T.L. & Armstrong, D.L. Hippocampal sclerosis. in *Epilepsy: A Comprehensive Textbook* Vol. 13 (eds. Engel, J.J. & Pedley, T.A.) 133–155 (Lippincott-Raven Publishers, Philadelphia, 1997).
49. Cavazos, J.E., Golarai, G. & Sutula, T.P. Mossy fiber synaptic reorganization induced by kindling: time course of development, progression, and permanence. *J. Neurosci.* **11**, 2795–2803 (1991).
50. Hu, K. *et al.* Expression profile of microRNAs in rat hippocampus following lithium-pilocarpine-induced status epilepticus. *Neurosci. Lett.* **488**, 252–257 (2011).
51. Tao, J. *et al.* Deletion of astroglial dicer causes non–cell-autonomous neuronal dysfunction and degeneration. *J. Neurosci.* **31**, 8306–8319 (2011).
52. Araki, T., Simon, R.P., Taki, W., Lan, J.Q. & Henshall, D.C. Characterization of neuronal death induced by focally evoked limbic seizures in the C57BL/6 mouse. *J. Neurosci. Res.* **69**, 614–621 (2002).
53. Lee, B. *et al.* The CREB/CRE transcriptional pathway: protection against oxidative stress-mediated neuronal cell death. *J. Neurochem.* **108**, 1251–1265 (2009).
54. Brandt, C., Potschka, H., Loscher, W. & Ebert, U. N-methyl-D-aspartate receptor blockade after status epilepticus protects against limbic brain damage but not against epilepsy in kainate model of temporal lobe epilepsy. *Neuroscience* **118**, 727–740 (2003).
55. Jimenez-Mateos, E.M. *et al.* Hippocampal transcriptome after status epilepticus in mice rendered seizure damage-tolerant by epileptic preconditioning features suppressed calcium and neuronal excitability pathways. *Neurobiol. Dis.* **32**, 442–453 (2008).
56. Nägerl, U.V., Eberhorn, N., Cambridge, S.B. & Bonhoeffer, T. Bidirectional activity-dependent morphological plasticity in hippocampal neurons. *Neuron* **44**, 759–767 (2004).
57. Kim, C.H. & Lisman, J.E. A role of actin filament in synaptic transmission and long-term potentiation. *J. Neurosci.* **19**, 4314–4324 (1999).
58. Pavlowsky, A. *et al.* A postsynaptic signaling pathway that may account for the cognitive defect due to IL1RAPL1 mutation. *Curr. Biol.* **20**, 103–115 (2010).
59. Wermeling, D.P. Intranasal delivery of antiepileptic medications for treatment of seizures. *Neurotherapeutics* **6**, 352–358 (2009).

SPONSOR FEATURE

Complete solution for discovery and validation of microRNA biomarkers in biofluids

EXIQON
Seek Find Verify

At Exiqon we have combined superior LNA™-enhanced microRNA profiling technologies with expertise and knowledge from our Diagnostics and Service divisions to develop a complete solution for microRNA profiling in biofluids. We offer world leading products and services covering workflows from sample preparation to data analysis.

The promise of microRNA biomarkers in biofluids

microRNAs are non-coding RNAs that have been shown to play important regulatory roles in most cellular and developmental processes and have been implicated in a large number of human diseases. Due to their wide-ranging biological potential and the fact that microRNAs are relatively stable in a number of readily available biofluids, these small 20-22 nt molecules are prime candidates for use as minimally invasive biomarkers in molecular diagnostics of disease and other clinical conditions, including toxicology.

However, microRNA profiling in biofluid samples is challenging and the development of robust biomarkers for clinical applications requires not only a highly sensitive and accurate microRNA detection method, but also optimized and standardized procedures for sample handling and preparation as well as reliable methods for sample and data qualification.

At Exiqon we have many years' experience with microRNA profiling in biofluid samples. Over the past few years we have been involved in several projects to discover and validate microRNA biomarkers in serum, plasma and urine and have gained extensive insights into the requirements for sample handling and RNA isolation as well as quality control and data processing. In particular, our project to discover microRNA biomarkers for early detection of colorectal cancer (CRC) has shed light on several challenging aspects and led to the development of innovative solutions and new products.

Figure 1. Superior sensitivity and linearity for microRNA profiling. The microRNA assays are all (95%) wet-lab validated to be linear down to 5-10 copies of microRNA target in the PCR reaction. Median Cq values for 179 microRNA assays on the Serum/Plasma Focus Panel are shown.

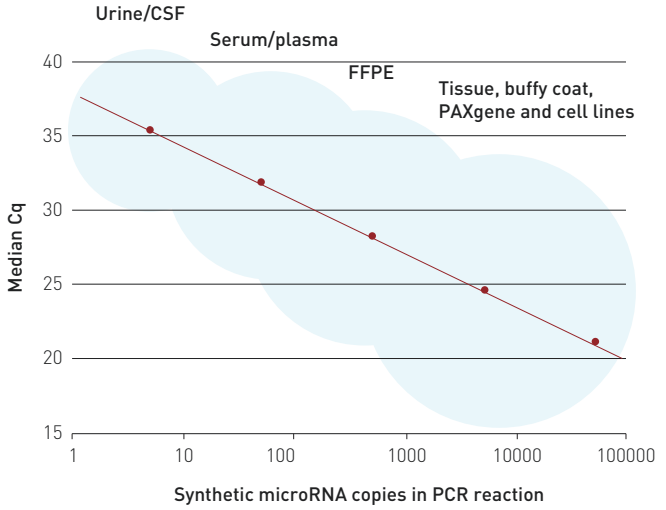

Accurate and robust microRNA profiling

The accurate and robust measurement of microRNAs in biofluids is made challenging by a number of factors. Firstly the divergent nature of the microRNA sequences means that the detection method must ensure accurate simultaneous detection of short sequences with widely varying GC contents. In addition, because individual members of microRNA families are highly similar, the detection method must also be able to distinguish single nucleotide mismatches. The inclusion of locked nucleic acids (LNA™) in microRNA PCR primers overcomes both these challenges.

We have developed a method for microRNA qPCR in which a single truly universal cDNA synthesis reaction is followed by PCR amplification using two microRNA-specific, LNA™-enhanced primers. The inclusion of LNA™ in the PCR primers allows the design of short, yet specific, high affinity primers even for AT rich sequences[1]. In combination with a highly optimized SYBR® Green PCR master mix this results in a uniquely sensitive microRNA profiling system with high specificity (Figure 1).

The miRCURY LNA™ Universal RT microRNA PCR system has proved to be especially well suited to analysis of biofluid samples with limited RNA content[2]. Profiling of up to 378 microRNAs is routinely done from 20ng total RNA or the equivalent of 20µL biofluids such as serum/plasma or urine without the need for pre-amplification. The absence of a pre-amplification step not only streamlines the workflow, but also reduces the risk of introducing artificial bias.

This accurate and reliable system is available in ready-to- use PCR plates compatible with a number of common qPCR instruments. A selection of panels is available that is compatible with the various phases of biomarker discovery and validation (Figure 2). The optimized and simple workflow is easily adapted to high-throughput applications and well-suited for a clinical automatable workflow.

The importance of high quality samples

Biofluid samples are challenging to work with in many ways. They contain low levels of RNA, high levels of inhibitors and are susceptible to pre-analytical variables. The low levels of RNA mean that reliable and reproducible isolation of microRNAs requires careful attention to the RNA isolation procedure. Recent studies have shown that column-based approaches give higher yields and better performance compared with traditional TRIzol®-based methods[3]. In addition, we have previously shown that the addition of carrier to the RNA isolation improves yield and reproducibility[4]. The recently introduced miRCURY™ RNA Isolation Kit for biofluids is optimized for the isolation of small RNA (<1000nt) from samples with low RNA content and has been shown to offer the best RNA isolation from serum[3].

In addition to RNA isolation, sample procurement, handling and storage can also be sources of pre-analytical variation. A number of recent papers have discussed various pre-analytical variables for microRNA profiling in serum and/or plasma. These studies have shown that cellular contamination and hemolysis (or the presence of red blood cell lysate in the sample) can be a major cause of variation in microRNA levels preventing detection of other biological differences. During the discovery phase of the CRC biomarker project, we found that samples from different hospitals varied in their microRNA profiles, and that these source-related differences could hamper the identification of CRC related microRNA signatures. The variation was linked to hemolysis and also correlated with the different blood collection tubes used. Our experience with the analysis of large numbers of biofluid samples from a variety of sources enables us to make specific recommendations for our customers and partners to ensure high quality starting material[5].

Figure 2. Overview of Ready-to-Use microRNA PCR panels available for the biomarker discovery process.

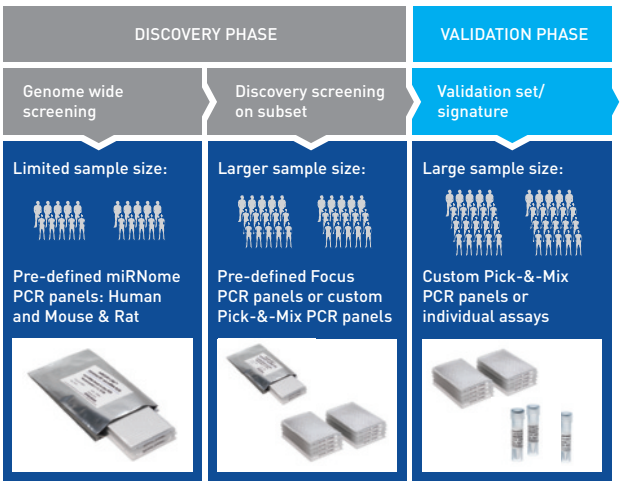

Ensuring high quality and reliable data

In addition to high quality samples and a sensitive and reliable microRNA profiling system, the identification of robust biomarkers also requires careful attention to RNA and data quality. Our experience in Exiqon Diagnostics and Exiqon Services has enabled us to develop an extensive QC and data analysis pipeline to identify and eliminate pre-analytical and technical variables in samples[6]. To control the quality of RNA samples and reduce sample related technical variation we have developed a set of synthetic small RNAs that are spiked into the sample at various stages during isolation and cDNA synthesis. The spike-ins are used to monitor yield and possible contamination by inhibitors and form part of a RNA QC panel recommended for checking the quality of RNA from biofluids before performing microRNA profiling.

As mentioned earlier, contamination of cell free samples with cellular RNA (e.g. hemolysis of serum/plasma samples) is a pre-analytical variable that can affect microRNA profiling results significantly[7]. Due to our extensive database of results from biofluid samples we have been able to generate reference ranges for microRNAs commonly expressed is such samples[4]. This allows us to compare any new sample to the reference range in order to identify outliers and detect e.g. unwanted cellular contamination. To overcome the issue of hemolysis in the CRC study, we developed a microRNA-based hemolysis indicator using on the relative expression of the erythrocyte-specific miR-451 and the stable miR-23a. We have shown that applying a pre-set cut-off for indications of hemolysis on a dataset from clinical plasma samples could improve the sensitivity and specificity of a microRNA signature for early colorectal cancer significantly[8].

A first step in qPCR data qualification is the analysis of melting curves to eliminate data where more than one amplicon was generated or where the amplicon melting point differs from expectations. Next, background levels are set based on negative controls performed on each assay and this is used to determine whether a signal is a true signal or just background. In addition to pre-processing of the data to make sure only high quality samples and data are included in the final analysis, proper normalization of the data is vital for high quality results. Exiqon's GenEx qPCR software offers a straightforward and user friendly solution where different methods of normalization can be explored. Based on our experience we provide researchers with advice and recommendations for microRNA data analysis from a variety of biofluids.

Concluding remarks

At Exiqon we have strict requirements for quality and reliability in our biomarker projects and therefore rely on using the most accurate and sensitive microRNA tools available. We run numerous large projects and are therefore dependent on fast and straightforward workflows to ensure timely delivery of results. Our complete product portfolio for microRNA profiling in biofluids provides both us and our partners and customers with a high performance platform to exploit the promise of microRNA biomarkers in biofluids.

Authors

Thorarinn Blondal, Ditte Andreasen, Maria Wrang Teilum, Peter Mouritzen, Johan Wahlin and Ina K. Dahlsveen.
Exiqon A/S, Skelstedet 16, 2950 Vedbæk, Denmark

References

1. N. Jacobsen *et al.*, Profiling microRNAs by real-time PCR. Methods Mol Biol. 732 (2011) 39–54.
2. S.G. Jensen *et al.*, Evaluation of two commercial global miRNA expression profiling platforms for detection of less abundant miRNAs, BMC Genomics. 12 (2011) 435.
3. M. A. McAlexander *et al.*, Comparison of methods for miRNA extraction from plasma and quantitative recovery of RNA from plasma and cerebrospinal fluid. Front. Genet. (2013) 4:83.
4. D. Andreasen *et al.*, Improved microRNA quantification in total RNA from clinical samples, Methods. 50 (2010) S6–9.
5. www.exiqon.com/biofluids
6. T. Blondal *et al.*, Assessing sample and miRNA profile quality in serum and plasma or other biofluids, Methods 59 (2013) 164–169.
7. C.C. Pritchard *et al.*, Blood cell origin of circulating microRNAs: a cautionary note for cancer biomarker studies., Cancer Prevention Research (Philadelphia, Pa.). 5 (2012) 492–7.
8. S. J. Nielsen *et al.*, A universal method for elimination of haemolyzed plasma samples that improves miRNA signature performance for early detection of colorectal cancer, AACR Annual Meeting. LB-476 (2012).

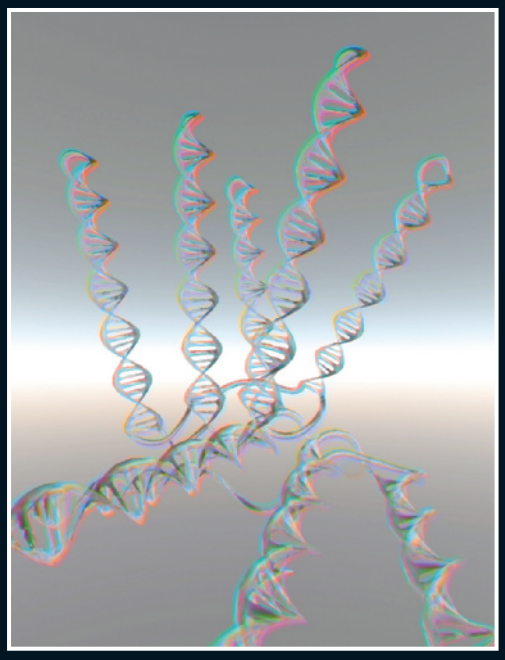

nature

www.nature.com/reprintcollections/microrna_2013